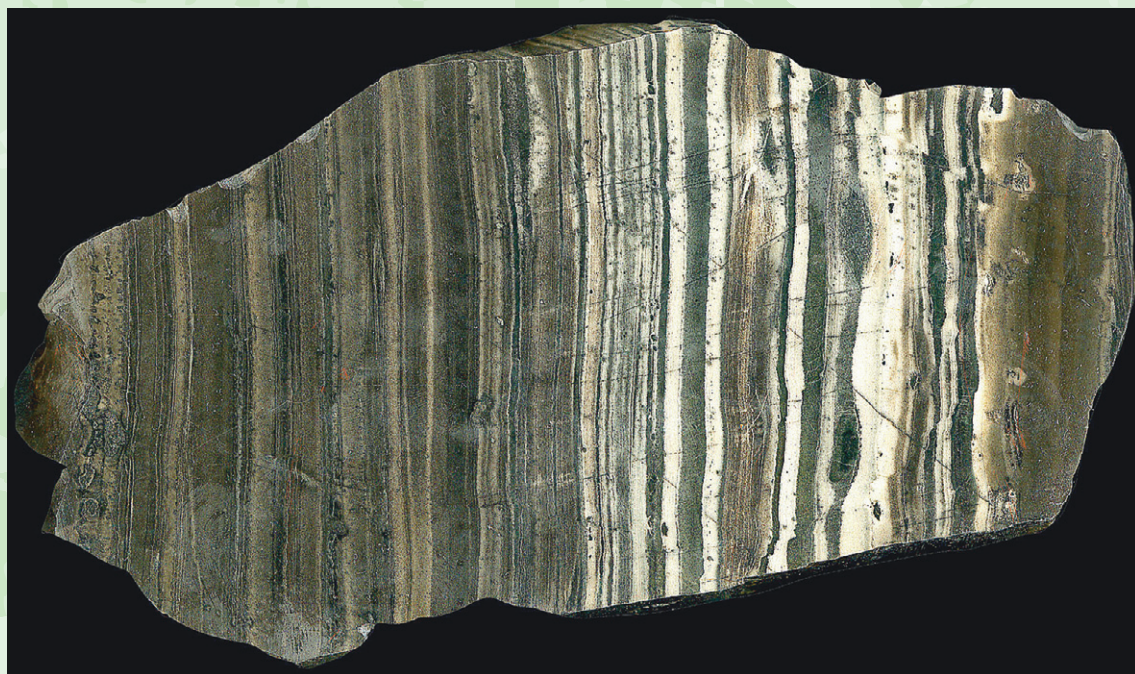


Rapporter och meddelanden 107

The geology of the Palaeoproterozoic limestone-hosted Dannemora iron deposit, Sweden

Ingemar Lager



SGU

Sveriges Geologiska Undersökning
Geological Survey of Sweden

Rapporter och meddelanden 107

**The Geology of the Palaeoproterozoic
Limestone-hosted Dannemora Iron Deposit, Sweden**

Ingemar Lager

Sveriges Geologiska Undersökning
2001

ISSN 0349-2176
ISBN 91-7158-666-0

Cover: Photograph of a rock sample from the upper unit of the upper formation in the Dannemora syncline. Brown, volcanoclastic turbidites can be seen in the left part of the photo and brown, volcanoclastic turbidites interbedded with zoisite-altered volcanoclastic turbidites (white) and limestone (dark) in the right part.

All photographs in this publication: Ingemar Lager

© Sveriges Geologiska Undersökning
Geological Survey of Sweden

Layout: Agneta Ek, SGU
Print: Elanders Tofters, Östervåla 2001

CONTENT

Sammanfattning	4
Abstract	4
Introduction	4
Regional geology	5
The Dannemora syncline	8
Shape and extent	8
Metamorphism	8
Rock types	8
Formations	8
Depositional environments	8
Depositional sequences	9
Deformation	9
Description and genetic interpretation of rock types	9
Volcaniclastic rocks	9
The pyroclastic flow deposits	10
The pyroclastic breccia deposit	13
The pyroclastic fall deposits	13
Redeposited pyroclastic deposits	16
Carbonate rocks	21
The calcite limestones	21
The dolomitic limestone	23
Chlorite felses	28
Eolian chlorite fels deposits	28
Chlorite fels turbidite or tempestites	29
Skarn (Fe-Mn-Ca-Mg-silicate rocks)	29
Iron ores	30
Sulphide ores	32
Massive sulphide vein deposits	32
The stratabound sulphide deposits	33
The sulphide fracture mineralizations	34
Dyke and sill complexes	34
Granodiorite	34
Evidence of primary organic life	34
Dolomitization	36
Stratigraphy and palaeogeographic interpretation	37
The lower formation	37
The depositional sequence 1 of the 1st order	37
The depositional sequence 2 of the 1st order	37
The depositional sequence 3 of the 1st order	38
The upper formation	38
Model of supracrustal evolution	39
The lower formation and the basal unit of the upper formation	39
The upper formation	39
Stage 1	40
Stage 2	40
Stage 3	41
Stage 4	41
Stage 5	41
Discussion	42
Conclusion	42
Acknowledgements	43
References	43
Plates	45

SAMMANFATTNING

Järnmalmfyndigheten i Dannemora består av ungefär 25 kroppar av både manganrik och manganfattig kalk- och skarnjärnmalm vilka var föremål för gruvbrytning under flera hundra år fram till år 1992. Fyndigheten omfattar också några sulfidmineraliseringar som bröts kring förra sekelskiftet. Vård- och sidobergarter till malmerna utgörs av brant stupande enheter av svagt omvandlade sedimentära och felsiska vulkaniska bergarter tillhörande den svekofenniska "leptitformationen" med en ålder av ca 1,9 miljarder år. Ursprungliga bergartsstrukturer och texturer är väl bevarade och har gett goda möjligheter till faciesanalyser och tolkningar av de ursprungliga sedimentära miljöerna. Fyndigheten antas ha bildats i ett område med rhyolitisk vulkanism och kalderabildning och sedimentationen antas ha ägt rum i flera olika miljöer: öppen marin, lagunartad och saltbildningsplatser. Upplyftning och nersänkning på grund av vulkanismen föreslås som huvudskälet till de upprepade regressionerna och transgressionerna inom området. Detta har möjliggjort återkommande avsättningar av vulkanoklastiska tidvat-tenavlagringar, dolomitiska karbonatavlagringar av sabkha-typ och saltskorpeavlagringar. De sistnämnda har varit ytterst viktiga för malmbildningen då de har fungerat som effektiva fällor för metallutfällningar från laterala, metallförande hydrotermala lösningar i många av sedimentationssekvenserna.

ABSTRACT

The Dannemora ore deposit consists of about 25 bodies of both manganese-rich and manganese-poor limestone and skarn iron ore, which were mined for several hundred years until 1992. It also contains a few sulphide mineralizations, which were mined in earlier times. The deposit is hosted by steeply dipping units of slightly altered sedimentary and felsic volcanic rocks belonging to the Svecofennian "leptite formation" with an age of around 1.9 Ga. Original rock structures and textures are well preserved and have provided good opportunities for facies analysis and interpretation of original sedimentary environments. A model for the geological evolution of the deposit based on a basin analysis is proposed. The deposit is interpreted to have formed in a rhyolitic, caldera region with sedimentation in an open marine, lagoonal, and salina environment. Volcano-induced uplift and subsidence is proposed as the primary reason for the repeated regressions and transgressions within the area. These have produced recurring depositional sequences of volcanoclastic tidal deposits, dolomitic carbonate sabkha deposits, and salt pan deposits. The latter have been paramount for the ore formation, as they have functioned as efficient traps for metal precipitation from lateral metalliferous, hydrothermal solutions in many of the depositional sequences.

Keywords: Palaeoproterozoic, Svecofennian, Dannemora iron deposit, depositional sequences, volcanoclastic rocks, bubble-wall shards, accretionary lapilli, stromatolites, evaporites.

INTRODUCTION

The Dannemora ore deposit is situated in the eastern part of central Sweden, about 45 km NNE of Uppsala and 120 km north of Stockholm (Fig. 1). It contains about 25 bodies of both manganese-rich and manganese-poor limestone and skarn iron ore. Many of them have been known for more than 500 years and have been mined for iron during several hundred years until 1992 when the mining operations finished. The deposit also comprises a small number of sulphide mineralizations, which were mined in earlier times. The deposit and its surroundings have previously been described in Erdmann (1851), Törnebohm (1878), Nyström (1922), Tegengren (1924), and Geijer & Magnusson (1944) and others. However, these authors only described the surface bedrock, or very limited and

shallow parts of the deposit. Through extensive mining and continued exploration, down to a depth of more than one thousand metres between 1944 and 1986, significantly larger portions of the Dannemora deposit have been exposed than were previously available for investigation, thereby revealing a multitude of new geological data. Some of the recent data have previously been presented by Lager (1986), but further geological investigations until 1992 revealed many new features, thus prompting an amplification and revision of earlier results and interpretations. This paper contains a more comprehensive summary, with updated geology of the Dannemora ore deposit, than presented by Lager in 1986.

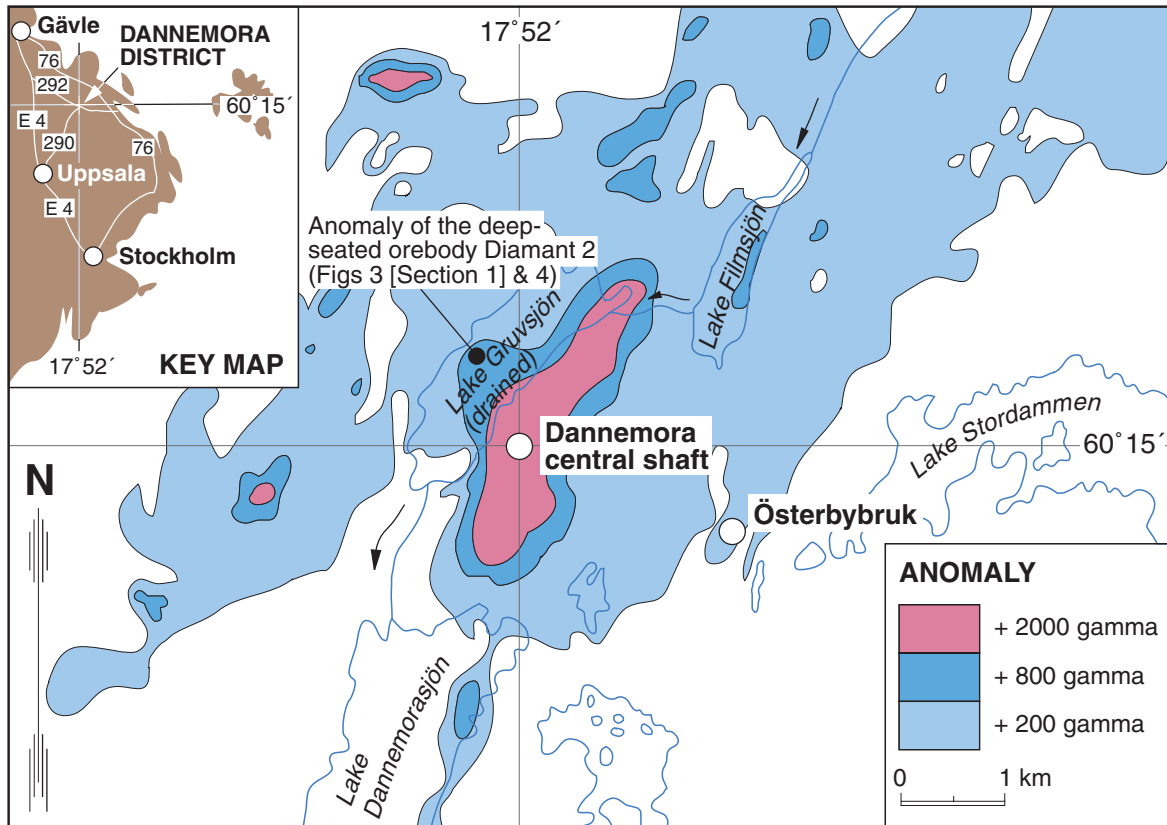


Fig. 1. Simplified aeromagnetic total-intensity survey of the Dannemora district.

REGIONAL GEOLOGY

The Dannemora deposit is hosted by Palaeoproterozoic, c. 1.9 Ga, Svecofennian, metavolcanic rocks of the "leptite formation" (see Lundqvist 1979). They probably belong to the uppermost part of a volcanic sequence, which characterizes the whole of the metalliferous Bergslagen area in southern, central Sweden (Lundström et al. 1998). During the Svecokarelian orogeny, these rocks were deformed and metamorphosed to low, medium, and high grades of regional low pressure metamorphism (Stephens et al. 2000, Stålhös 1991). A number of well preserved areas are described from western Bergslagen (e.g. Sundius 1923, Magnusson 1925, Björk 1986, Oen 1987, Lundström 1995). Due to the generally stronger regional metamorphism, such areas are rare in the eastern, coastal areas. However, the rocks in the Uppsala-Dannemora area are reasonably well preserved. The regional geology of eastern Bergslagen is described by Stålhös (1991).

The bedrock within the Dannemora area and its surroundings, here called the Dannemora district (Fig. 2), is

characterized by steeply dipping strata of well preserved sedimentary and felsic volcanic rocks. These units occur in belts of variable thicknesses between early orogenic granitoids (granites, granodiorites etc.). Perpendicular to the extension of the Dannemora deposit the belt is thickened due to isoclinal folding with low-angle fold axes. There the belt consists of two synclines, separated by an anticline, where the Dannemora deposit is part of the ESE syncline, here called the Dannemora syncline. The deposit stands out on the aeromagnetic map of the area (Fig. 1) as an extensive magnetic anomaly with high gamma values. Note the widened anomaly caused by the deep-seated Diamantmalm 2 ore body (Fig. 3 and Fig. 4, cross-section 1). The aeromagnetic map also shows other magnetic anomalies, but these all have a limited extension and low gamma readings. These anomalies are also caused by iron ore bodies of which several have been explored and exploited in earlier times (Fig. 2, "iron ore mines [closed]").

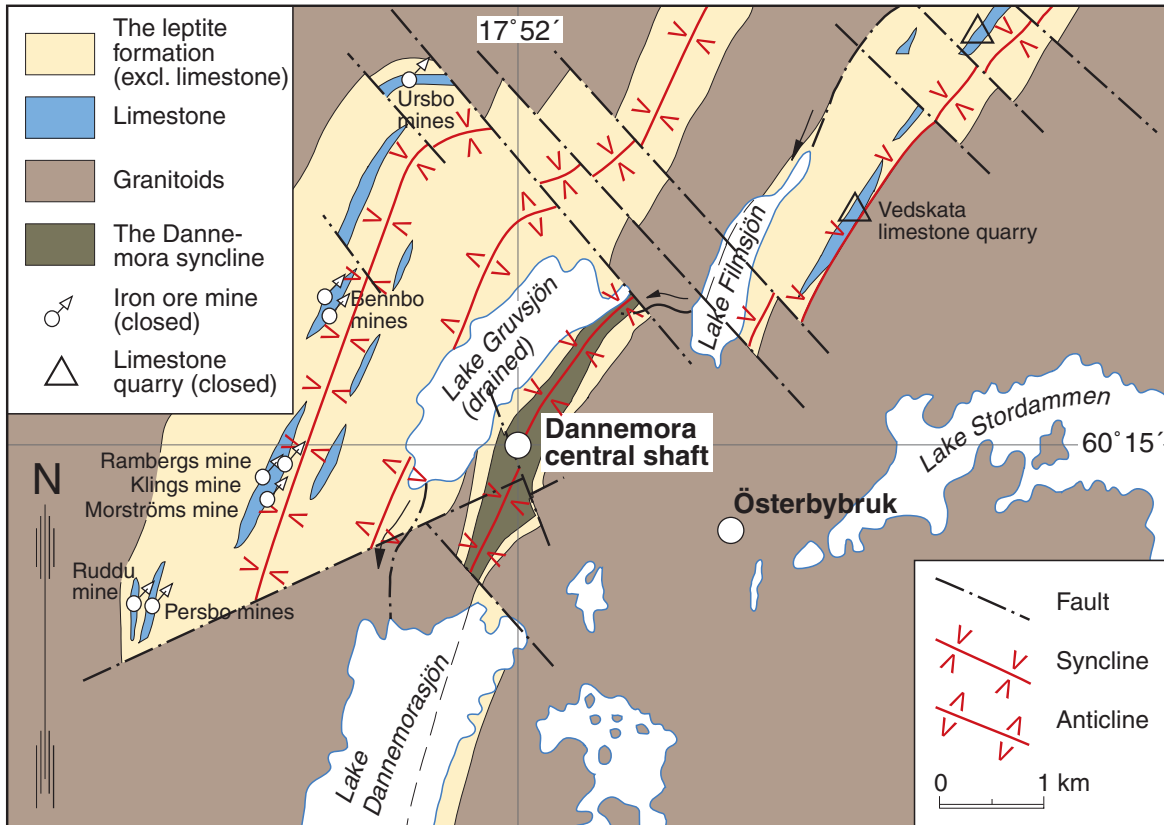


Fig. 2. Simplified geologic map of the Dannemora district.

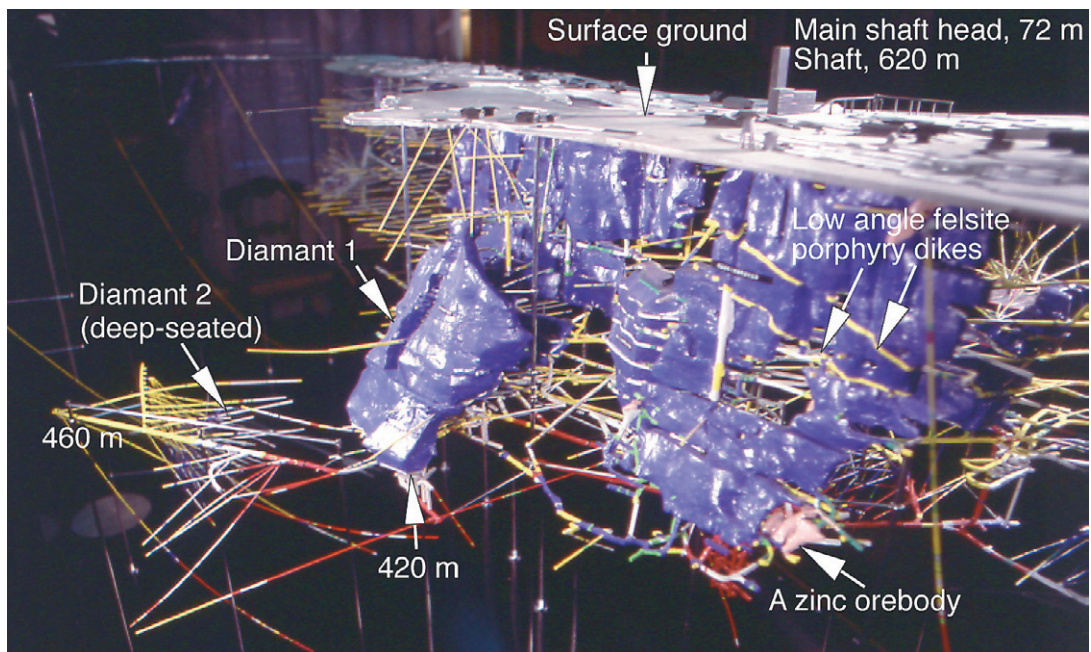


Fig. 3. Three-dimensional model of the Dannemora mines seen from the south towards north. Blue = iron ore or open rooms from iron ore mining, yellow = volcaniclastic rocks or "felsite porphyry" dykes, white = limestone, red = granodiorite, and light brown = zinc ore.

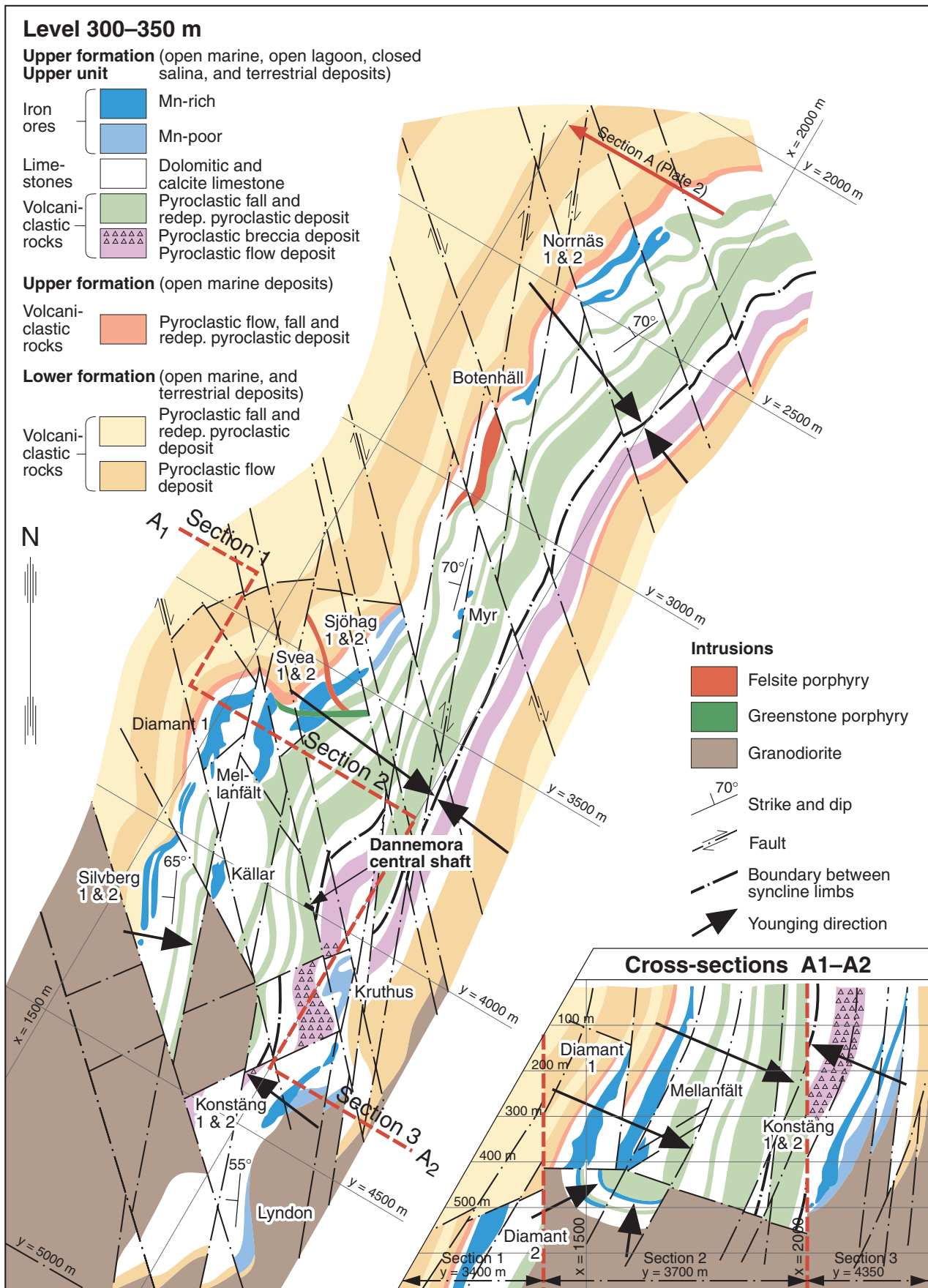


Fig. 4. Geologic map of the Dannemora syncline at the 300–350 m level.

THE DANNEMORA SYNCLINE

Shape and extent

The shape and extent of large parts of the Dannemora syncline at the 300–350 m level can be seen in Figure 4. The carbonate and ore-bearing section of the syncline, the Dannemora ore deposit, has a total length of about 3 km and a width of about 400 to 800 m. The deposit strikes approximately N30°E and dips between 80 and 90° towards the northwest at the surface and between 55° and 70° at the 350 m level. The Dannemora syncline, which plunges a few degrees towards the northeast, is composed of two steeply dipping fold-limbs of which the WNW-limb is slightly overturned (Fig. 4, cross-section A₁–A₂). The stratigraphy is similar in both limbs and the original way-up directions of bedding have been determined by grading, cross-bedding, erosional surfaces, and the orientation of stromatolite-like structures. The hinge of the syncline has only been observed within the southern part of the deposit (Fig. 4, cross-section A₁–A₂). Despite investigations of the bedrock towards the north, the hinge has not been revealed there. In the north, it is possible to trace the "leptite formation" down to a depth of 1150 m (ore down to 1000 m) with the aid of diamond drilling and it most likely continues even deeper.

Metamorphism

The mineral parageneses of the rocks must have changed many times after deposition. Particularly, the regional metamorphism during the Svecokarelian orogeny must have had potential to change the mineral parageneses. However, the rocks are structurally so well preserved, that the post-depositional (post-volcanic-hydrothermal) processes can be assumed to have been essentially isochemical. Therefore, the mineralogical composition of the skarns and chlorite felses etc. may essentially reflect the geochemical alteration created by the syndepositional, diagenetic or hydrothermal processes.

The rocks in the exposed parts of the Dannemora syncline are mainly metamorphosed in low greenschist facies, but locally up to lower amphibolite facies within hydrothermally altered areas. The "meta-"prefix should therefore precede the rock names. However, primary structures and textures are generally preserved well enough to allow their recognition and allow interpretations of the origin of the rocks. Therefore, both sedimentary, and magmatic names will be used without the prefix – alongside with some commonly used metamorphic names such as quartzite, chlorite fels, and skarn.

Rock types

The rock types in the Dannemora syncline include both primary supracrustal rocks, such as volcanoclastic and carbonate rocks, and diagenetically and hydrothermally altered supracrustal rocks, such as chlorite fels, skarn (Fe-Mn-Ca-Mg silicate rocks), iron and sulphide ores, as well as intrusive rocks, e.g. felsic and "greenstone" porphyries, diorite, and granodiorite, of which most are to be found in Figure 4. Many of the supracrustal rocks occur as finely laminated heteroliths too thin to be reproduced on the current map scales. In Figure 4, such rocks have been labelled with the name of the dominant lithology within the unit. Furthermore, the chlorite fels, skarn, sulphide ores and many of the intrusive rocks have not been included in Figure 4 due to their negligible thickness.

Formations

The stratigraphic sequence in the Dannemora syncline has been divided informally into a lower and an upper formation (Fig. 4 and Plate 1c). In addition, the upper formation is divided into a basal unit and an upper unit. The lower formation is composed exclusively of volcanoclastic rocks. The basal unit of the upper formation consists also solely of volcanoclastic rocks, but the volcanic rocks contain lithic clasts of iron ore, which are lacking in the lower formation. Beds of iron ore and carbonate rocks are completely missing there. The upper unit of the upper formation on the other hand, is composed of beds of volcanoclastic rocks as well as beds of iron ore and carbonate rocks.

Depositional environments

Several different depositional environments are proposed for the deposits of the Dannemora syncline. The main types of names used here for depositional environments are *open marine*, *open lagoon*, *closed salina*, and *terrestrial environment*. They have been used with the following meanings: *open marine* – oceanic environment without any protecting barrier, *open lagoon* – a body of water with a protecting barrier, but partly in connection with the ocean and its equilibrating effects, through superficial channels, *closed salina* – a body of water, near the ocean coast with sea-water recharge, but without any superficial connection with the ocean and its equilibrating effects, and *terrestrial environment* – the dry land.

Depositional sequences

The stratigraphy of the Dannemora syncline is divided into three depositional sequences of the 1st order (Plates 1 and 2). They are interpreted as transgressive-regressive sequences. The depositional sequences 1 and 2 of the 1st order constitute the basal part of the lower formation. They are suggested to have been deposited in open marine and terrestrial environments (see “Stratigraphy and paleogeographic evolution” below and Plate 2). The depositional sequence 3 of the 1st order consists of the upper part of the lower formation, and the basal and upper unit of the upper formation (Plates 1 and 2). The upper part of the lower formation and basal unit of the upper formation are considered to have been deposited in an open marine environment (see “Stratigraphy and paleogeographic evolution” below and Plate 2). The upper unit of the upper formation is suggested to have been deposited in repeated open marine, open lagoon, closed salina, and terrestrial environments (see “Stratigraphy and paleogeographic evolution” below and Plates 1 and 3). This unit is divided into 14 depositional sequences of the 2nd order (open marine, open lagoon, closed salina, and terrestrial deposits), thought to be transgressive-regressive (see “Stratigraphy and paleogeographic evolution” below and Plates 1 and 3). At the bottom of these sequences the sediments may be sorted in depositional sequences of the 3rd order (two types: one with foreshore, beach, and tidal flat deposits and one with subtidal and sabkha deposits), considered as transgressive-progradational (shallowing upwards) sequences (see “Stratigraphy and paleogeographic evolution” below and Plate 4). In the upper portion of these sequences there are in many cases also depositional sequences of the 3rd order (primary evaporative gypsum and hal-

ite deposits), regarded as dilution-aggradation (drying upwards) sequences (see “Stratigraphy and paleogeographic evolution” below and Plate 4). Furthermore, in the depositional sequences of 3rd order, the sabkha deposits sometimes can be separated into depositional sequences of the 4th order (spring and storm flood, chert, primary algal mats, and evaporative gypsum deposits). They are interpreted as dilution-aggradation (drying upwards) sequences (see “Evidence of primary organic life” below).

Deformation

During the period of granitic magmatism, the originally horizontal layers of the supracrustal rocks were raised to a steeply dipping position. Apart from this intrusion-related folding, faulting with associated minor drag-folding is the dominating deformation style in the Dannemora iron ore deposit. Secondary foliations exist only in close association with fault zones, and lineations occur only locally parallel with the fold axes in minor folds. Slaty, fracture and crenulation cleavages have been observed in fault zones with associated deformation of e.g. accretionary lapilli.

Several major fault zones are horizontal or gently dipping (Figure 4, sections 1 and 2). These zones always show top-to-the-south kinematics. The greatest known horizontal displacement is 400 m. The Diamant 1 orebody is faulted 400 m towards the south in relation to the Diamant 2 orebody at the 420 m level (Fig. 3). Two conspicuous parallel systems of steeply dipping fault zones also occur. One strikes N15°W and dips 60–90°W, the other strikes N10°E and dips 85°W (Fig. 4). As a rule, dextral kinematics are indicated for these zones.

DESCRIPTION AND GENETIC INTERPRETATION OF ROCK TYPES

Below, the following rock types in the Dannemora syncline are described: volcanoclastic rocks, carbonate rocks, chlorite felses, skarn, iron ores, sulphide ores, dyke and sill complexes, and granodiorite. Evidence of primary organic life, and dolomitization are also treated in this chapter, but as separate topics.

Volcanoclastic rocks

The volcanoclastic rocks in the Dannemora syncline are rhyolitic in composition, commonly with a high potassium content (Table 1). All of them have a low sodium content with the exception of the pyroclastic flow deposits, which are a little higher in sodium. The reported compositions of the pyroclastic flow deposits, however, are mean values for 10 analyses, and the spread in the potas-

sium and sodium content is high. The sample localities of the 14 samples of pyroclastic flow and fall deposits are shown in Plate 2. From the reported values, it is evident that the potassium content increases and the sodium content decreases twice upwards in the stratigraphy. A high sodium content is correlated with a higher amount of sodium feldspar phenocrysts, and hence the K_2O/Na_2O ratio is, at least partially, due to primary magmatic differences. This is in accordance with the presence of two types of dykes, i.e. low sodium content “felsite” dykes with quartz phenocrysts and high sodium content “greenstone porphyry” dykes with sodium feldspar phenocrysts. The main minerals are quartz, albite, microcline, and sericite, but in some cases illite, chlorite, calcite, or epidote may occur.

Table 1. Chemical compositions of different rocks (mean values of chemical analyses made by SGAB Analyis using ICP. The Fe₂O₃-content is calculated).

Rocks	No. samples	SiO ₂ %	TiO ₂ %	Al ₂ O ₃ %	Fe ₂ O ₃ %	FeO %	MnO %	MgO %	CaO %	K ₂ O %	Na ₂ O %	P ₂ O ₅ %	LOI %	Sum %	Ba PPM
Upper formation															
Pyroclastic fall deposits	7	74,17	0,12	13,62	0,82	0,70	0,09	1,09	2,18	4,90	0,55	0,02	1,50	99,76	538
Pyroclastic breccia	1	61,60	0,09	9,96	0,45	1,50	0,37	1,19	16,00	3,86	0,24	0,01	4,30	99,57	113
Redep. pyroclast. dep. coarse	21	68,53	0,25	12,42	4,00	2,80	0,13	1,31	1,63	5,10	0,66	0,05	1,33	98,21	8107
Redep. pyroclast. dep. fine	4	56,33	0,16	17,18	0,68	1,58	0,20	1,90	11,46	6,69	0,65	0,02	2,83	99,68	633
White spherical structures	2	71,90	0,06	10,50	0,97	1,25	0,42	0,45	11,60	0,24	0,05	0,01	2,40	99,85	75
Calcite limestone	12	15,92	0,04	1,75	1,12	1,50	0,55	1,72	45,54	0,49	0,06	0,02	31,14	99,85	119
Dolomitic limestone	17	6,79	0,03	1,02	4,66	5,14	1,52	11,26	32,94	0,15	0,05	0,03	35,86	99,45	63
Chlorite fels	4	36,83	0,20	14,30	3,57	8,70	0,99	14,76	6,46	4,25	0,23	0,08	8,60	98,97	362
Jaspilite	3	71,33	0,07	5,11	13,44	3,30	0,04	0,54	1,20	2,08	0,32	0,03	0,93	98,39	7163
Skarn (Mn-poor silicates)	1	-	0,09	5,31	14,75	3,20	1,25	1,22	29,60	0,03	0,05	0,08	-	55,58	9
Skarn (Mn-rich silicates)	2	-	0,01	0,09	1,89	31,45	22,49	2,92	0,84	0,02	0,03	0,00	-	59,74	8
Iron ore (Mn-poor)	3	-	0,01	0,36	45,77	22,67	0,28	4,31	3,55	0,09	0,07	0,08	-	77,19	1
Iron ore (Mn-rich)	5	-	0,03	1,40	43,21	21,94	3,99	6,41	3,12	0,44	0,03	0,03	-	80,60	124
Lower formation															
Pyroclastic flow deposits	10	70,18	0,21	14,14	1,76	1,43	0,07	0,85	1,92	5,44	1,99	0,05	1,53	99,57	997
Pyroclastic fall deposits	7	73,56	0,20	13,52	1,20	0,93	0,04	0,85	1,42	5,63	0,66	0,02	1,64	99,67	716
Intrusions															
Felsite porphyry	2	74,70	0,07	13,05	0,53	1,20	0,07	0,61	0,36	6,90	0,77	0,01	1,05	99,32	3259
Greenstone porphyry	1	69,70	0,27	14,30	0,75	2,50	0,06	0,84	2,21	4,07	3,22	0,03	1,40	99,36	1592
Diorite	2	47,65	0,91	14,30	2,83	9,25	0,43	8,14	8,46	0,79	1,36	0,31	4,30	98,73	399
Granodiorite	5	67,92	0,39	14,28	1,00	3,04	0,10	1,32	3,47	3,08	2,75	0,14	1,94	99,43	822

The volcanoclastic rocks are composed of thousands of laminae and beds with very varied appearance. An attempt to subdivide similar beds and bed sequences into genetic types has been made. Some deposit types, such as pyroclastic surge deposits, have been grouped together with other types because they are too thin or are too difficult to discern in the thin drill cores used for facies analysis. Therefore, only the following four genetic groups of volcanoclastic rocks have been distinguished (Fig. 4 and Plates 1–4); pyroclastic flow deposits, pyroclastic breccia, pyroclastic fall deposits, and redeposited, pyroclastic deposits. In some areas the genetic groups alternate so intimately that far from all can be presented on the map at the scale presented here. In these cases, only the dominant rock types have been used.

The pyroclastic flow deposits

Pyroclastic flow deposits of two types have been identified in the Dannemora syncline, namely, 1) subaerial pyroclastic flow deposits (pumice flow deposits or ignimbrites) and 2) subaqueous pyroclastic flow deposits (pumice flow deposits or ignimbrites).

1) The subaerial pyroclastic flow deposits (pumice flow deposits or ignimbrites) are found solely within the depositional sequence 2 in the lower formation (Plate 2). These deposits constitute a group of several flow beds, with a bed thickness of 1.5–14 m. Each bed consists of a thick, red or greyish-red basal unit and a thinner, grey upper unit. The basal unit contains numerous black and red pumice clasts, which are poorly sorted and normally ungraded (Fig.

5a). Locally the pumice clasts have irregular shapes as in Fig. 5a, but mostly they are flattened and found as c. 1–5 mm thick and 1–10 cm long clasts (Figs. 5b–c and 6a–c). Typical of the basal unit is also abundant 1–5 mm large feldspar phenocrysts and/or 1–7 mm large blue-coloured quartz phenocrysts (Figs. 6a–c). Lithic clasts are also common in the basal unit, for example, of older felsic, pyroclastic rocks (Fig. 7a). The upper unit is characterized by dispersed, dark grey, angular pumice without flattening and 1–3 mm large feldspar and/or white quartz phenocrysts (Fig. 7b).

Poor sorting and variable amounts of ash, pumice lapilli and blocks is typical for pyroclastic flow deposits (pumice flow deposits or ignimbrites) (e.g. Cas and Wright 1987). Red colour of the pumice may result from thermal oxidation, a process that reflects cooling of hot material while in contact with air (e.g. McPhie et al. 1993). The alternation between the red or greyish-red basal units and the grey upper units in the flow deposits in Dannemora indicates that the red colour in the basal units is caused by early thermal oxidation rather than later processes. Flattening of pumice may have several origins, e.g. post-emplacment welding, burial compaction and tectonic foliation or lineation. The alternation between flattened pumice in the basal units and non-flattened pumice in the upper units in Dannemora suggests that the flattening of the pumice is caused by post-emplacment welding and not by burial compaction or tectonic foliation or lineation. Welding and thermal oxidation are features suggesting a hot, gas-supported emplacement of the material (McPhie et al. 1993).



Fig. 5. Parts of pyroclastic flow deposits with juvenile fragments: a) with red, irregular, non-flattened, pumice fragments. b) with red, flattened, pumice fragments. c) with grey, slightly flattened, pumice fragments. Dark spots are phenocrysts of quartz. Photographs of drill-core samples from red or greyish-red basal units of flow beds in the lower formation.



Fig. 6. Parts of pyroclastic flow deposits with different phenocrysts and juvenile fragments: a) with feldspar phenocrysts (light spots) and black and red, flattened, pumice fragments (black and red lenses). b) with quartz phenocrysts (white spots) and flattened pumice fragments (red lenses). c) with feldspar (light red spots) and quartz (bluish-grey spots) phenocrysts and pumice fragments not seen in the photograph. Photographs of rock samples from red basal units of flow beds in the lower formation.

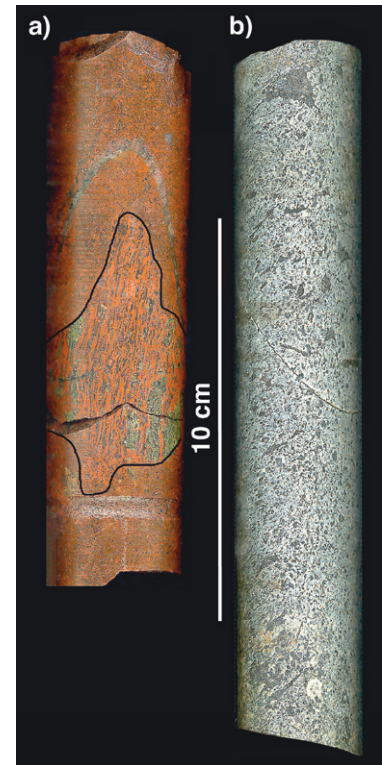


Fig. 7. Parts of pyroclastic flow bed units: a) with a red lithic clast (clast margin is outlined with black) with a strongly welded structure. Photograph of drill-core sample from the red basal unit of a flow bed in the lower formation. b) with dispersed, dark grey, angular pumice without flattening. Photograph of a drill-core sample from the grey upper unit of a pyroclastic flow bed in the lower formation.

The poor sorting, the content of numerous pumice lapilli, the red colour of the pumice, and the existence of flattened pumice in the basal units thus indicate that this type of deposits in the Dannemora area originally formed as pyroclastic flows. The grey upper units with grey, angular pumice without flattening suggest emplacement of more chilled material at the top of the flows. The intense red coloration and flattening of the pumice in the basal units, the absence of normal grading in the flow beds, and their lack of interbedding with turbidites suggest that the emplacement of these deposits was subaerial.

2) The subaqueous pyroclastic flow deposits (pumice and ash flow deposits or ignimbrites) occur within all three depositional sequences in the lower formation (Plate 2) and in the basal unit of the upper formation (Plate 2, the deposits are included in the signature for pyroclastic flow, fall and redeposited pyroclastic deposits). Besides that, a single bed of a subaqueous, pyroclastic flow deposit has been observed in the upper formation in the ESE limb of the syncline (see below under "Pyroclastic breccia",

Fig. 4). Disregarding this single bed the subaqueous pyroclastic flow deposits are to be found in groups of several flow beds, with bed thicknesses of 1–15 m. The subaqueous flow deposits are mostly very similar to the sub-aerial pyroclastic flow deposits but they are more greyish, although they locally contain red flattened pumice clasts. Sometimes, as in the basal unit of the upper formation, the subaqueous pyroclastic flows are more fine-grained and lack pumice (ash flow deposits). They consist of abundant bubble-wall shards and 1–7 mm large, often corroded, blue phenocrysts of quartz (Fig. 8). Zones of non-flattened bubble-wall shards (Figs. 9–10) and flattened bubble-wall shards (Fig. 11) alternate in this type of pyroclastic flow deposit.

The subaqueous pyroclastic flow deposits are also characterized by a faint normal grading and a high content of yellow-green, epidote-rich, lithoclasts (Fig. 12) associated with a conspicuous epidotization. Some of the flow beds in the basal unit of the upper formation also contain lithoclasts of iron ore. The subaqueous pyroclastic

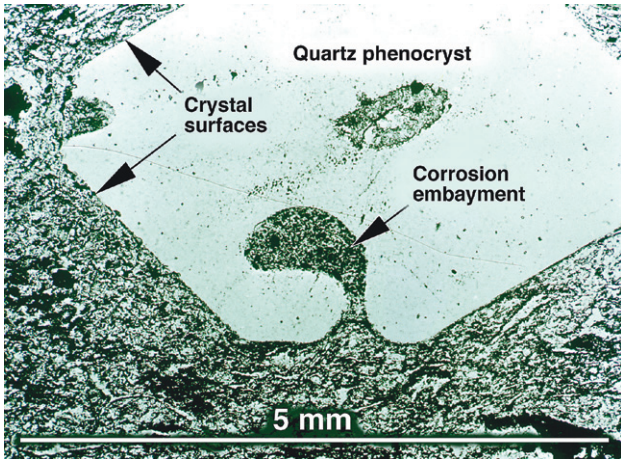


Fig. 8. A quartz phenocryst in a pyroclastic flow deposit (ash flow deposit) with non-flattened bubble-wall shards. Photomicrograph of a specimen from the basal unit of the upper formation. Plane polarized light.

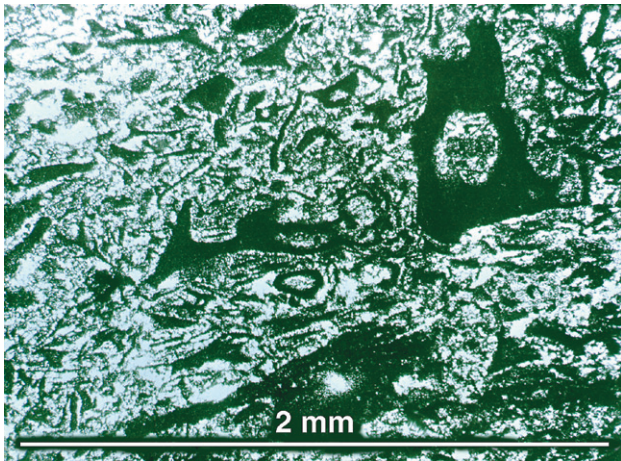


Fig. 9. A part of a pyroclastic flow deposit (ash flow deposit) with non-flattened bubble-wall shards. Dark is fine-grained shards of feldspar. Transparent is cement of quartz. Photomicrograph of a specimen etched with hydrofluoric acid, from the basal unit of the upper formation. Plane polarized light.

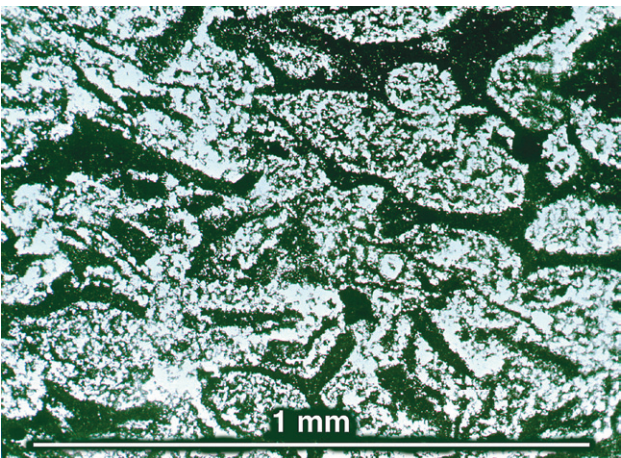


Fig. 10. A part of a pyroclastic flow deposit (ash flow deposit) with non-flattened bubble-wall shards. Dark is fine-grained shards of feldspar. Transparent is cement of quartz. Photomicrograph of a specimen etched with hydrofluoric acid, from the basal unit of the upper formation. Plane polarized light.

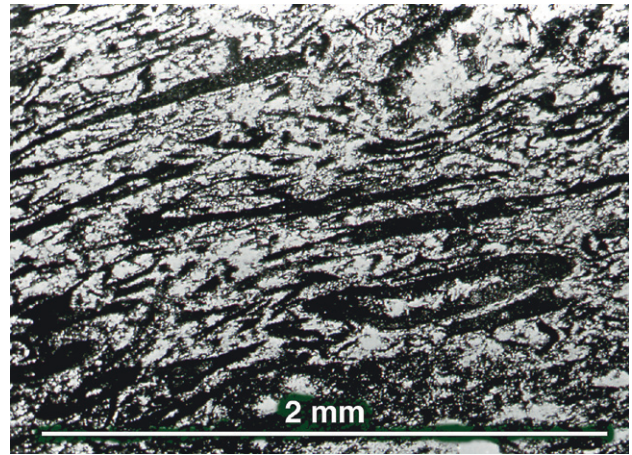


Fig. 11. A part of a pyroclastic flow deposit (ash flow deposit) with flattened bubble-wall shards. Dark is fine-grained shards of feldspar. Transparent is cement of quartz. Photomicrograph of a specimen etched with hydrofluoric acid, from the basal unit of the upper formation. Plane polarized light.



Fig. 12. A part of a pyroclastic flow deposit with greenish-yellow, epidote-altered, lithic fragments. Photograph of a drill-core sample from the lower formation.

flow deposits are often interbedded with normally graded, greyish-brown, volcanoclastic turbidites.

The similarity of these deposits to the subaerial pyroclastic flow deposits in Dannemora suggests that also they are pyroclastic flow deposits. Welding is also possible in subaqueous environments (Howells et al. 1991), but is much less common than in subaerial environments (Cas and Wright 1991). The faint normal grading in the subaqueous pyroclastic flow deposits and their interbedding with volcanoclastic turbidites indicate that the emplacement of these deposits was subaqueous.

The pyroclastic breccia deposit

A pyroclastic breccia deposit occurs in a funnel-shaped structure in the ESE limb of the Dannemora syncline, within the upper unit of the upper formation (Fig. 4, the shape is not apparent at the 350 m level). The structure locally cuts the surrounding rocks. Upwards, the funnel-shaped breccia gradually changes to a laterally extended, 50 m thick bed of a subaqueous pyroclastic deposit of the same type as described above. The funnel-shaped structure is composed of a massive, light-red breccia with 1–10 cm large angular lithic fragments of pink volcanoclastic rocks, dark dolomitic limestone, and locally magnetite (Fig. 13a). It also contains abundant 2–6 mm large quartz phenocrysts. It is hydrothermally altered to varying degrees and is also partially hydrothermally brecciated (Fig. 13b).

The shape and the composition suggest that this deposit was formed as a pyroclastic breccia, deposited and hydrothermally altered within a volcanic explosion vent. The breccia deposit has a somewhat lower SiO₂ content than the pyroclastic flow and fall deposits, which may be due to the presence of limestone xenoliths in the pyroclastic breccia, but possibly also to the hydrothermal alterations.

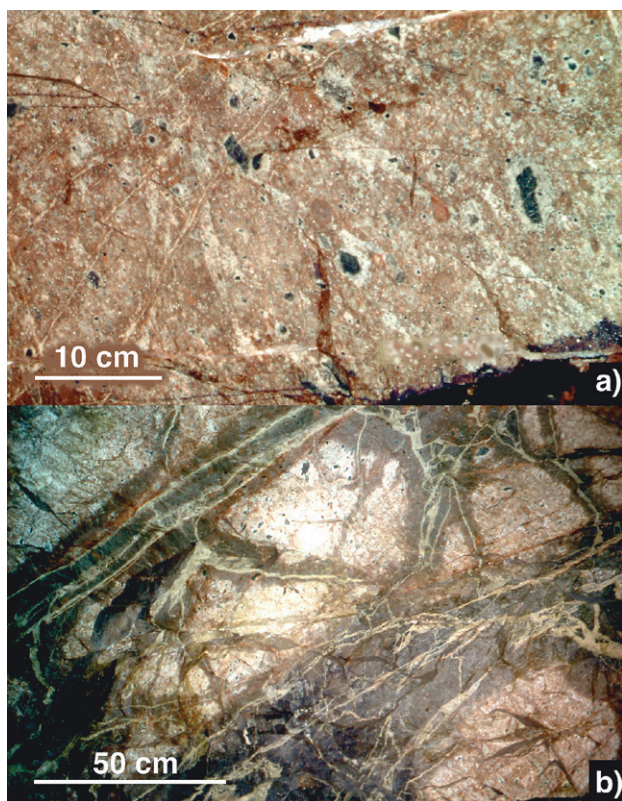


Fig. 13. a) A part of a pyroclastic breccia deposit with light red fragments of volcanoclastic rocks and dark of dolomitic limestone. b) A part of a brecciated pyroclastic breccia deposit with the same fragments as in figure a). Photographs of drift walls in the mine from the upper unit of the upper formation.

The pyroclastic fall deposits

Two types of pyroclastic fall deposits have been recorded in the Dannemora syncline: 1) subaerially emplaced and 2) water-settled pyroclastic fall deposits. The chemical compositions of the pyroclastic fall deposits are reported in Table 1.

1) Subaerially emplaced pyroclastic fall deposits (facies A in Plate 4) have been recorded in both the lower and upper formation. In the lower formation (Fig. 4 and Plate 2) they occur in the depositional sequences 1 and 2. There they are found in up to one hundred metres thick units, which can be divided into diffuse, 1–2 m thick beds or in more distinct cm-thick layers. There are no signs of interlayering of pyroclastic flow deposits, volcanoclastic turbidites or tempestites. The subaerially emplaced pyroclastic fall deposits in the lower formation are grey, fine-grained and rather well sorted, but they may locally contain dispersed black, 2–40 mm large, cusped-shaped pumice and white, silicified, lithic clasts. Some beds are also characterized by a high content of 1–5 mm large white quartz phenocrysts. The phenocrysts and clasts locally define a diffuse normal grading. Silicification and sericitization appear to be common in many beds but bubble-wall shards have nevertheless been observed within many of them.

In the upper formation, the subaerially emplaced pyroclastic fall deposits occur in the upper unit in e.g. the depositional sequence 8 (Plate 3). They may be found as solitary or repeated beds, from 0.1 metre up to several metres in thickness. There are no signs of interlayering of volcanoclastic turbidites or tempestites. The subaerially emplaced pyroclastic fall deposits in the upper formation vary in grain size between clay, silt and sand and they are rather well sorted. They are brown to brownish black and consist mainly of illite with diffuse bubble-wall shards. They may also contain 1–4 mm large, commonly idiomorphic quartz phenocrysts and up to dm-sized lithic clasts, which, in some cases have caused evident bomb-sag structures. Also, many beds are characterized by non-graded accretionary lapilli (Figs. 14a, b) of which some have a light-coloured core of ash material (cored lapilli) (Fig. 14a), while others are composed of multiple concentric shells. The lapilli are broken in places (Fig. 14b).

Relatively good sorting and varying amounts of internal stratification or lamination in pyroclastic material are typical for pyroclastic fall deposits (e.g. Cas & Wright 1987). The subaerially emplaced pyroclastic fall deposits in the lower formation consist of bubble-wall shards, cusped-shaped pumice, lithic clasts, and quartz phenocrysts. They are rather well sorted and more or less stratified, which suggests that they are pyroclastic fall deposits. The lack of interlayering of volcanoclastic turbidites or tempestites indicates that they were subaerially emplaced.

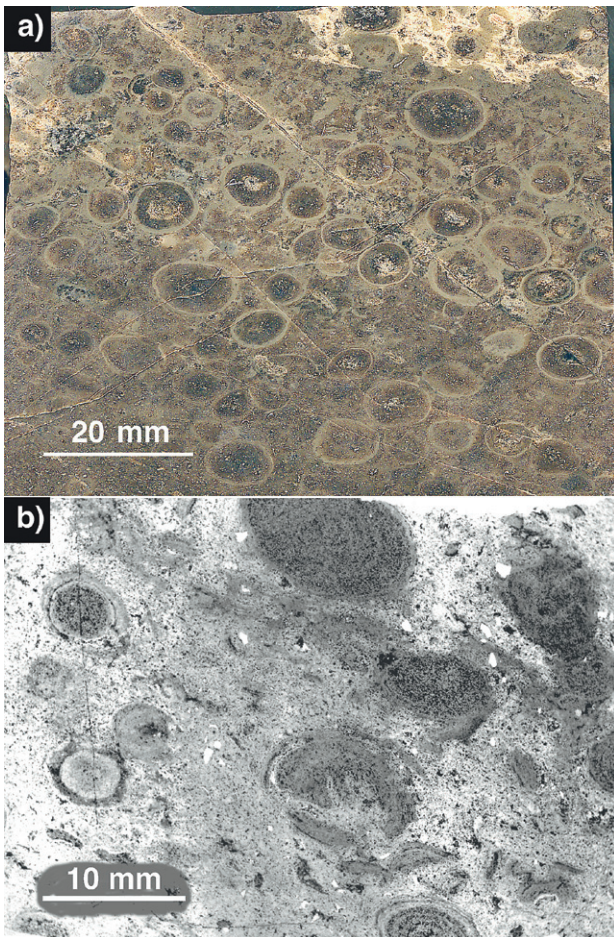


Fig. 14. a) A part of a brown, illitic, subaerially deposited, pyroclastic fall deposit with accretionary lapilli. Note that several of the lapilli have a light core (cored lapilli). Photograph of a rock sample from upper unit of the upper formation (sequence 8 in Plate 3). b) A part of a subaerially deposited pyroclastic fall, with accretionary lapilli and small quartz phenocrysts (white). Note the lapilli with several concentric shells at the bottom of the photo. Microphotograph of a specimen from the upper unit of the upper formation (sequence 8 in Plate 3). Plane polarized light.

During Plinian eruptions, large volumes of pumice are ejected and extensive pumice-fall deposits are produced. Near-vent deposits can be very coarse whereas they away from the vent deposits become fine-grained (Cas & Wright 1987). The subaerially emplaced pyroclastic fall deposits in the lower formation are found in up to one hundred metres thick units, demonstrating the very large volumes of ejected material, which implies an origin from explosive eruptions of Plinian type. Several eruptions must have contributed to the deposition as the units are too thick to have been deposited from one single eruption. The subaerially emplaced pyroclastic fall deposits in the lower formation are fine-grained and rather thinly bedded, which indicates that their deposition was distal.

The subaerially emplaced pyroclastic fall deposits in the upper formation consist of illite-altered bubble-wall shards, quartz phenocrysts, and locally accretionary lapilli

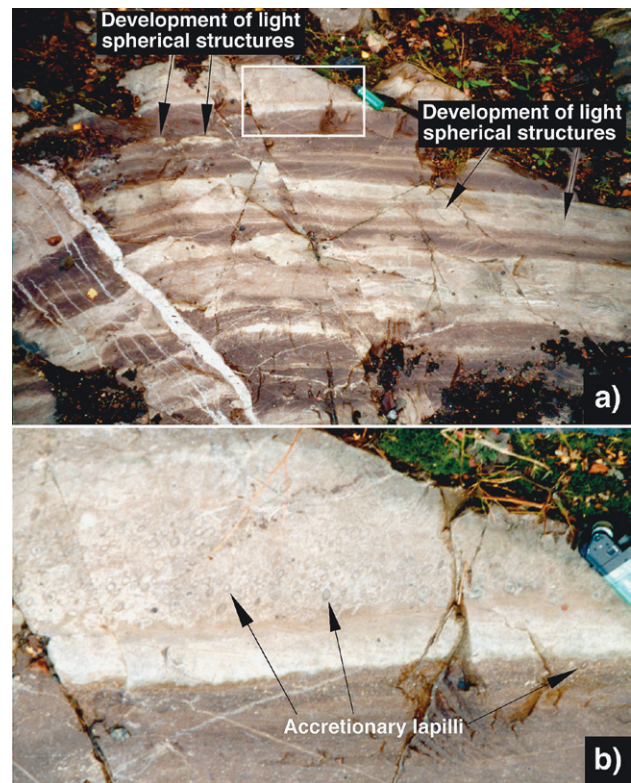


Fig. 15. a) Brown, illitic, water-settled, pyroclastic fall deposits interbedded with epidote-zoisite-cemented, volcanoclastic turbidites or tempestites (light beds). Evidence of development of light spherical structures can also be observed in figure. b) Weakly deformed accretionary lapilli occur both in the brown beds of pyroclastic fall deposits and in light, normal graded turbidites. Photographs of an outcrop in the basal unit of the upper formation. Outlined area in a) is enlarged in b).

and up to dm-sized lithic clasts. Accretionary lapilli are common in a wide variety of primary pyroclastic deposits, such as pyroclastic, surge, and fall deposits (McPhie et al. 1993). The subaerially emplaced pyroclastic fall deposits in the upper formation are rather well sorted and more or less stratified, which suggests that they are pyroclastic fall deposits. The content of up to dm-sized lithic clasts indicates a near-vent deposition. The lack of interlayered volcanoclastic turbidites or tempestites suggests subaerial emplacement.

2) The water-settled pyroclastic fall deposits have only been recorded in the upper formation (Fig. 4 and Plate 3). They may occur in the lower formation as well, but it has not been possible to distinguish them from volcanoclastic turbidites or tempestites. In the basal unit (Plates 1 and 3) of the upper formation they are found between pyroclastic flow deposits and redeposited pyroclastic deposits (Fig. 15, between volcanoclastic turbidites or tempestites), whereas in the upper unit they are interbedded with volcanoclastic turbidites or tempestites and limestones (Fig. 16). They may occur as solitary or repeated beds, from 1 to 5 dm thick. Oscillatory ripple marks are ob-

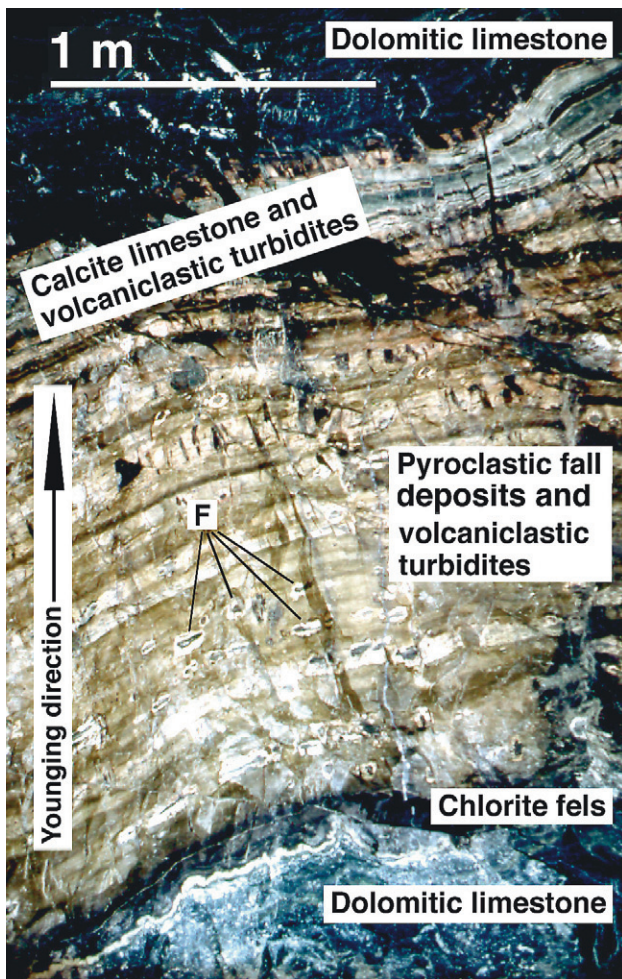


Fig. 16. Brown, illitic, water-settled pyroclastic fall deposits interbedded with volcanoclastic turbidites or tempestites (light beds) overlie chlorite fels and nodule bedded, dolomitic limestone. The uppermost part of the sequence is composed of calcite limestone (light grey beds) interbedded with volcanoclastic turbidites or tempestites (dark beds) and dolomitic limestone. Note the dark, lithic fragments with a pale grey, altered, outer rim (F) in the pyroclastic fall deposits and the contorted, white bed in the lower nodule bedded, dolomitic limestone (pseudomorph after a "chicken wire" anhydrite bed?). Photograph of a drift roof in the mine in the upper unit of the upper formation.

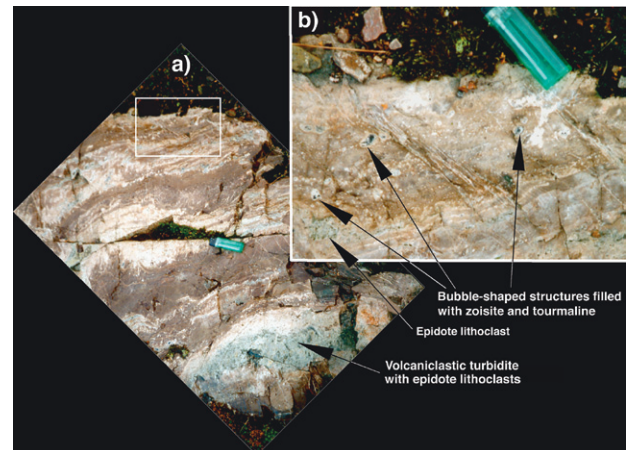


Fig. 18. Brown, illitic, water-settled pyroclastic fall deposits interbedded with epidote-zoisite-cemented, volcanoclastic turbidites or tempestites (light beds). Outlined area in a) is enlarged in b). a) A turbidite or tempestite bed with a large number of epidote lithoclasts can be seen at the bottom of figure. b) Epidote lithoclasts can also be found in the lowermost parts of the brown pyroclastic fall deposits. Some of the brown beds of pyroclastic falls contain bubble-shaped, light-coloured, 5–10 mm large structures filled with zoisite and tourmaline. Photographs of an outcrop in the basal unit of the upper formation.

served in some beds. Their grain size varies between clay, silt and sand. They may be graded with accumulations of crystals of quartz or feldspar and/or heavy fragments at the base and less dense or platy clasts in the upper parts (Fig. 17). The water-settled pyroclastic fall deposits are brown to brownish black in colour. They consist mainly of illite but may also contain 1–4 mm large, in many cases idiomorphic quartz phenocrysts and up to dm-sized fragments, commonly composed of epidotized volcanoclastic rocks (Figs. 16 and 18). Also the water-settled pyroclastic fall deposits may contain accretionary lapilli and are then overlain by volcanoclastic turbidites (Fig. 15). The water-settled pyroclastic fall deposits can also be rich in bubble-shaped, often light-coloured, 5 to 10 mm large structures, which are filled with zoisite, tourmaline, and axinite (Figs. 18 and 19). The two latter minerals explain a remarkably high boron content in this type of volcanoclastic deposit, up to c. 100 ppm. The water-settled pyroclastic fall deposits may also contain abundant conspicuous light-coloured, zoisite-rich, spherical, 1 dm large structures (Figs. 20a and b). Water-settled, pyroclastic fall deposits are not included as a facies in the suggested, hypothetical depositional sequence (Plate 4). In cases where a depositional sequence of the 2nd order (see "Depositional sequences" above) is terminated by a water-settled, pyroclastic fall deposit, it is characterized by interlay-

Fig. 17. A brown, illitic, water-settled, pyroclastic fall deposit with heavy crystals and fragments at the bottom and platy ash shards at the top. A layer of volcanoclastic turbidite or tempestite is situated above the pyroclastic fall deposit. Photograph of an outcrop in the basal unit of the upper formation.



Fig. 19. A part of a brown, illitic, water-settled pyroclastic fall deposit containing bubble-shaped, light-coloured, 5–10 mm large structures filled with zoisite, axinite and tourmaline. Photograph of a rock sample from the upper unit of the upper formation.

ering of volcanoclastic turbidites or tempestites with light-coloured, spherical structures.

The water-settled pyroclastic fall deposits resemble the subaerially emplaced deposits with respect to composition and stratification, which suggests that also they are fall deposits. They also contain accretionary lapilli, which is not contradictory to a subaqueous emplacement as accretionary lapilli may be deposited, redeposited or reworked even in subaqueous settings (McPhie et al. 1993). The water-settled deposits are interbedded with volcanoclastic turbidites or tempestites, which indicates a subaqueous emplacement. Besides, they may be graded with accumulations of crystals of quartz or feldspar and/or heavy fragments at the base and less dense or platy clasts in the upper parts. This may be evidence of water-settling of the material (McPhie et al. 1993). Some of the water-settled pyroclastic fall beds contain oscillatory ripple marks, which points to an emplacement above the storm-wave base. The bubble-shaped, light-coloured, 5 to 10 mm large structures in the water-settled pyroclastic fall deposits are interpreted as infilled gas cavities, and the abundant light-coloured, zoisite-rich, spherical, 1 dm large structures are

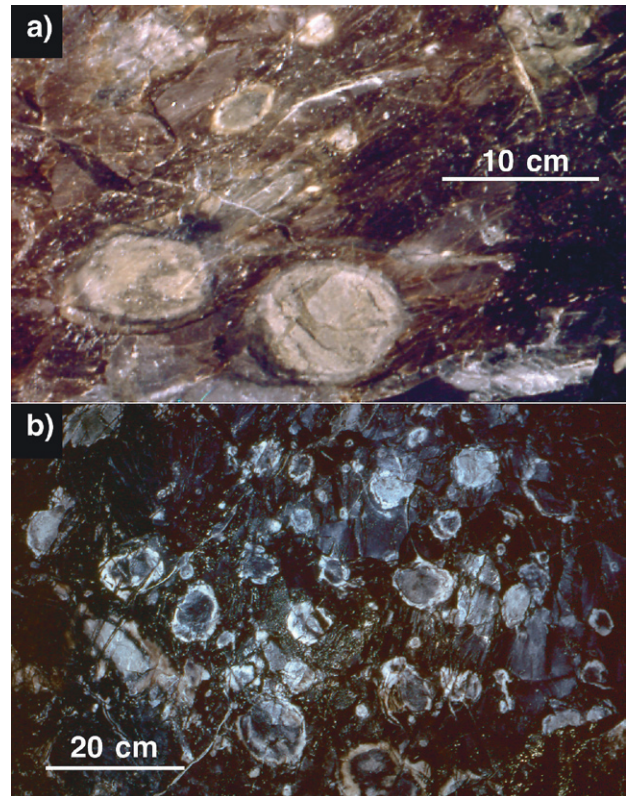


Fig. 20. a) A part of a brown, illitic, water-settled pyroclastic fall deposit containing some light-coloured, spherical, 1 dm large structures. Photograph of a drift wall in the mine in the upper unit of the upper formation. b) A part of a brownish-black, illitic, water-settled pyroclastic fall deposit containing a large number of light-coloured, spherical, 1 dm large structures. Photograph of a drift wall in the mine in the upper unit of the upper formation.

suggested to have formed as concretions during diagenetic remobilization of material in carbonate-cemented volcanoclastic turbidites or tempestites (Fig. 15).

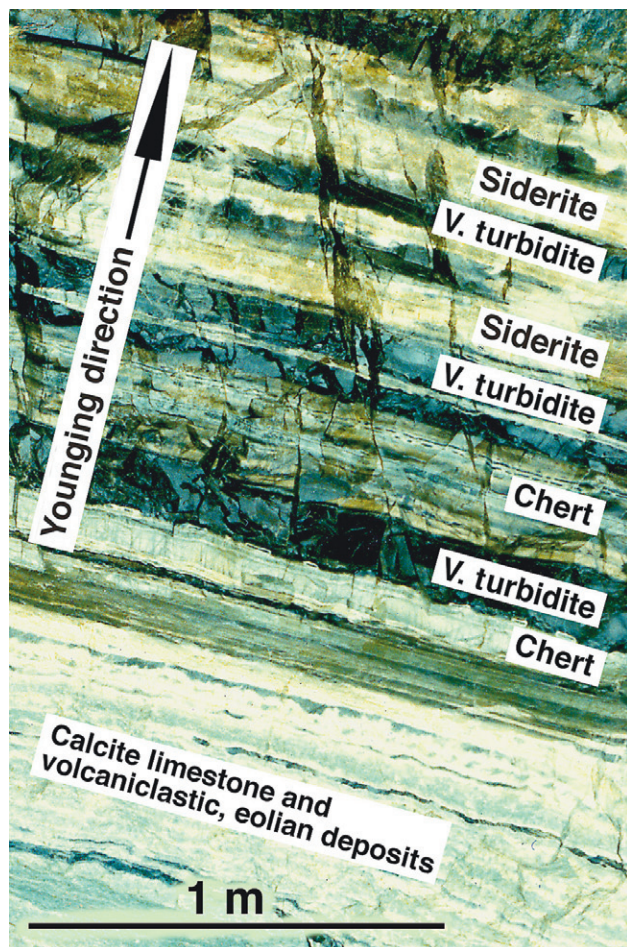
In the basal unit (Plates 1 and 3) of the upper formation, the water-settled pyroclastic fall deposits are interbedded with pyroclastic flows. This suggests that they were formed from ash clouds that accompanied pyroclastic flows (Cas & Wright 1987; McPhie et al. 1993). In the upper unit of the upper formation there is no stratigraphic relationship between pyroclastic fall and flow deposits. Nevertheless, pyroclastic flow deposits are demonstrated in connection with the pyroclastic breccia. Ash clouds and accompanying pyroclastic flows may have been deposited in different areas. In that case, both the water-settled and subaerially emplaced pyroclastic fall deposits in the upper unit of the upper formation have been formed from ash clouds that accompanied pyroclastic flows.

Redeposited pyroclastic deposits

Five main types of redeposited pyroclastic deposits have been distinguished in the Dannemora syncline: 1) volcanoclastic eolian deposits, 2) volcanoclastic beach and

shoreface deposits, 3) volcanoclastic tidal flat deposits, 4) volcanoclastic tidal channel deposits, and 5) volcanoclastic turbidites. The chemical compositions of the redeposited pyroclastic rocks are found in Table 1. Coarse, redeposited pyroclastic deposits have a composition, which resembles that of the pyroclastic flow and fall deposits. However, it does show a higher iron content compared to the pyroclastic flow and fall deposits, which is due to the presence of magnetite clasts. It also displays an unusually high barium content, which reflects a high baryte content. The fine-grained, redeposited pyroclastic deposits have both a lower SiO₂ content and a higher Al₂O₃, TiO₂ and CaO content. The lower SiO₂ content and the higher Al₂O₃ and TiO₂ content indicate strong leaching of SiO₂ and hence a concentration of Al₂O₃ and TiO₂. The higher calcium content depends on the fact that the material in the fine-grained, pyroclastic deposit is mixed with calcite and zoisite.

1) Volcanoclastic eolian deposits (parts of facies K in Plate 4) have only been observed in the upper unit of the upper formation and then only as solitary, 1–3 cm thick beds overlying calcite limestone with pseudomorphs after gypsum mush (see "Calcite limestone with pseudomorphs after gypsum mush" below). Apart from the lack of mag-



nesium alterations, they are equivalent to the chlorite fels beds in the dolomitic limestones with pseudomorphs after gypsum mush. They have a grain size between silt and clay as well as characteristically uneven bases and planar tops (Fig. 21, in the lower part of the photograph). They are brown and consist mainly of illite.

The composition of the volcanoclastic eolian deposits in the upper formation is similar to that in the fine-grained, illitic pyroclastic fall deposits, which suggests that the material of the eolian deposits primarily was volcanic. No textural or structural evidence that could tell whether these deposits are eolian or pyroclastic fall deposits has been found. The volcanoclastic eolian beds are interpreted as such as they always overlie calcite limestone with pseudomorphs after gypsum mush. Gypsum mush forms in the transitional zone between intertidal and supratidal conditions (e.g. Shinn 1983), which indicates that volcanoclastic eolian deposits in the upper formation are deposited in a zone, where also eolian sedimentation is common (e.g. Reading 1986).

2) The volcanoclastic beach and shoreface deposits (facies M and P in Plate 4) have only been recorded in the upper unit of the upper formation in the depositional sequences 1–3, 7–9, 11, and 13 (Plate 3). They show a cyclic alternation of layering with an initial transgressive phase of volcanoclastic beach and shoreface deposits (facies M) and a final depositional phase with 1 to 3 metres thick beds of prograding volcanoclastic beach and shoreface (facies P) and tidal flat deposits (depositional sequences of the 3rd order). The transgressive beach deposits are often planar bedded with alternating pebbly and sandy beds. The shoreface deposits are cross-bedded and consist of sandy beds. The volcanoclastic beach and shoreface deposits are rather well sorted. They are brown, grey, black, or pale red in colour. The pebbly beds normally contain somewhat worn fragments of grey, pink, or white silicified, volcanoclastic rocks, accretionary lapilli, brown illitic pyroclastic fall deposits, dark chlorite fels, dolomitic limestone, and iron ore (Figs. 22–24). The sandy units contain abundant winnowed quartz phenocrysts and are classified as quartzites (Figs. 22–25).

The content of clasts of silicified, volcanoclastic rocks, accretionary lapilli, brown illitic pyroclastic fall deposits, and winnowed quartz phenocrysts indicates that most of the material of the volcanoclastic beach and shoreface deposits was primarily volcanic. The initial transgressive

Fig. 21. Brownish-black, volcanoclastic turbidites (V. turbidite) interbedded with chert and siderite on top of calcite limestone interbedded with rocks interpreted as volcanoclastic eolian deposits. Note the uneven base and the planar top surface of some beds in the calcite limestone interbedded with volcanoclastic, eolian deposits (see text for explanation). Photograph of a drift roof in the mine in the upper unit of the upper formation.



Fig. 22. A part of a volcaniclastic beach deposit with grey and white altered, rounded, redeposited, pyroclastic fragments and brownish-black, partly broken, redeposited accretionary lapilli. Photograph of a rock sample from the upper unit of the upper formation.

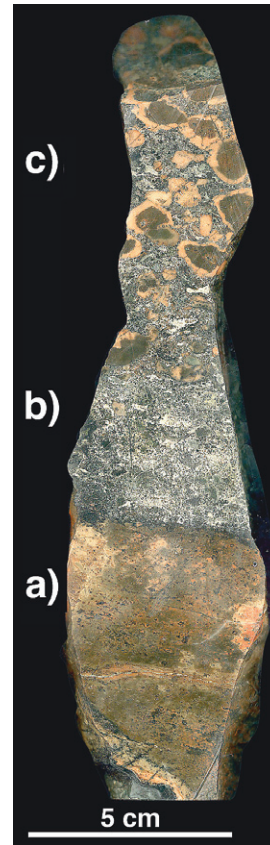


Fig. 24. Redeposited pyroclastic rocks (b and c) overlie brown, illitic, pyroclastic fall deposits (a): a) fine-grained, brown, illitic, pyroclastic fall deposit. b) a beach deposit with clastic, winnowed quartz phenocrysts (volcanic quartzite). c) a beach deposit with rounded fragments of brown, illitic, pyroclastic fall deposits (volcanic conglomerate). Photograph of a rock sample from the upper unit of the upper formation.

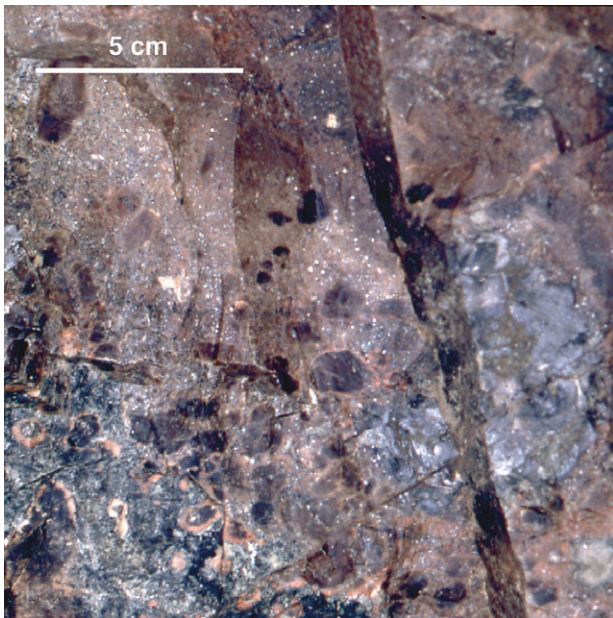


Fig. 23. A part of a volcaniclastic beach deposit with clastic, winnowed quartz phenocrysts (white spots, volcanic quartzite) in the upper part of the photo and rounded fragments of brown, illitic, pyroclastic fall deposit (volcanic conglomerate) in the middle and lower part. Photograph of a drift wall in the mine in the upper unit of the upper formation.



Fig. 25. A part of a volcaniclastic beach deposit with clastic, winnowed quartz phenocrysts (white and grey spots). Photograph of a rock sample in the upper unit of the upper formation.

phase with planar bedded pebbly and sandy beds followed by cross-bedded sandy beds suggests a transgressive deposition of beach and shoreface deposits (e.g. McCubbin 1982). The final phase with prograding volcanoclastic beach and tidal flat deposits supports this. It is possible that the deposits are too poorly sorted to be interpreted as beach and shoreface deposits (Figs. 22–25) and that a rapid volcano-induced subsidence better could explain the unusually poor sorting.

3) Volcanoclastic tidal flat deposits (facies O in Plate 4) have only been observed in the upper unit of the upper formation (in the depositional sequences 8 and 9, Plate 3; facies O in Plate 4). They occur in 1–2 m thick units made up of 1–5 cm thick beds, with sandy bases and clayey tops, which together may show wavy, lenticular and flaser bedding, locally with bipolar cross-lamination. The sandy bases are dominated by winnowed quartz phenocrysts.

The content of winnowed quartz phenocrysts and silicified bubble-wall shards suggests that most of the material of the volcanoclastic tidal flat deposits was primarily volcanic. The composition of the beds (sandy bases and clayey tops), the wavy, lenticular and flaser bedding, and the bipolar cross-lamination indicate that the volcanoclastic tidal flat deposits in the upper unit of the upper formation really are tidal flat deposits (Weimer 1982).

4) Volcanoclastic tidal channel deposits (parts of facies N in Plate 4) have only been observed in the upper unit of the upper formation together with volcanoclastic tidal flat deposits (in the depositional sequences 8 and 11, Plate 3) They occur as 0.2–1.5 m thick units with lensoidal shape. The units are sandy and consist mostly of winnowed quartz phenocrysts. They are cross-bedded with clayey foresets.

Due to the content of winnowed quartz phenocrysts it seems that most of the material of the volcanoclastic tidal channel was primarily volcanic. The lensoidal shape of the volcanoclastic tidal channel deposits indicates that they are such. Their occurrence together with volcanoclastic tidal flat deposits and their composition of sandy, cross-bedded material with clayey foresets, imply that they are tidal (Clifton 1982, Weimer et al. 1982).

5) Volcanoclastic turbidites or tempestites (parts of facies L in Plate 4) are found in the lower as well as the upper formation. In the lower formation, and locally in the upper, they appear as millimetre to metre thick beds on top of each other (Fig. 26). In the upper formation they

may also be found as isolated beds in limestone and interlaminated or interbedded with pyroclastic fall deposits (Figs. 15–18), chert (Fig. 21), siderite (Fig. 21) or calcite limestone (Fig. 16, upper part and Fig. 27). Jaspilite can also be found in the uppermost parts of the beds (Fig. 28). Silicified bubble-wall shards have been observed in the jaspilite in several cases. The volcanoclastic turbidites or tempestites have a grain size, which alternates between clay, sand, and granule in both formations. They are normally graded. In a few cases ripples have been observed at the top of respective beds. The volcanoclastic turbidites are brown, grey, light grey or light red. They may contain clasts of chert and epidote-altered, volcanoclastic rocks (Figs 17 and 18a), as well as winnowed quartz phenocrysts. In the upper formation they also contain clasts of illitic, pyroclastic fall deposits and chlorite fels and in some cases accretionary lapilli (Fig. 15).

The presence of clasts of epidote-altered, volcanoclastic rocks and brown illitic pyroclastic fall deposits, accretionary lapilli, and winnowed quartz phenocrysts indicate that most of the material of the volcanoclastic turbidites was primarily volcanic. The normal grading in the volcani-



Fig. 26. In the lower part of the Figure, several brown, volcaniclastic turbidites can be seen. In the upper part of the figure, brown, volcaniclastic turbidites interbedded with zoisite-altered volcaniclastic turbidites (white) and limestone (dark) are visible. Photograph of a rock sample from the upper unit of the upper formation.



Fig. 27. Volcaniclastic turbidites interbedded with calcite limestone. Volcaniclastic turbidites are brown, zoizite-altered volcaniclastic turbidites are light red, calcite limestone is grey. Note the crenulation cleavage on top surface (left). Photographs of a rock sample from the upper unit of the upper formation. Left half of photo – from above. Right half of photo – from the right.

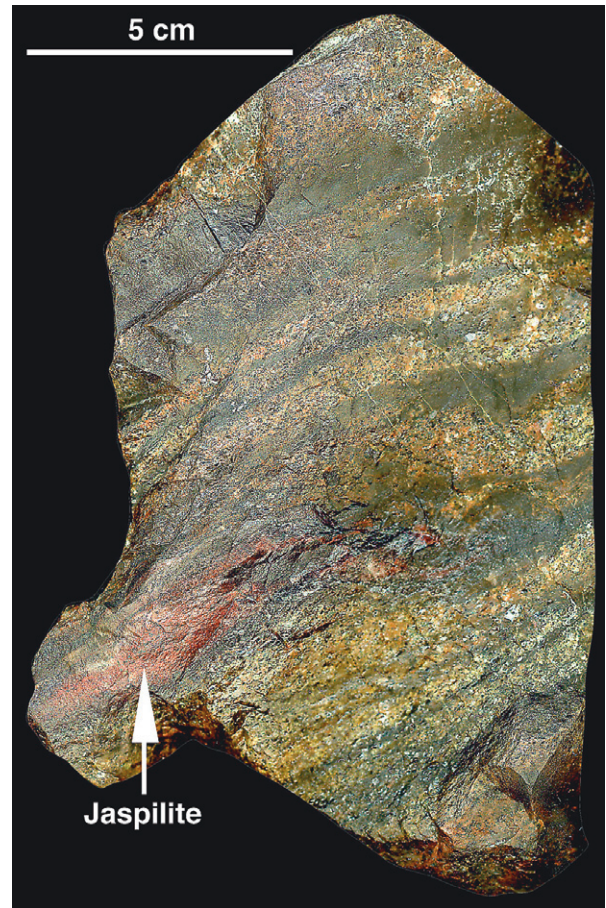


Fig. 28. A part of a volcaniclastic turbidite or tempestite deposit with sandy and clayey beds and jaspilite. Photograph of a rock sample in the upper unit of the upper formation.

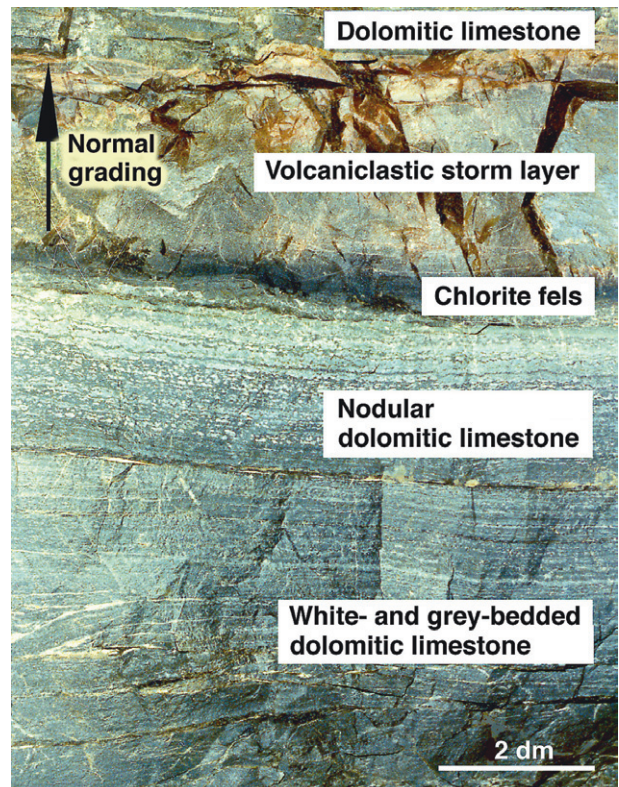


Fig. 29. A volcaniclastic, normal graded storm layer on the top of chlorite fels, and nodular and white- and grey-bedded, dolomitic limestone. The storm layer contains a large number of winnowed quartz phenocrysts. Photograph of the roof in the mine in the upper unit of the upper formation

clastic turbidites suggests that they are turbidites or tempestites (storm layers). However, most volcanoclastic tempestites that occur in the Dannemora syncline are called volcanoclastic turbidites as there have been difficulties to discern wave ripples, hummocky cross-stratification and other distinguishing features of tempestites. In a few cases, tempestites have been distinguished on the basis of their position in the stratigraphy. For example, a bed in the inter- and supratidal part of the upper formation has been interpreted as a volcanoclastic storm layer (a tempestite bed, Fig. 29) created by a storm flood after a rapid subsidence. The occurrence of chert and siderite intercalated with this type of redeposited volcanoclastic rock is not well understood and should be further studied.

Carbonate rocks

Carbonate rocks are only found in the upper unit of the upper formation (Fig. 4 and Plate 1c). Two different varieties of carbonate rocks have been distinguished: calcite limestones and dolomitic limestones. The latter are much more frequent. The chemical composition of the two types is presented in Table 1. The calcite limestones are always light-coloured (white, light grey or light red), calcium-rich and contain only small amounts of Mg, Fe and Mn. The dolomitic limestones are normally much darker (dark grey or black), magnesium-rich and have an iron content of between 5 and 30 % (30 % Fe is the limit

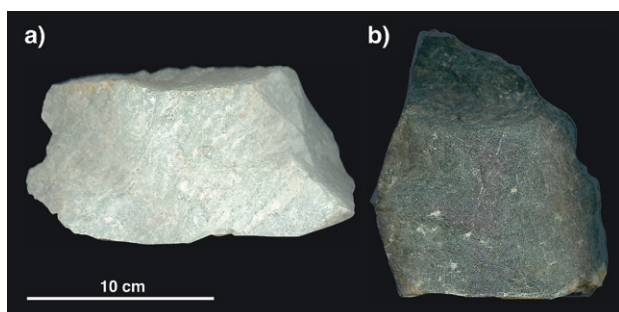


Fig. 30. Limestones: a) Light, calcite limestone. b) Dark grey, dolomitic limestone. Photographs of rock samples from the upper unit of the upper formation.

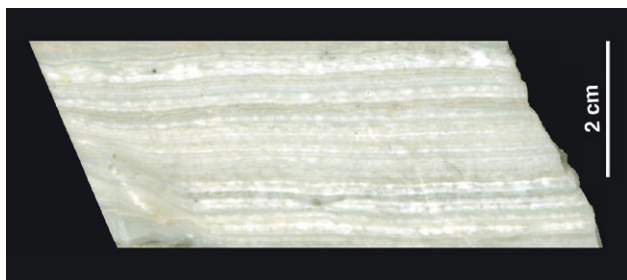


Fig. 31. Nodular calcite limestone intercalated with calcite limestone with signs of algal mats (tufted laminae and fenestral porosity, not visible in the figure). Photograph of a rock sample from the upper unit of the upper formation.

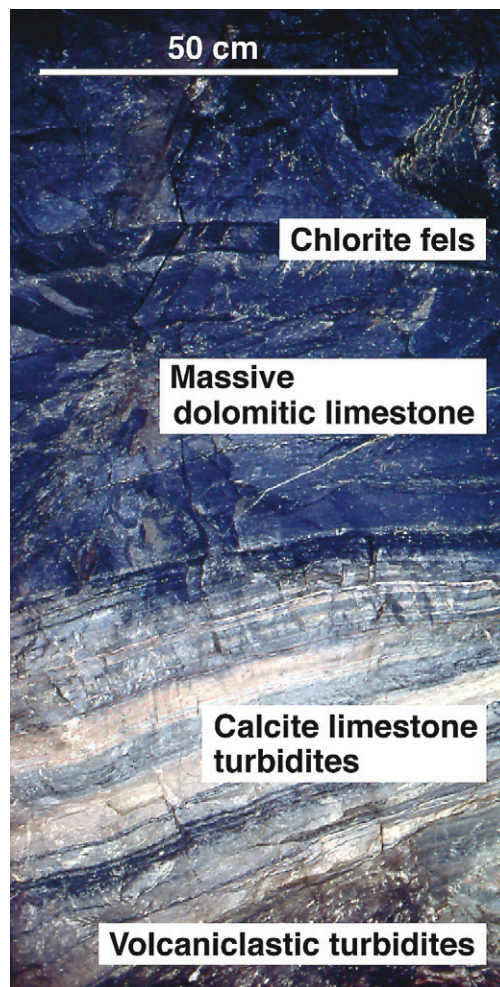


Fig. 32. A sequence with volcanoclastic turbidites at the base, followed upwards by calcite limestone turbidites and massive dolomitic limestone. In the massive dolomitic limestone a chlorite fels bed occurs. Photograph of a drift roof in the mine in the upper unit of the upper formation.

between iron ore and Fe-bearing dolomitic limestone on the mine maps) and a manganese content between 0.5 and 1.5 % (Figs. 30–32). The dark colour of the dolomitic limestones is due to the presence of fine-grained magnetite, graphite, and subordinate chlorite. No systematic investigation of the distribution of these minerals has been done, even though this could shed light on variations of the redox conditions in the palaeo-environment.

The calcite limestones

Calcite limestones occur in metre to several metres thick units. They are either composed of laminae or beds deposited on top of each other (Figs. 31 and 32) or intercalated with other deposits, e.g. volcanoclastic turbidites, dolomitic limestone or siderite (Figs. 21 lower part, 28, 33, and 34). Calcite limestones, with or without interlaminae of other rocks, commonly occur on top of redeposited pyroclastic units and are overlain in turn by dolomitic limestones (Fig. 32). In special cases (as in sequence 11 in the



Fig. 33. Calcite limestone (light grey) interbedded with dolomitic limestone (black), volcanoclastic, eolian deposits (brown) and zoisite-altered volcanoclastic, eolian deposits (white). Note the uneven base and the planar top surface of some beds (see text for explanations). Photograph of a drift roof in the mine in the upper unit of the upper formation.

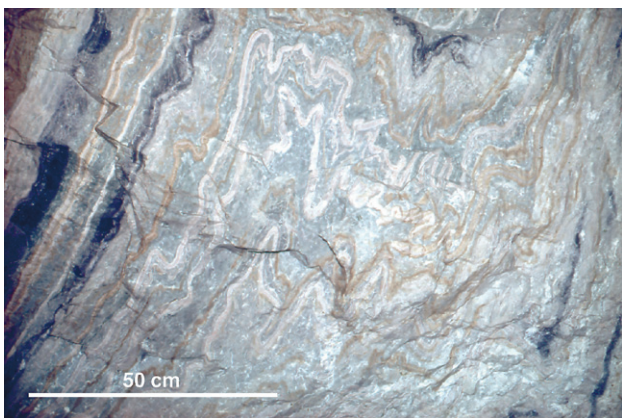


Fig. 34. Calcite limestone (grey) interbedded with dolomitic limestone (black), siderite (brown), and zoisite-altered redeposited pyroclastic rocks (white). The beds are folded. Photograph of a drift roof in the mine in the upper unit of the upper formation.

upper formation, Plate 3), interbedding between calcite and dolomitic limestones occur (Figs. 33 and 34). The calcite limestones are generally very finely crystalline and it is often possible to observe an original clast size, which varies between clay, silt, and sand. The calcite limestones can genetically be divided into four different facies: 1) calcite limestone turbidites, 2) nodular calcite limestones, 3) calcite limestones with pseudomorphs after gypsum mush, and 4) calcite limestones with signs of primary algal mats.

1) Calcite limestone turbidites (parts of facies L in Plate 4) are found in most of the depositional sequences 1–14 in Plate 3, on top of volcanoclastic turbidites. They are composed of 1 to 25 mm thick laminae or beds deposited on top of each other (Fig. 32) or intercalated with other types of calcite limestones or other types of deposits. They consist of clasts of calcite and usually have a normal grading between silt and clay. In cases where the limestone is interbedded with volcanoclastic turbidites (Fig. 28) it is partly composed of the limestone turbidites and partly of what is interpreted as beds of carbonate particles settled out of suspension.

The normal grading in the calcite limestone turbidites suggests that they are turbidites or tempestites (storm layers). However, most calcite limestone tempestites that occur in the Dannemora syncline are called calcite limestone turbidites as there have been difficulties to discern distinguishing features between the two types of deposits.

2) Nodular calcite limestones (facies K in Plate 4) have only been observed in the depositional sequences 10 and 11 (Plate 3). They are composed of 5 to 10 mm thick layers deposited on top of each other, consisting of laminae with white nodules alternating with laminae of calcite limestone with signs of primary algal mats (Fig. 31). The latter laminae are composed of crenulated, brownish, carbonate laminae with interlayered flat pores filled with clear, greyish-blue calcite, which is difficult to discern in Figure 31.

The shape of the nodules in the nodular calcite limestone laminae indicates that nodules primarily have formed by diagenetic transition of gypsum to anhydrite (Schreiber & Kinsman 1975; see also "Nodular dolomitic limestone" below). The crenulated carbonate laminae and the calcite-filled pores points to primarily tufted algal mats and fenestral porosity (see "Evidence of primary organic life" below).

3) The calcite limestones with pseudomorphs after gypsum mush (part of facies J in Plate 4) have been observed in depositional sequences 10, 11, and 13 (Plate 3). They are composed of 1–5 cm thick beds of light-coloured calcite limestone with planar bases and uneven, white, nodular tops intercalated with 1–4 cm thick beds of volcanoclastic, eolian deposits (see "Volcanoclastic eolian de-

posits" above) (Fig. 21, lower part, and Fig. 33). The calcite limestone beds consist of clasts of calcite. They usually have a grain size between silt and clay. The beds of volcanoclastic, eolian deposits have uneven bases and planar tops and are clay–silt-sized.

The shape of the nodules in the top of the limestone beds indicates that nodules primarily formed by diagenetic transitions of gypsum to anhydrite (Schreiber & Kinsman 1975). This in turn suggests that the nodules primarily formed from gypsum mush created on top of spring or storm tide beds of carbonate clasts, as gypsum mush forms in the transitional zone between intertidal and supratidal conditions (Butler 1965, Kendall & Skipwith 1969, Kinsman 1964). Volcanoclastic, eolian deposits covered the uneven surface of mush and may have protected the mush from dissolution. Spring or storm tide floods eroded the tops of the eolian sediments.

4) Calcite limestones with signs of primary algal mats (parts of facies J in Plate 4) have only been observed in depositional sequence 10 (Plate 3), but may also exist in other sequences. They are found in tidal sediments in 1–3 cm thick beds of cyclically repeated sequences of calcite limestone with pseudomorphs after gypsum mush and chert. The calcite limestones with signs of primary algal mats are characterized by the content of tufted laminae and fenestral porosity (see "Evidence of primary organic life" below).

The dolomitic limestone

The dolomitic limestones occur most often in one to several metres thick units, which are generally composed of a number of stacked beds with slightly different characteristics. On rare occasions, 5 to 10 cm thick beds of dolomitic limestone are found interlayered with the calcite limestone (Figs. 33 and 34). However, the most common occurrence is a sharp transition from calcite limestone to dolomitic limestone upwards in the sequence (Fig. 32). Locally, the dolomitic limestones are intercalated with chlorite fels (in the upper part of Fig. 35). The dolomitic limestones are normally very fine-grained but some units, such as carbonate layers occurring in the proximity to stromatolite-like structures, may be coarse-grained with a crystal size up to 5–10 mm. The texture in the dolomitic limestones is more diffuse than in the calcite limestones. Thus, clastic textures can rarely be discerned with the exception for accumulation of 1 to 20 cm large clasts of light-coloured carbonate in two dolomitic limestone beds (Fig. 36) along unconformity surfaces in the ESE limb. As this variety of limestone occurs along the unconformity surfaces and occurrences of pseudomorphs after evaporites are common in the Dannemora ore deposit (see below) it is interpreted as formed through dissolution of

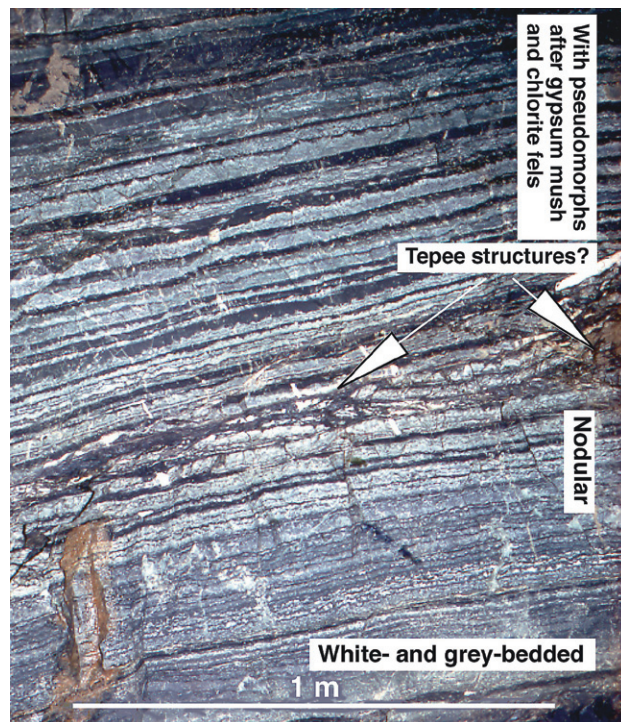


Fig. 35. A section of what is interpreted as a prograding sabkha sequence of dolomitic limestone. At the base white- and grey-bedded dolomitic limestone can be seen, which is overlain by nodular dolomitic limestone (mainly white) and dolomitic limestone with pseudomorphs after gypsum mush (grey and white) intercalated with chlorite fels (black). Between the latter two units there are structures similar to tepee structures. Note the uneven bases and the planar top surfaces of some of the chlorite fels beds. (See text for explanations). Photograph of a drift roof in the mine in the upper unit of the upper formation.

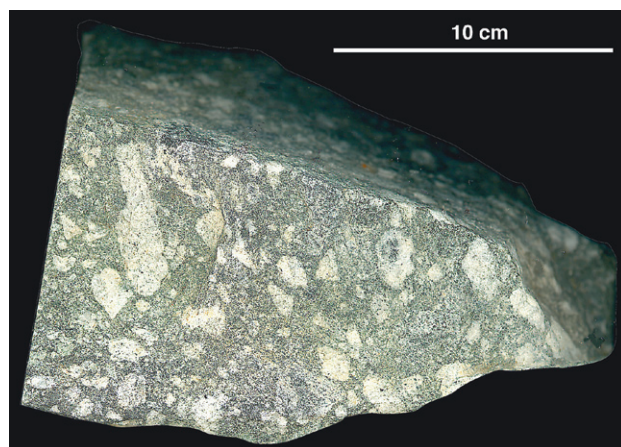


Fig. 36. Dolomitic limestone collapse breccia. Photograph of a rock sample in the upper unit of the upper formation.

evaporites with ensuing collapse of overlying sedimentary strata (i.e. limestone collapse breccia, James 1984).

The dark colour of the dolomitic limestone makes the identification of structures difficult. Nonetheless, attempts have been made to sub-divide the dolomitic limestones into groups with the help of different textures and structures. The following nine different types have been

distinguished: 1) massive dolomitic limestones, 2) white- and grey-bedded dolomitic limestones, 3) nodular dolomitic limestones, 4) dolomitic limestones with pseudomorphs after gypsum mush, 5) dolomitic limestones with pseudomorphs after bottom-growing gypsum, 6) spotted dolomitic limestones, 7) dolomitic limestones with stromatolite-like structures, 8) dolomitic limestones with pseudomorphs after massive halite, and 9) dolomitic limestones with box-work structures.

1) Massive dolomitic limestones (facies G in Plate 4) are found in most of the depositional sequences (Plate 3). They constitute large portions of the dolomitic limestones. Locally, they may contain beds of chlorite fels (upper part of Fig. 32). The massive dolomitic limestones are usually very fine-grained (micritic), dark grey to black, massive, and structureless. The dark colour may be due to a high graphite content.

Their fine-grained texture and the lack of bedding indicate that they were deposited in the deeper parts of the basins, where they precipitated mainly from a suspension. The graphite content suggests a voluminous organic production with a contemporaneous stratification of the water column. This resulted in a reducing environment.

2) White- and grey-bedded dolomitic limestones (facies F in Plate 4) occur in the depositional sequences 3–6, 10, 12, and 13 (Plate 3), either above or below the massive dolomitic limestones. They are diffusely separated into 1–20 cm thick, white and grey, fine-grained beds (lower part of Figs 29 and 35). Locally they contain pseudomorphs after gypsum (see “Spotted dolomitic limestone” below).

The alternating white and grey beds may have formed through interbedding of carbonate precipitated from suspension with material deposited by turbidity currents.

3) Nodular dolomitic limestones (part of facies I in Plate 4) have been found in the depositional sequences 1–4, 6–7, and 9–10 (Plate 3). They are composed of alternating fine-grained beds of dark, dolomitic limestone and white beds with 5–15 mm large nodules and locally pseudomorphs after gypsum (central parts of Figs. 29, 35, and 37). This type of dolomitic limestone may also contain contorted white layers (lower part of Fig. 16).

Structurally, the nodular dolomitic limestone closely resembles the supratidal sediments deposited along the Abu Dhabi coast of the Persian Gulf, described by e.g. Shearman (1966), Kinsman (1969), Butler (1970), Bush (1973), and Kendall (1984). Evaporites found in these types of sediments have been interpreted as formed by diagenetic processes within supratidal environments because of their close resemblance to the sedimentary sequence in the progradational wedge along the Abu Dhabi coast. The nodules formed during diagenetic transition from primary gypsum to anhydrite. The nodular dolomitic limestones

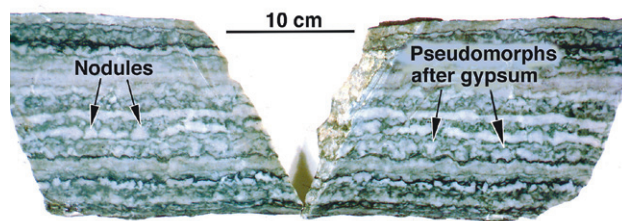


Fig. 37. Nodular dolomitic limestone composed of white nodules, pseudomorphs after gypsum and dissolution surfaces (stylolite-like) with overlying chlorite. Photograph of two rock samples from the upper unit of the upper formation.

are believed to have formed in a similar fashion as the supratidal sabkha deposits. The contorted white layers resemble “chicken wire structures”, described by e.g. Shinn (1983). These structures can be seen in many ancient gypsum and anhydrite deposits.

4) Dolomitic limestones with pseudomorphs after gypsum mush (part of facies I in Plate 4) have been observed in the depositional sequences 1–3, 7, and 9–10 (Plate 3). They are composed of 1–5 cm thick beds of dark dolomitic limestone with planar bases and uneven, white, nodular tops. The dolomitic limestone beds are intercalated with 1–40 mm thick beds of chlorite fels (upper part of Fig. 35). They normally have a grain size between silt and clay. The chlorite fels beds have uneven bases but planar top surfaces, and they are composed of clay–silt-sized chlorite, sometimes with winnowed quartz phenocrysts. Apparent “tepee-like structures” have been observed under the dolomitic limestone with pseudomorphs after gypsum mush (Fig. 35).

The similarity between the calcite and dolomitic limestones with pseudomorphs after gypsum mush suggests that they have the same origin (see “Calcite limestones with pseudomorphs after gypsum mush” above). The nodules were primarily gypsum mush created on top of spring or storm tide beds of carbonate clasts. However, the dolomitic limestones were dolomitized. The mode of occurrence of the chlorite fels indicates that its unaltered precursor was composed of windblown volcanoclastic material (see “Chlorite fels eolian deposits” below). The occurrence of tepee structures is common in intertidal and supratidal environments (Burri et al. 1973; Warren & Kendall 1985).

5) Dolomitic limestones with pseudomorphs after bottom-growing gypsum (facies D in Plate 4) are encountered in the depositional sequences 4–7 and 12 (Plate 3). They are characterized by more than cm-thick layers of dolomitic limestone composed of white, vertical, and elongated bodies. These often contain laminations with sharp-edged corners, visible in sections cut perpendicular to the depositional surface (Fig. 38). If cut parallel to the depositional surface, they appear as more isomet-

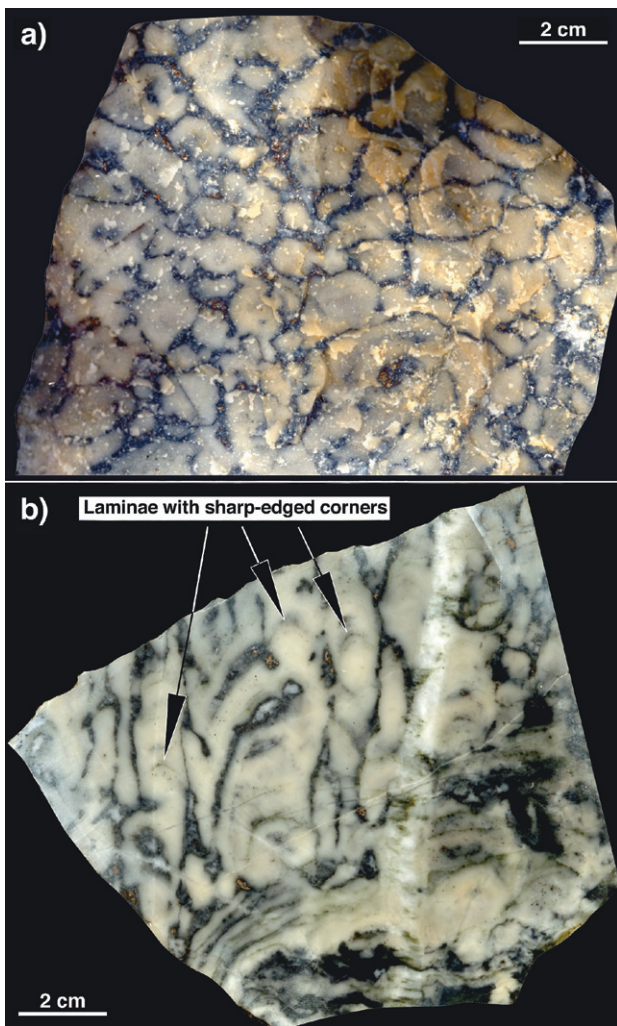


Fig. 38. Dolomitic limestone with pseudomorphs after bottom-growing gypsum: a) cut parallel to the deposition surface. Isometric, angular, white bodies with a network of chlorite between the individuals are visible. b) cut perpendicular to the deposition surface. Elongate, vertical, white bodies with diffuse growth laminae with sharp-edged corners that grew on top of dolomitic limestone with stromatolite-like structure. Photographs of a rock sample from the upper unit of the upper formation.

ric, angular bodies, separated by a thin network of chlorite (Fig. 38).

Morphologically, the elongated bodies resemble pseudomorphs after gypsum crystals grown on the bottom of a coastal salina, e.g. as in Marion Lake, Australia (Warren 1982, Reading 1986). Therefore, such an interpretation is also suggested here.

6) Spotted, dolomitic limestones (facies F in Plate 4) have been found in the depositional sequences 4, 6–7, 10, and 12 (Plate 3). They are encountered above the massive dolomitic limestones and below bedded, dolomitic limestones with stromatolite-like structures, and locally under the nodular dolomitic limestones. The spotted dolomitic limestones are composed of dark, massive or white- and grey-bedded dolomitic limestone with scattered, white,

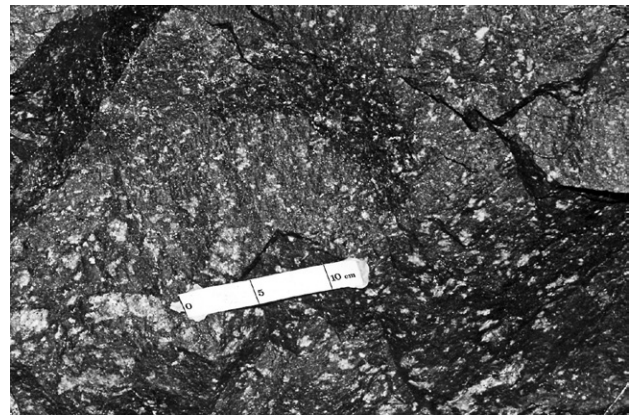


Fig. 39. Spotted dolomitic limestone with pseudomorphs after displacive gypsum, now composed of calcite (light spots). Photograph of a drift wall in the mine in the upper unit of the upper formation.

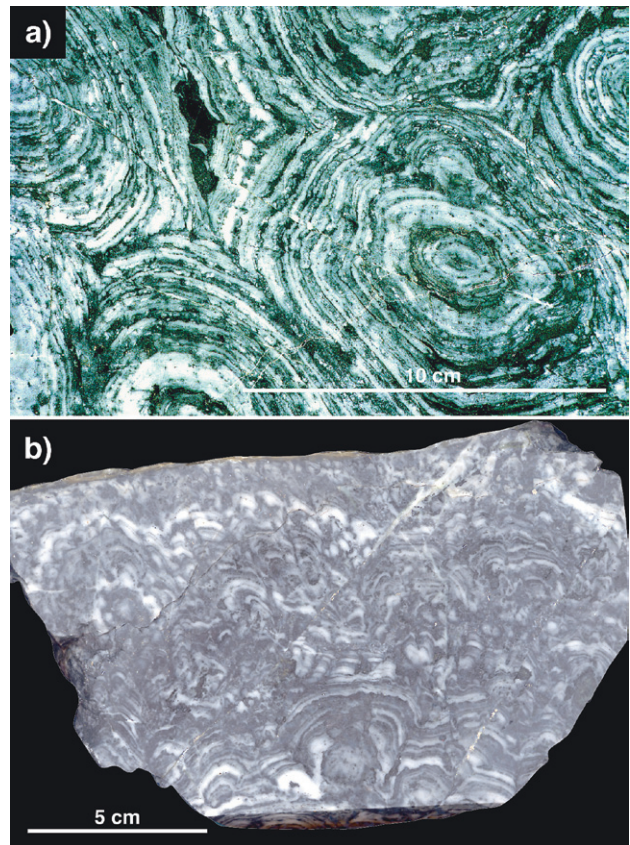


Fig. 40. Dolomitic limestone with stromatolite-like structures: a) a surface parallel to the depositional surface exposes almost circular, concentric laminations can be seen. b) a surface perpendicular to bedding displays dome shaped structures in the lower part and pseudomorphs after fan-like growth of gypsum crystals in the upper part. Photographs of rock samples from the upper unit of the upper formation.

1–10 mm large, often lenticular, spots (Fig. 39).

The spots are composed of carbonate. However, their shape is very similar to diagenetically grown replaced crystals of gypsum, found in different types of sabkhas

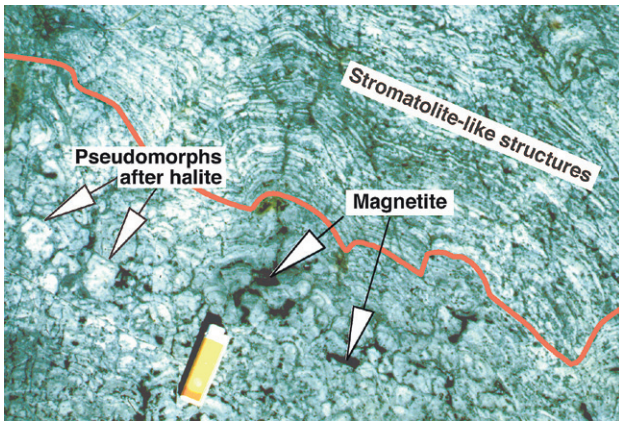


Fig. 41. Dolomitic limestone with a bed of stromatolite-like structures (above the red curve) on top of a bed with pseudomorphs after massive halite. Photograph of a rock sample from the upper unit of the upper formation.

(Dronkert 1977; Schreiber 1978). The spots are therefore interpreted as pseudomorphs after replaced gypsum.

7) Dolomitic limestones with stromatolite-like structures (facies E in Plate 4) have been observed in the depositional sequences 2, 4–7, and 12 (Plate 3). They are the most spectacular of the limestones occurring in the Danemora area. They are formed by laminated units, which in cross-section parallel to the bedding (Fig. 40a) are circular and if cut perpendicular to the depositional surfaces are more or less dome-shaped (Fig. 40b lower part, Fig. 41 upper part, and Fig. 42 central part). The dome-shaped units have a diameter between 1 and 50 cm (normally around 10 cm) and a height of between 0.2 and 2 dm. Laminae are distinguished by an alternation between lighter- and darker-coloured, 0.5–10 mm thick, carbonate laminae and commonly paper-thin, chlorite laminae. The light colours of the laminae facilitate identification of the stromatolite-like structures in the otherwise dark dolomitic limestones.

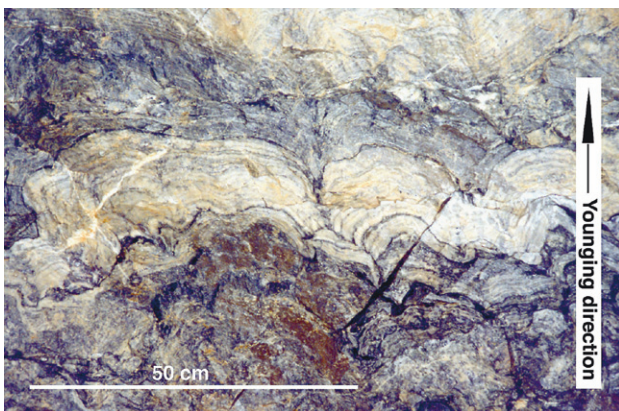


Fig. 42. Interbedded dark and light, dolomitic limestone. The light limestone is laminated and shows stromatolite-like structures cut perpendicular to the deposition surface. Several dissolution surfaces can be observed. Photograph of a drift roof in the mine in the upper unit of the upper formation.

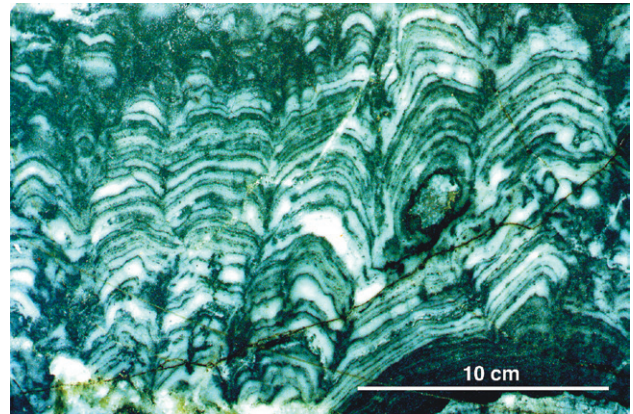


Fig. 43. Dolomitic limestone with stromatolite-like structures cut perpendicular to the depositional surface. Note the shifts between laminations with rounded surfaces (dissolution surfaces) and with sharp-edged corners (growth surfaces). Photograph of a rock sample from the upper unit of the upper formation.

Parts of the light-coloured laminae commonly have a nodular appearance suggesting that the lighter-coloured laminae primarily formed through formation of nodules during diagenetic transition from gypsum to anhydrite. Many of the laminae are not round but show a distinct tendency of having sharp-edged corners (Figs. 43 and

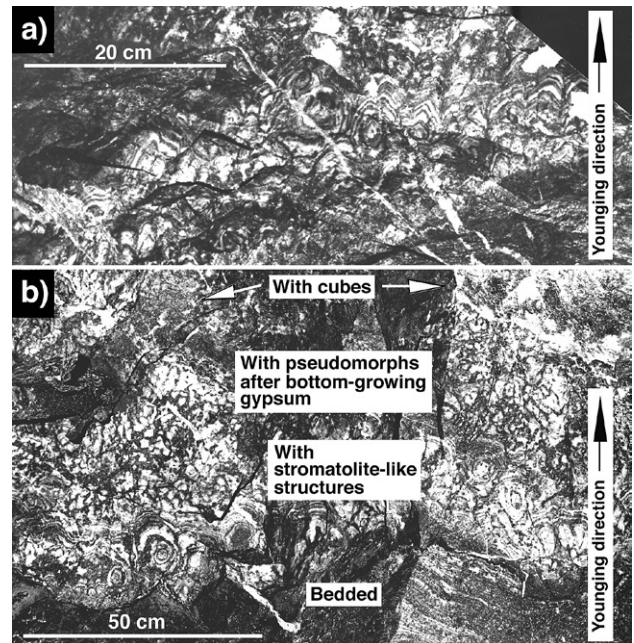


Fig. 44. Dolomitic limestone with stromatolite-like structures cut perpendicular (a) and partly oblique (b) to the depositional surface. a) Stromatolite-like structures with sharp-edged corners. b) A section beginning with bedded, dolomitic limestone and continuing upwards with dolomitic limestone with stromatolite-like structures, dolomitic limestone with pseudomorphs after bottom-growing gypsum and with cubic pseudomorphs after massive halite (not visible in the figure). This section is interpreted as an aggrading, sublittoral sequence of pseudomorphs after evaporites in dolomitic limestone (a drying upwards sequence). Photographs of drift walls in the mine in the upper unit of the upper formation.

44a). In Figure 43, the shape of the laminae alternates between rounded and sharp-edged. This closely resembles the alternation between dissolution surfaces (rounded shapes) and growth surfaces (sharp-edged shape) on bottom-growing gypsum in modern salinas described by Schreiber & Kinsman (1975), Schreiber (1978), and Warren (1982). Many, more extensive, dissolution surfaces can be observed in Figure 42 in the stromatolite-like structures. In an evaporite environment these would represent dissolution surfaces formed during transgressions. Richter-Bernburg (1973) reported fan-like growth of gypsum beds, forming domed structures termed "cavoli" or "cabbage structure" from Sicily. Warren (1982) described fanned crystal beds or domes of gypsum that nucleated on the bottom of ponds. In the upper parts of Figure 40b, structures that closely resemble the primary fan-like growth of gypsum can be seen. Also these structures contain dissolution surfaces.

In the comprehensive literature on stromatolites, e.g. in Walter (1976), they are often reported as having formed organically. Carbonate particles settled on sticky algal mats and the shape of the stromatolites formed through a complicated combination of successive growth of new algal mats, carbonate laminae, and erosion. Many of the lighter-coloured laminae in the stromatolite-like structures in the Dannemora area are too thick to have formed through accumulation of carbonate particles on algal mats. Fenestral porosity appears to be missing, and no microfossils have been found. All the above-mentioned characteristics of the stromatolite-like structures in the Dannemora area instead suggest that a primary gypsum production combined with dissolution has dominated the formation of the stromatolite-like shapes rather than algal mats. The primary gypsum laminae could very well have been interlaminated with algal mats, especially where the thickness of the laminae is minimal. This has, however, not been proven. The literature describes several cases of interlaminations between evaporites and algal mats from younger environments, e.g. in Poland (Vai & Ricchi-Lucchi 1977).

8) Dolomitic limestones with pseudomorphs after massive halite (facies C in Plate 4) have been encountered in the depositional sequences 5–7 and 12 (Plate 3). They consist of 5 dm to several metres thick, commonly dark grey layers, which contain more or less visible square- or cube-like inclusions within a dark rock matrix (Fig. 42 and 44b). In exceptional cases, these squares or cubes may contain light-coloured laminae and their shape becomes more evident (Fig. 41). Pores and cavities between the cubes are commonly magnetite-filled. The dark dolomitic limestones with pseudomorphs after massive halite

are often interbedded with light-coloured beds of dolomitic limestone with stromatolite-like structures (Fig. 42). Another example of alternating layers of light and dark dolomitic limestone can be seen in Figure 44b. The base consists of white- and grey-bedded dolomitic limestone, which upwards changes into dolomitic limestone with stromatolite-like structures and dolomitic limestone with pseudomorphs after bottom-growing gypsum and ends with dolomitic limestone with pseudomorphs after massive halite.

The distinct shape of squares and cubes in the dolomitic limestones indicates that they are pseudomorphs after primary evaporites, most likely halite. If the stromatolite-like structures in Figure 44b represent large crystals and the pseudomorphs after bottom-growing gypsum smaller crystals, then this represents a natural evolution for a drying-upwards sequence where the number of crystal nuclei increases with the increase of the concentration of the evaporitic brine. The laminae in the stromatolite-like structures are interpreted as mainly composed of dissolution surfaces formed by repeated dissolution at lower concentrations during the early stages of the sequence, whereas the laminae in the dolomitic limestones with pseudomorphs after bottom-growing gypsum chiefly constitute growth surfaces during higher concentrations and less dissolution. The sequence terminates with dolomitic limestone with pseudomorphs after massive halite, which confirms an increasing concentration in the evaporitic brine. This type of sequence can be repeated several times towards the end of the depositional sequences of the 2nd order (Plate 4). There it forms sequences of the 3rd order, which preferentially occur towards the centre of the different depositional basins. These sequences are referred to as primary evaporite pans in Plate 4.

9) Dolomitic limestones with box-work structure (not represented in Plate 4 but may occur there in facies C, D, and E) have only been identified below channel-shaped formations of pyroclastic fall and redeposited pyroclastic deposits (depositional sequence 8 and 9 in Plate 1) in the depositional sequences 6 and 7 (Plate 1). They contain abundant 1–5 cm large pores among remnants of stromatolite-like structures and pseudomorphs after evaporites. The pores are filled with magnetite and carbonate (Figs. 45 and 46) and in places this type of limestone is intruded by veins, filled with the same minerals (Figs. 46 and 47).

The pores in the dolomitic limestones with box-work structure appear to have formed through dissolution of evaporites and carbonates, for example, through circulation of sea-, ground-, or hydrothermal waters, similar to what has happened in the salinas in South Australia (Warren & Kendall 1985).

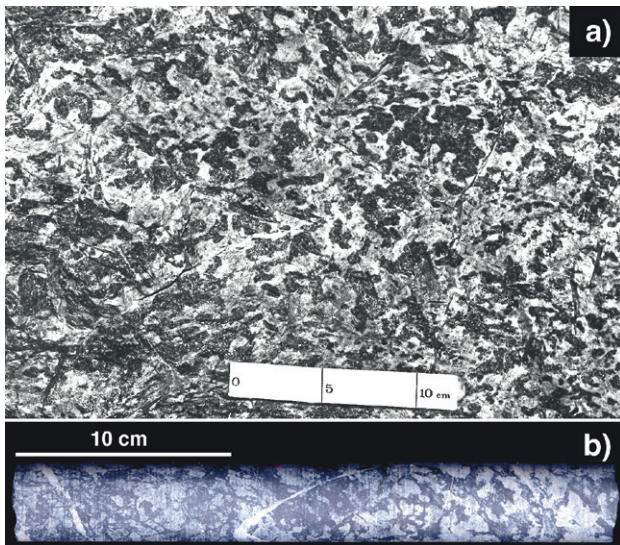
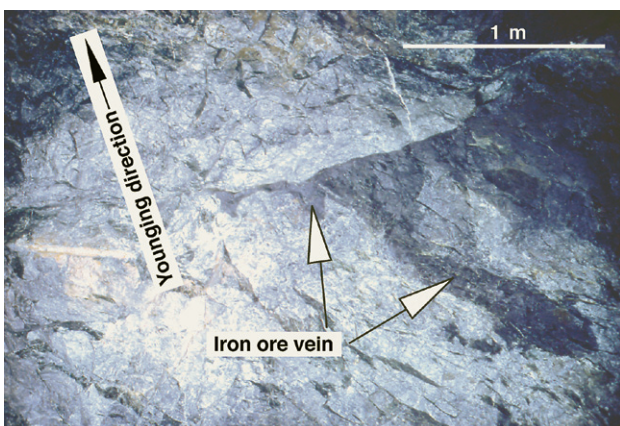


Fig. 45. Dolomitic limestone with boxwork structure. a) Vugs in the dolomitic limestone (white and light grey) filled with magnetite (dark grey and black). Photograph of a drift wall in the mine in the upper formation. b) The right hand part of the drill-core similar to a). The left hand side is composed of spotty iron ore with spots of carbonate (light grey) in a groundmass of magnetite (bluish grey-dark grey). Photograph of a drill core from the upper unit of the upper formation.



Fig. 46. Magnetite (black) in pores and in a vein in dolomitic limestone (white and grey) with boxwork structure. Note that the vein and even some of the pores are also partly filled with carbonate. Photograph of a rock sample from the upper unit of the upper formation.



Chlorite felses

Chlorite felses are only found in the upper unit of the upper formation (Fig. 3 and Plate 1c). Two different varieties of chlorite felses have been discerned: eolian chlorite fels deposits and chlorite fels turbidites. The chemical composition of the two types is presented in Table 1. It is controlled by the content of the mineral chlorite and therefore characterized by a low SiO_2 and a high MgO content. The chlorite felses are found as millimetre to several metres thick laminae or beds in the lower and upper parts of the dolomitic limestone deposits in the depositional sequences of the 2nd order (Plates 3 and 4). Likewise, they occur above the iron ore or dolomites with stromatolite-like structures and pseudomorphs after evaporites in the top of these sequences, laterally outside the profile B in Plate 3 (skarn in Plates 3 and 4). These beds are too thin to be presented on the map in Figure 3, but are important for the interpretation of the evolution of the area. The chlorite felses are dominated by clay- to silt-sized particles and mainly composed of the minerals chlorite, dolomite, calcite, and quartz. Quartz occurs as somewhat worn clasts of phenocrystic quartz crystals with partially preserved crystal faces and corrosion embayments.

The existence of phenocrystic quartz crystals in the chlorite felses points towards a volcanoclastic origin for them. The chlorite felses only occur in dolomitic limestone, which suggests that the alteration from volcanoclastic deposits to chlorite felses occurred in connection with the dolomitization of calcite limestones (see Dolomitization below). The chemical composition of the chlorite felses compared with that of the fine-grained redeposited pyroclastic deposits shows that both have a relatively high Ti, Al, and K content (Table 1). If fine-grained, redeposited pyroclastic deposits have been precursors to chlorite felses, a removal of Si and Ca, and an addition of Fe, Mn and Mg must have occurred. Thus, a similar exchange of elements seems to have happened as during the dolomitization of the calcite limestone to dolomitic limestone. The presence of frequent clasts of chlorite felses in overlying sediments indicates that the alteration of the volcanoclastic deposits was prior to the deposition of the overlying depositional sequence.

Eolian chlorite fels deposits

Eolian chlorite fels deposits (parts of facies I in Plate 4) are found in the depositional sequences 1–3, 4 (laterally outside profile B in Plate 3, in which the chlorite fels corresponds to skarn), 6–7, and 9–10 (Plate 3). They may

Fig. 47. Iron ore vein in dolomitic limestone with stromatolite-like structures and pseudomorphs after evaporites. Photograph of a drift wall in the mine in the upper unit of the upper formation.

occur either as 1–40 mm thick beds in sabkha sediments, where they are intercalated with dolomitic limestone with pseudomorphs after gypsum mush (upper part of Fig. 35), or as 10 centimetre to 1 metre thick repetitions of beds on top of limestone or iron ore, as the uppermost part of closed salina deposits. The chlorite fels intercalated in the sabkha sediments have characteristically uneven bases and planar tops and have a black colour.

The composition and the mode of occurrence of the chlorite fels eolian deposits imply that their unaltered precursor was composed of windblown volcanoclastic material.

Chlorite fels turbidites or tempestites

Chlorite fels turbidites or tempestites (parts of facies E and H in Plate 4) occur in the depositional sequences 4, 5 (laterally outside profile B in Plate 3, in which the chlorite fels corresponds to skarn), and 6–7 (Plate 3). They were deposited in the sublittoral parts of the dolomitic limestones, partly as isolated or repeated 1–50 cm thick beds in the massive dolomitic limestone (Fig. 32) or above eolian chlorite fels deposits in the basal part of the overlying sequence. Partly, they were deposited as 1–10 mm thick laminae or beds in the dolomitic limestone with stromatolite-like structures and pseudomorphs after evaporites. The chlorite fels turbidites or tempestites have a normal grading. Pseudomorphs after gypsum have been noted in some of the chlorite fels beds (Fig. 48).

The composition of the chlorite fels turbidites or tempestites suggests that the unaltered precursor was volcanoclastic material. The primary material of the chlorite fels beds in the dolomitic limestone with stromatolite-like structures and pseudomorphs after evaporites was most

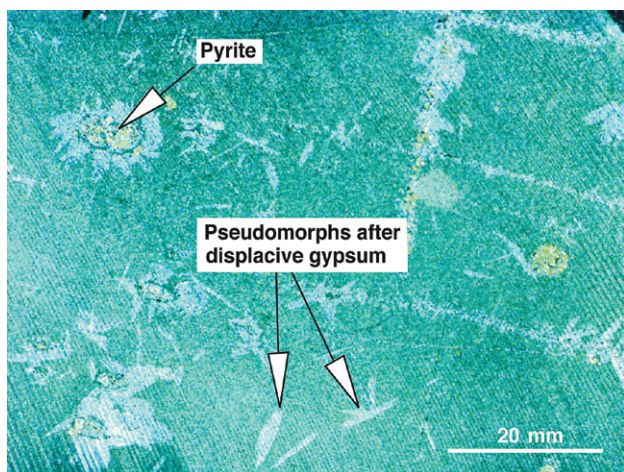


Fig. 48. Chlorite fels with pseudomorphs after displacive gypsum, now composed of calcite (light lenses). Pyrite crystals are sometimes seen in connection with the pseudomorphs. Photograph of a rock sample from the upper unit of the upper formation.

likely deposited as volcanoclastic turbidites or tempestites. This was later altered to chlorite during the dolomitization event. The occurrence of chlorite beds in the sublittoral massive dolomitic limestone indicates that the chloritic material was redeposited. The normal grading in the chlorite fels of this type suggests that they are turbidites or tempestites (storm layers). They may have been deposited sublittorally among clastic dolomitic material, when settling out of suspension. Bedded chlorite fels in the basal part of some sequences above eolian chlorite fels deposits also seem to be turbidites or tempestites. The chlorite fels turbidites and tempestites have not been separated as a consequence of difficulties to discern distinguishing features of tempestites.

Skarn (Fe-Mn-Ca-Mg-silicate rocks)

Skarn is a relatively rare rock type in the Dannemora syncline and it occurs only in the upper unit of the upper formation. Two types of skarn have been observed. One type is green with reddish inclusions, Mn-poor and Ca-rich, and composed of the minerals diopside, actinolite, garnet, and varying amounts of magnetite. The other type is brown and Mn-rich with a manganese content up to 25 %, composed of the minerals knebelite, dannemorite, serpentine, and varying amounts of magnetite. The chemical composition of the skarn can be seen in Table 1. Skarn occurs in 1–7 m thick beds, too thin to be shown on the current map scales. Generally, the Mn-poor beds are found above Mn-poor skarn iron ore and Mn-rich beds above Mn-rich skarn iron ore as massive, uppermost layers in the depositional sequences, for example in the sequence 4 (Plate 3 and facies B in Plate 4). This type of skarn has a very limited lateral extent and either pinches and swells or locally disappears completely. Some skarn rocks are laminated or bedded and form the basal parts of the depositional sequences, for example in sequence 5 (Plate 3). The grain size of the skarn varies between 1 mm and several cm.

The chemical composition of the skarn, with low contents of the less mobile elements Ti and Al, suggests that the skarn precursor was limestone and not volcanoclastic rocks or chlorite fels (Table 1). However, the identical stratigraphic positions of skarn and eolian chlorite fels deposits or chlorite fels turbidites or tempestites, imply that the latter are the skarn precursors. The close relationship between skarn and iron ore indicates alteration of the chlorite fels to skarn by similar hydrothermal fluids that gave rise to the iron ore. If chlorite fels was the precursor to skarn, a removal of Ti, Al and K, and an addition of Fe, and to the Mn-rich skarn also Mn, must have occurred. The hydrothermal fluids must in that case have been warm enough to facilitate this alteration. The lim-

ited lateral extent of the skarn beds and the locally overlying laminated and bedded skarn beds suggest that erosion of skarn beds has occurred and that the bedded skarn was redeposited. This, and the occurrence of clastic fragments of skarn in overlying sediments, indicate that the process of altering the precursor to skarn occurred prior to the deposition of the overlying depositional sequence.

Iron ores

Iron ores have only been found in the upper unit of the upper formation where they occur in 8 out of 14 investigated depositional sequences of the 2nd order (Plate 1). The iron ores are always found in the upper parts of the sequences, especially in the central parts of the sedimentary basins. They are normally massive and strata-bound to the parts of the dolomitic limestone that have stromatolite-like structures and pseudomorphs after evaporites, which the iron ores have partially or completely replaced. They are thickest in the central parts and thin towards the edges. Due to both primary and tectonic features, the beds of iron ore are separated into c. 25 bodies situated at different depths in the mine.

The iron ores are composed of aggregates of several minerals, although the main constituent is magnetite. The aggregates may contain silicate minerals such as knebelite, dannemorite, diopside, actinolite, chlorite, and serpentine as well as carbonate minerals such as calcite, dolomite, siderite, and rhodochrosite. Depending on the distribution of these minerals within the ore, and the iron and manganese content, the ore has traditionally been classified as Mn-rich skarn iron ore, with an iron content varying between 30 and 50 % and a manganese content between 1 and 6 %, and Mn-poor skarn and carbonate iron ore, with an iron content varying between 30 and 50 % and a manganese content between 0.2 and 1 %. The cut off grade was 30 % Fe. The chemical composition of the iron ores can be seen in Table 1. Unfortunately the SiO₂ content is missing. The SiO₂ content varies depending on whether the ore is skarn-hosted or carbonate-hosted. The iron is mostly bound to magnetite, Fe₃O₄, but also to silicates such as knebelite (Fe,Mn)SiO₄ and dannemorite (Fe,Mn,Mg)₇Si₈O₂₂(OH)₂. Apart from Fe and O, the magnetite also contains some manganese. The manganese content of the magnetite in 10 different orebodies in the deposit is given in Table 2. Note that the manganese content of the magnetite in one of the orebodies (Konstäng 2) is as high as 3.1 %. In the remaining analysed orebodies, the Mn content in magnetite is relatively low, even if the manganese content of the ore is high. This indicates that most of the manganese in the iron ore in Dannemora is bound to other minerals than magnetite, e.g. knebelite and dannemorite, except in the Konstäng 2 orebody.

The iron ores are, as a rule, dense or very fine-grained. In the ESE fold-limb of the Dannemora syncline, a coarser grain size (up to 0.5 mm) has been observed. They are mostly spotted iron ores, with 1–50 mm big silicate concentrations (in skarn iron ores) or carbonate minerals (in carbonate-hosted iron ores) surrounded by a fine-grained matrix of magnetite (Fig. 49a). Rare, bedded iron ores occur with alternating magnetite and carbonate or skarn beds (Fig. 49b). The latter morphologically resemble the dolomitic limestone with pseudomorphs after gypsum mush intercalated with the chlorite fels. The skarn beds often have uneven bases and planar top surfaces, similar to the chlorite fels in the limestone. Stromatolite-like structures have been observed in the ores and, in some cases, also structures resembling pseudomorphs after evaporites (Fig. 50).

Laterally, outside the ores, where the total iron content does not exceed 30 %, magnetite is often found in vugs in the dolomitic limestone (Figs. 45 and 46) with box-work structures, described in “Dolomitic limestones with box-work structures” above. This variety locally grades into carbonate-spotted iron ore (Fig. 45b). It also contains 1 cm to approximately 2 m thick veins of magnetite or iron ore (Figs. 46 and 47). The veins and the vugs in the dolomitic limestone may also contain carbonate, which was deposited prior to the magnetite (Fig. 46). It seems probable that the pores formed primarily through dissolution of material, which was followed by deposition of carbonate on the walls of the resulting cavities. The remaining cavities were later filled with magnetite. It is suggested that the evaporites dissolved first, starting with halite. Where the dissolution and subsequent precipitation were extensive, only relics of the original sediment remain where the remnant carbonate forms spots in a matrix dominated by magnetite (Fig. 45b). In some cases, the iron ores resemble collapse breccias formed through the dissolution of evaporites with subsequent collapse of overlying sedimentary strata (James 1984). This could partially explain the for-

Table 2. Manganese content in magnetite in 10 different ore bodies (microprobe analyses made by the Geological Survey of Sweden). Manganese content in magnetite in 10 different ore bodies.

Ore bodies	% Mn in ore samples	% Mn in magnetite
Svea	3.90	0.42
Konstäng 2	3.40	3.10
Sjöhag 1	0.48	0.09
Konstäng 4	0.75	0.33
Ström	2.30	0.28
Kruthus	0.43	0.10
Myr	1.80	0.16
Mellanfält	2.50	0.36
Lyndon	0.97	0.06
Norrnäs	1.90	0.17

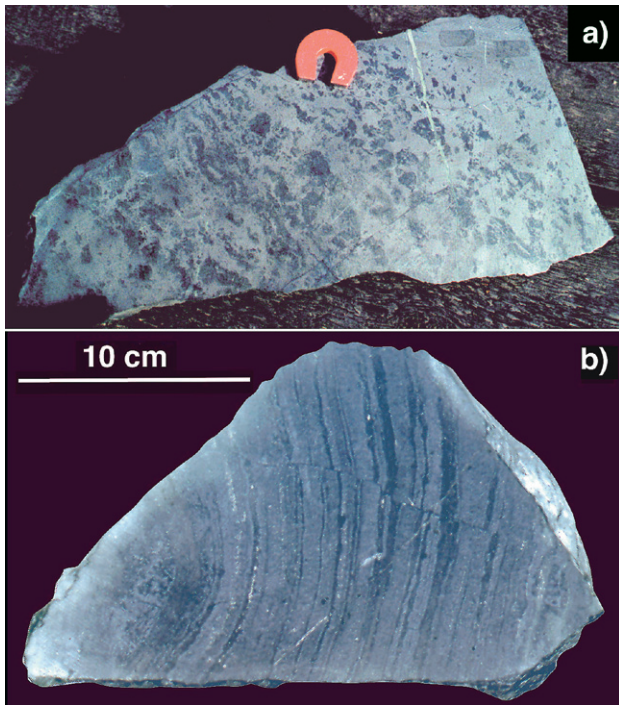


Fig. 49. a) A representative sample of spotted iron ore from the Dannemora deposit. The bluish-grey groundmass is magnetite and the dark spots are Fe, Mn, Mg, and Ca- skarn minerals. b) A rare sample of bedded iron ore in Dannemora deposit. The bluish-grey beds consist of magnetite and the dark beds are Fe, Mn, Mg, and Ca-skarn minerals. Photographs of rock samples from the upper unit of the upper formation.

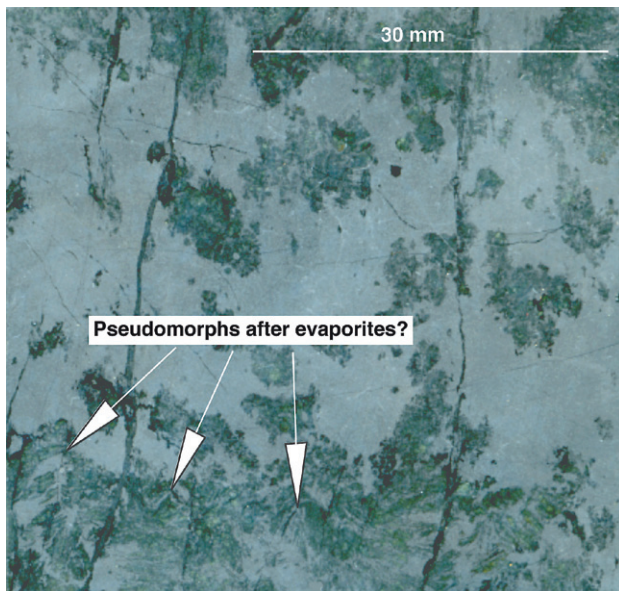


Fig. 50. Iron ore with pseudomorphs after evaporites? (magnetite and skarn laminae with sharp- edged corners). The grey groundmass is magnetite and the dark spots are Fe, Mn, Mg, and Ca-skarn minerals. Photograph of a rock sample from the upper unit of the upper formation.

mation of skarn-spotted iron ores. The skarn spots would then represent altered fragments of collapsed overlying, eolian volcanoclastic sediments.

The bedding, the stromatolite-like structures, and the pseudomorphs after evaporites occur in some parts of the iron ores either as continuous or discontinuous beds and laminae of skarn. In these cases, it appears most likely that beds and laminae of chlorite fels, which are common in areas containing bedding, stromatolite-like structures, and pseudomorphs after evaporites, have altered to skarn during replacement of the remaining sediments by the magnetite. This replacement is most obvious in the case of gypsum. The spots in the skarn-spotted iron ores could partially also have formed during this event.

The exsolution, pore formation, material replacement, and skarn formation must have involved large volume changes through material transport, indicating both removal and addition of new material. This, in turn, should be visible in the overlying strata as either doming or collapse depressions. If the ore formation occurred long after deposition of the overlying sequence, then this sequence should be affected. There are, however, no signs of this. Only collapse of the overlying beds (e.g. volcanoclastic eolian deposits) within the same sequence has been observed. This suggests an ore formation prior to the deposition of the overlying sequences. The facts that the iron ores locally, in both limbs of the Dannemora syncline, show evidence of early erosion (Plate 1) and that the overlying sediments often contain ore clasts, suggest that the ore formation occurred prior to the accumulation of the sediments in the overlying sequences. The occurrence of ore in 8 stratigraphic levels within the upper formation implies that a similar ore-forming process was repeated at least 8 times during deposition of the host sediments. The dolomitic limestone contains small amounts of both iron and manganese (Table 1). When iron ore occurs at the top of the depositional sequence, i.e. close to the palaeo-surface, it is possible that the ore formation occurred through weathering of the iron- and manganese-rich, dolomitic limestone with enrichment of iron and manganese in the near surface layers. However, the iron ores are situated within the central parts of the depositional basins, i.e. in depressions or low-lying areas in the palaeo-landscape. If ore deposition occurred through residual weathering only, then the iron ores would not only be concentrated in the low-lying areas of the basin but also in the topographically higher areas along the margins, unless extensive erosion has taken place.

The enrichment of iron and manganese appears instead to have been caused by circulation of iron- and manganese-rich hydrothermal fluids. These fluids are suggested to have been warm enough to alter the silica-rich units, such as the chlorite felsens, to skarn containing Fe- and Mn-silicates. No alteration zones occur below the ore in the investigated area, which indicates that vertical transport of Fe and Mn did not take place there. However, ver-

tical conduits must have been located elsewhere. A lateral transport of Fe and Mn is very likely in the area as the ores were deposited in an environment controlled by volcanic activity, probably with a high hinterland relief. The hydrothermal fluids migrated from the hinterland towards low-lying areas. Some deposition of Fe and Mn occurred in the carbonate sediments during transport but the bulk of the elements were deposited in the centre of the depositional basin in the evaporite pan deposits. Here, the fluids were concentrated through evaporation with an increasing accumulation of evaporites. This setting was exceptionally favourable for dissolution, precipitation, and material redistribution. The latter is indicated by the occurrence of stromatolite-like structures and pseudomorphs after evaporites in the iron ore. That the ore deposition was repeated at least 8 times during accumulation of the supracrustal rocks in the Dannemora area is most likely linked to the variations in the supracrustal evolution and volcanic activity (see chapters “Stratigraphy and supracrustal evolution” and “Conclusions”).

Sulphide ores

Sulphide ores and mineralizations have only been observed in the upper formation of the Dannemora syncline. The sulphide ores can be divided into two categories based on their mineralogical composition. One category contains sphalerite and galena with traces of silver (up to 20 ppm) and the other contains chalcopyrite, pyrite, arsenopyrite, and pyrrhotite with traces of gold (up to 4 ppm). The distinction is not always sharp. According to

mode of occurrence, the sulphide ores can also be divided into three groups: massive sulphide vein deposits, stratabound sulphide deposits, and sulphide fracture mineralizations.

Massive sulphide vein deposits

Only one massive sulphide vein deposit has been found in the Dannemora syncline, namely in the shallower parts of the Silbergsmalmen ore (Fig. 4) in Södra fältet (the southern field) within the Svelgruvan mine. The mine has been inaccessible for many years. It was described by Bäckström (1923) and Tegengren (1924) who state that the sulphides in the southern field occur both as a massive vein deposit truncating the iron ore layers in Svelgruvan and as bands, schlieren, and impregnations in the Fe-ore bodies. A map of the massive vein deposit (Svelgruvan) at the 40 m level is shown in Figure 51. The sulphides there are sphalerite, pyrite, pyrrhotite, and arsenopyrite with subordinate galena and chalcopyrite.

Bäckström (1923) and Tegengren (1924) interpreted the sulphide ore genesis as epigenetic and mainly younger than the iron formation, since they regarded the alteration of an intrusive metadolerite, as related to the ore formation. It was also suggested that the sulphide ores in Dannemora are genetically linked to the “Uppsala granite”, i.e. the granodiorite found within the syncline (Fig. 4). This view cannot be evaluated due to the inaccessibility of the southern field. However, considering that most of the other studied sulphide ore deposits in Dannemora are stratabound it is likely that also the massive vein deposit

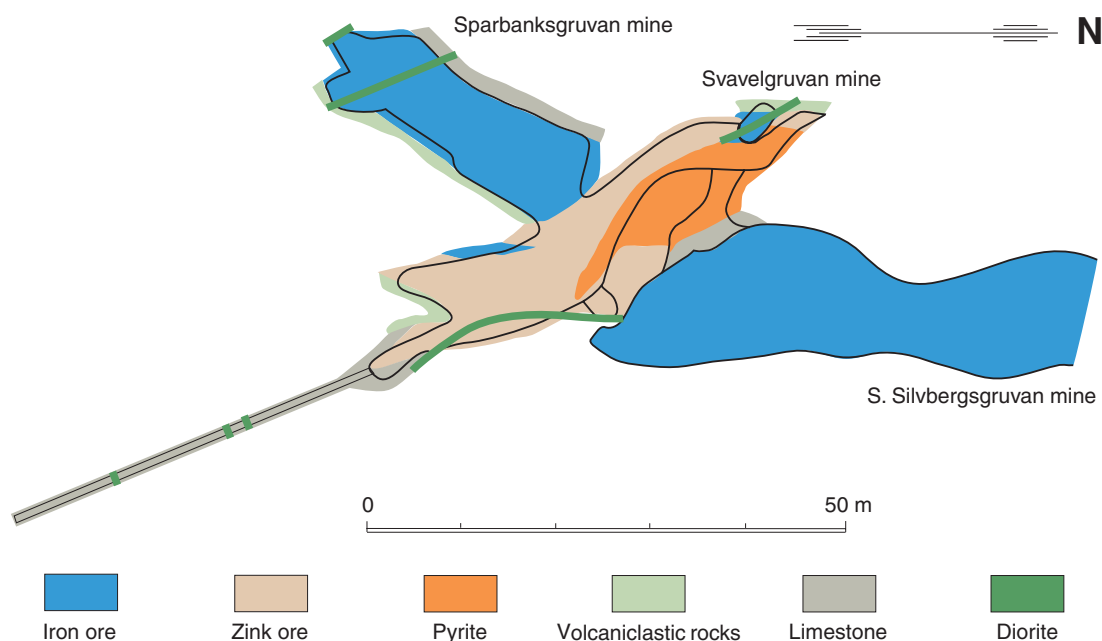


Fig. 51. Geologic map of the Svelgruvan mine at the 40 m level in the Silbergsmalm ore. See Figure 4 for location. Modified from Tegengren et al. (1924).

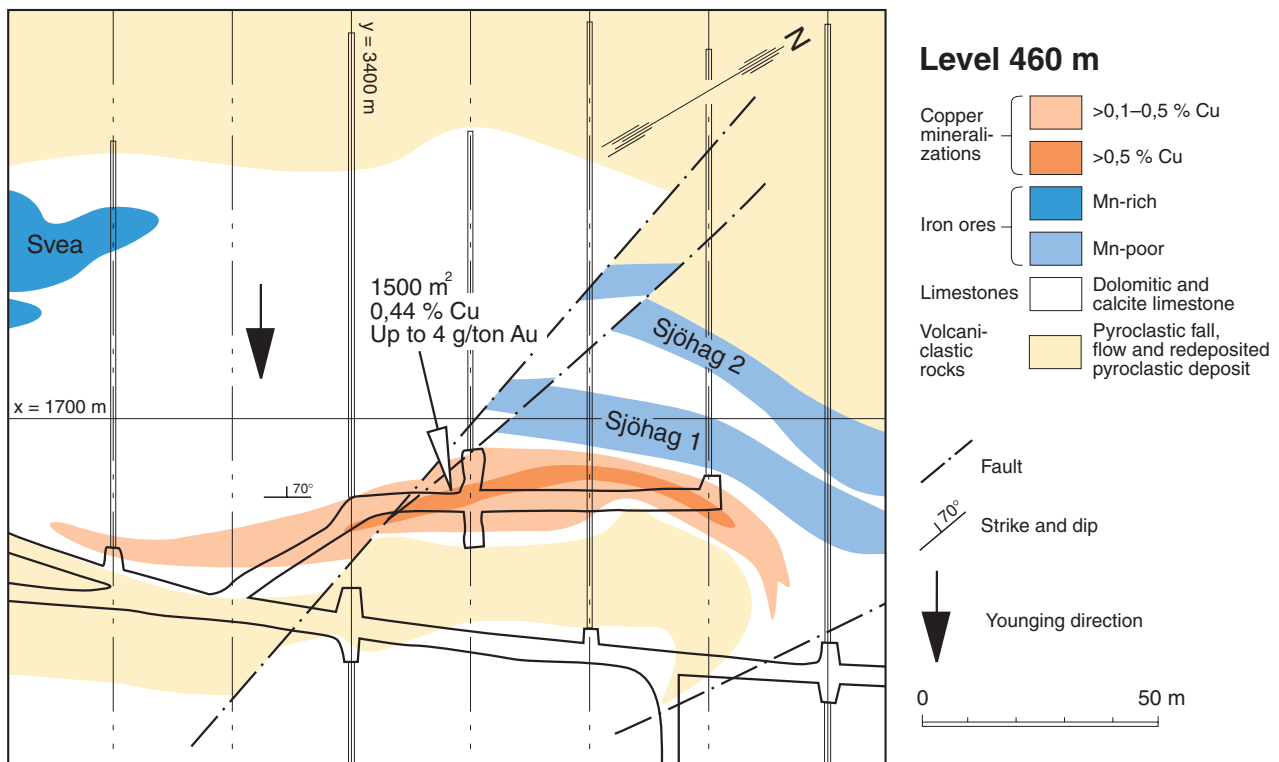


Fig. 52. Geologic map of a copper mineralization in the upper formation at the 460 m level. Modified from a mine map. The approx. location of the sulphide ore can be seen in Figure 4 (see local grid for reference).

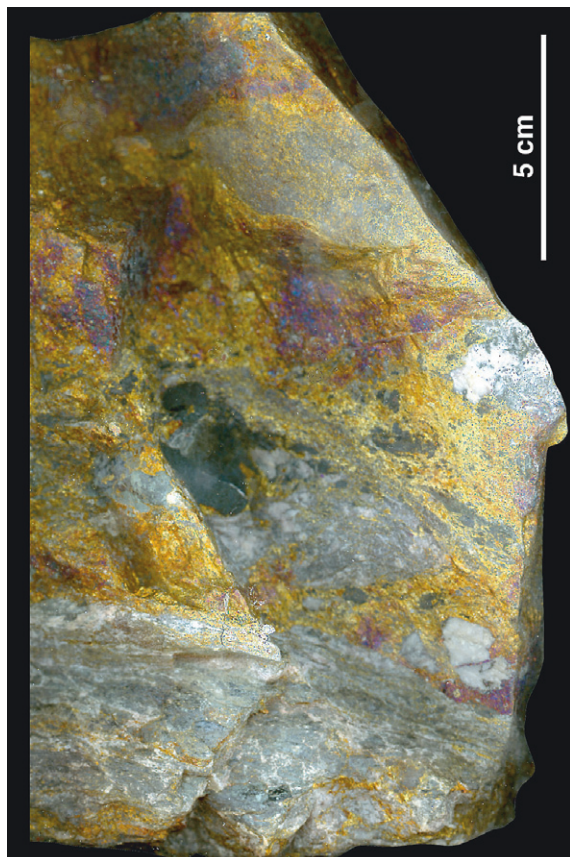


Fig. 53. A chalcopyrite-cemented breccia with fragments of chlorite fels and limestone. Photograph of a rock sample in the upper unit of the upper formation.

(Svavelgruvan) is stratabound. The vein-like appearance of the latter may well be due to deformation and drag faulting, or alternatively, the altered “metadolerite” may simply be a misinterpreted layer of skarn.

The stratabound sulphide deposits

Stratabound sulphide deposits have been identified on both sides of the iron ore (Plate 1), in the uppermost part of the depositional sequence 6 (Plate 3) within the upper formation of the WNW limb. On the NNE side of the iron ore, the sulphide deposit consists of chalcopyrite, pyrite, arsenopyrite, and pyrrhotite with traces of gold and to the SSW of the iron ore it consists of sphalerite and galena with traces of silver. A few deposits of sphalerite and galena have been found in the ESE limb in similar stratigraphic positions. All deposits have very low metal contents and are not economic. The extent of the NNE deposit at the 460 m level in Plate 1 is shown in Figure 52. It should be noted that the sulphide mineralizations are hosted by sequence 6, while iron ore Sjöhag 1 is hosted by sequence 3 and Sjöhag 2 by sequence 2.

The temporal relationship between the central iron ore in sequence 6 and the surrounding sulphide mineralizations is difficult to determine as large parts of sequence 6 have been eroded away (Plate 1). The sulphide mineralizations are parallel to the bedding (Fig. 52) and always

occur, as do the iron ores, in the dolomitic limestone with stromatolite-like structures and pseudomorphs after evaporites. These sulphide mineralizations are not as massive as the iron ores but occur as disseminations and thin vein-fillings in the dolomitic limestone and locally also as sulphide-cemented breccias above the stromatolites (Fig. 53). In the sulphide-bearing limestone, tremolite-bearing fracture fillings are common. These fractures may have resulted from doming related to the volcanic activity.

The age relationship between the stratabound sulphide deposits and the iron ores, overlying sediments, and sulphide ores in the southern field has not been established with any certainty. It cannot be excluded that the stratabound sulphide deposits, like the iron ore, are older than the sedimentary rocks in the overlying sequence. Support for this idea is the fact that all stratabound sulphide deposits are found within the same stratigraphic level in both the WNW and ESE limb of the syncline. If the sulphide mineralization took place after the formation of the whole upper formation then many more suitable host rocks would have been available within other sequences. It seems probable that the stratabound sulphide deposits, like the iron ores in Dannemora, formed by metals precipitating from laterally flowing, hydrothermal fluids into the areas containing stromatolites and evaporites before overlying layers were deposited. This means that a change in the composition of the hydrothermal fluids took place from Fe- and Mn-enriched to Cu-, Zn-, and Pb-enriched fluids. The tremolite-bearing fracture fillings in the sulphide-bearing limestone indicate that the latter fluids also were Si- and Mg-rich.

The sulphide fracture mineralizations

Sulphide fracture mineralizations have only been observed in the proximity of the suggested explosion vent in the ESE limb (see “Pyroclastic breccia deposit” above). An extensive system of planar fractures, filled with sphalerite, galena, and arsenopyrite emanate from this structure and continue into and cut the nearby Kruthus iron orebody (Fig. 4). The pyroclastic breccia deposit in the explosion vent (Fig. 12) is intensely hydrothermally altered.

The pyroclastic breccia deposit, hydrothermal alteration and fracture mineralization can most likely be attributed to the same volcanic event. The Kruthus iron ore, body formed during deposition of sequences 2 and 3 and the above-mentioned volcanic event took place during the evolution of depositional sequence 6 (Plate 3). The area around and below the vent may have served as a vertical conduit for the metalliferous hydrothermal fluids prior to the explosion. The hydrothermal fluids then flowed laterally and resulted in the mineralizations in depositional sequence 6.

Dyke and sill complexes

There are two types of porphyritic dykes in the area. In the local mine nomenclature, these were called “felsite porphyry” and “greenstone porphyry”. However, both have a rhyolitic composition. The third type of dyke is known as “diorite”, but is in fact andesitic. Their chemical compositions are shown in Table 1. The “felsite porphyry” (with a low sodium content) is brown, and contains phenocrysts of quartz whereas the “greenstone porphyry” (with a moderate sodium content) is grey-green and contains sodium feldspar phenocrysts. The “diorite” is massive and homogeneous. All three dyke rocks are fine-grained. The “felsite” and “greenstone porphyries” have only been identified in the upper formation, but should also occur in the lower formation. The “diorite” is common in both the lower and the upper formations. All three rock types occur as 10 cm to 10 m wide, steeply dipping dykes, but the “felsite” and “greenstone porphyries” also occur as low angle dykes (Fig. 3) and sills (Fig. 4). Only a few are wide enough to be shown on the map (Fig. 4). The dykes intrude all supracrustal rocks within the deposit. The “greenstone porphyry” also cuts the “felsite porphyry”. The “felsite” and “greenstone porphyries” are probably subvolcanic intrusions. The “diorite” occurs only as steep dykes and intrudes all rocks within the deposit, including the granodiorite (see below) and is thus the youngest rock type in the Dannemora area. None of the dykes appears to have been affected by the ore related hydrothermal fluids.

Granodiorite

The granodiorite (the chemical composition is shown in Table 1) is composed of quartz, microcline, albite, and biotite. The grain size is normally around 1 mm and the colour is mostly grey, but may occasionally be red. It also contains dark enclaves, around 10 cm in size, which are interpreted as the result of magma mixing. The granodiorite belongs to the early orogenic granitoid suite, c. 1.89 Ga in age, and is visible in the southwestern parts of the Dannemora syncline where the contact with the supracrustal rocks is fault-bounded and sharp. No intrusive contact between the granodiorite and the supracrustal rocks has been observed, nor any contact with signs of erosion and subsequent sedimentation. In the north-eastern parts of the syncline the granodiorite has not been encountered.

Evidence of primary organic life

Signs of primary organic life have been observed in some calcite limestones. An example of this is shown in Figure 54, where a number of cyclically recurring depositional sequences of the 4th order are shown. Several of the lime-

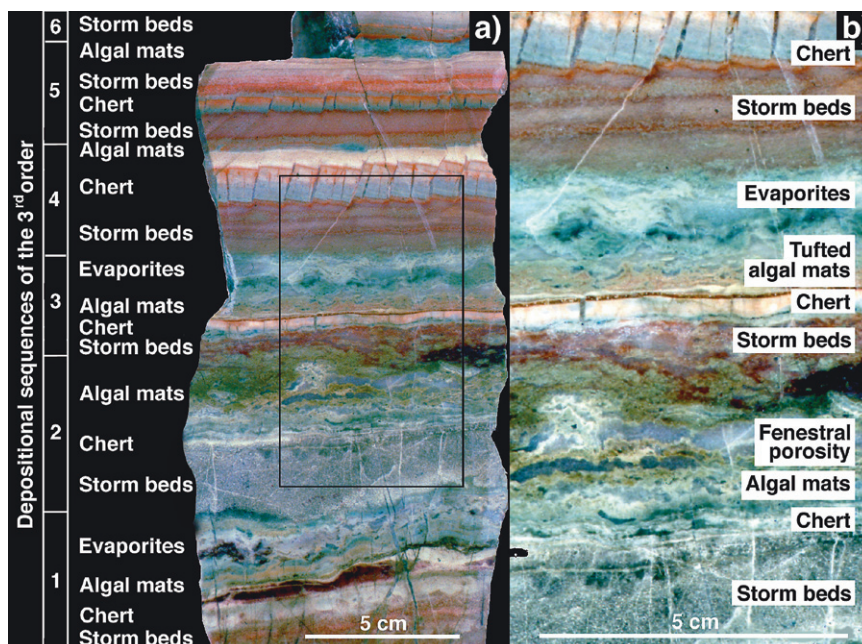


Fig. 54. a) cyclic depositional sequences of the 4th order with evidence of earlier organic life (fenestral porosity and tufted algal mat-limestone laminae) in chert bedded, calcite limestone. A complete sequence starts with storm beds of calcite limestone (primary evaporite clasts?) and continues upwards with chert, algal mats, and calcite limestone with pseudomorphs after evaporites. Photographs of a rock sample in the upper unit of the upper formation. Outlined area in a) is enlarged in b).

stone beds, shown in Figure 54 contain calcite-filled vugs, which resemble “bird’s eye” structures (Shinn 1968) or “fenestrae” or “fenestral porosity” (Shinn 1983). Where these structures occur in predominantly muddy rocks, they are considered to be reliable indicators of supratidal deposition. Volume shrinkage and gas bubbles in the mud are the most likely causes of fenestral porosity. If these structures occur together with algal mats, then organic decay is an obvious explanation for the gas formation. Evidence for this process includes wavy limestone laminae, which closely resemble the shape of the algal mats described by Hoffman (1976) (see Fig. 54). A complete sequence (Fig. 54) starts with storm beds of limestone, followed by chert, limestone with algal mats and, uppermost, limestone with pseudomorphs after evaporites (gypsum mush). If this interpretation is correct, then the sequence could be called a “drying upwards sequence”, which started with a transgression (storm flood). Occasional storms deposited storm beds, possibly with evaporite clasts. After dilution, SiO_2 was precipitated out of solution. Thereafter blue-green algae flourished and carbonate clasts adhered to sticky algal mats. During evaporation, the salinity increased and the evaporites precipitated as gypsum mush. The occurrence of chert here is not well understood and should be more thoroughly investigated.

Traces of micro-organisms have only been found in jaspilite, in which 0.05 mm long threads of micro-crystals of hematite have been observed (Fig. 55). These thin threads resemble filaments of blue-green algae.

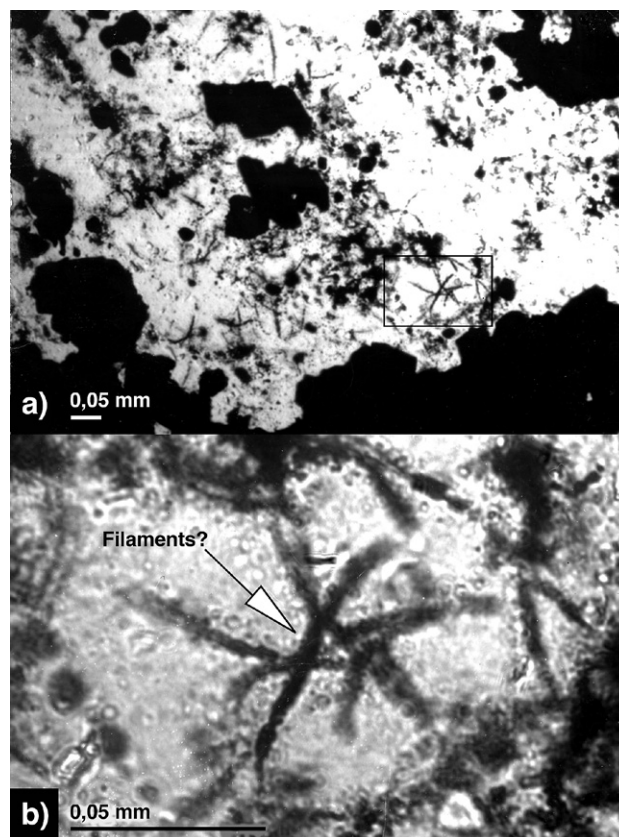


Fig. 55. Evidence of primary organic life? Small “threads” (filaments) now consisting of hematite in chert. Photomicrographs of a thin section from the upper unit of the upper formation. Plane polarized light. Outlined area in a) is enlarged in b).

Microfossils have not been found in the dolomitic limestones, nor in limestones with stromatolite-like structures. This does not, however, exclude the possibility of a rich organic life at the time of the original sedimentation of the dolomitic limestone, since morphological evidence of this may have been completely obliterated by subsequent diagenesis and metamorphism. There are other indications, which point towards the existence of organic life. The graphite in the dolomitic limestone, for example, could constitute remnants of primary organic life. Moreover, the dolomitic limestones, even those with stromatolite-like structures, often contain pyrite flecks, which could have formed from bacterial sulphate reduction of organic life forms during which both H_2S and Fe sulphides were produced (Kendall 1984). Both sulphates and iron were readily available in the dolomitic limestones.

Dolomitization

A lithostratigraphic evolution model for the formation of a depositional sequence of the 2nd order in the upper unit of the upper formation in the Dannemora ore deposit is presented in Plate 4. The lithologies at the bottom of the sequence are composed of redeposited pyroclastic rocks. Following upwards in the sequence occur calcite limestone, dolomitic limestone, and pyroclastic fall deposits. Different structures and pseudomorphs reflect the depositional environments; first an open marine environment with volcanoclastic shoreface, beach and tidal flat sedimentation, then an open lagoon with deposition of carbonate sabkha, after that a closed salina with formation of an evaporite pan with surrounding mudflats, and finally a terrestrial environment with pyroclastic fall deposition. Much of the original sediments has thus been replaced through different processes, especially the carbonates and the evaporite deposits. Dolomitization was one such process, and it was important during the evolution of the Dannemora deposit.

No single criterion can be used on ancient dolomite to propose a single dolomitization model (Warren, 1989). Many ancient dolomites show evidence of having passed through several dolomitization stages, probably associated with more than one replacement process. Dolomites which contain dolomite pseudomorphs after gypsum have been reported from both young and ancient rocks around the world (i.e. Beales & Hardy 1980; McClay & Carlisle 1978). These are thought to have been precipitated from hypersaline waters. As the sabkha sediments of the dolomitic limestone in the Dannemora upper formation are fine-grained and originally probably contained both organic material and evaporites, the dolomitization most likely took place according to the "sabkha model" (Kinsman 1964, McKenzie 1980, Warren 1989, Shinn & Loyd

1969, 1983). According to that model, dolomitization of pre-existing $CaCO_3$ tends to form at the surface on supratidal flats, a few cm above normal high tide. In this setting, phreatic groundwater is brought to the surface by capillary action, or seawater is supplied by surface flooding during storms. Subsequently, evaporites are formed from highly concentrated brines. Calcium is selectively removed from solution through precipitation of aragonite and gypsum, thus elevating the Mg/Ca ratio to levels many times higher than that of ordinary water. Changes in pH associated with respiration and photosynthesis of blue-green algae, as well as oxidation and the pumping action of fluctuating groundwater, may also be contributing factors in supratidal dolomitization. The removal of sulphate ions through bacterial sulphate reduction – the presence of which inhibits dolomite precipitation – is of great importance.

A suitable model for the dolomitization of the original closed salina sediments of dolomitic limestone in the Dannemora area is harder to find. These sediments are mostly fine-grained, except in some beds where they have a crystal size up to 5–10 mm. They have most likely also contained organic material and evaporites. The "brine reflux model", in which the palaeoenvironment is defined as a restricted lagoon behind some sort of sill or reef acting as a physical barrier to the free inflow of fresh seawater (Warren 1989), could therefore possibly fit the dolomitization process of some parts of these sediments. This model is very similar to the sabkha model. However, the brine reflux model is usually invoked for explaining thicker, much larger-scale ancient dolomites associated with evaporites. The formation of carbonates and evaporites occurred on the bottom of the lagoon. Once this began, the Mg/Ca ratio of the remaining brine increased, thereby raising the solution density and causing the magnesium-enriched solutions to sink down through and dolomitize the underlying limestones, as the solutions migrated seawards.

The recurring Mg-rich chlorite fels beds in the dolomitic limestone most likely formed by alteration of volcanoclastic beds according to the "sabkha model" or the "brine reflux model". The described models can partially explain the increased magnesium content in the carbonates, but hardly in all parts of the deposit. Iron ore precipitation with accompanying skarn formation, and sulphide fracture mineralizations with associated tremolite-bearing fracture fillings, suggest that the bedrock was also flushed by laterally flowing hydrothermal fluids. Some of these fluids may have leached Mg while flushing the bedrock in one place and caused dolomitization in another. Skarn for example, seems to have formed by the alteration of the Mg-rich chlorite fels by hydrothermal fluids. This alteration must have included release of Mg.

In addition to magnesium, the dolomitic limestones

also contain some iron and manganese (Table 1), which could have been incorporated in the same fashion as suggested by Eriksson et al. (1976) for the formation of some similar Proterozoic carbonate sequences in South Africa. The atmosphere was more reducing during the Proterozoic compared to today, and iron and manganese occurred

in solution in river and groundwater to a greater extent. If the pH increased, the Fe carbonates precipitated first, followed by Fe-Ca carbonates and, finally, by Fe-Ca-Mn carbonates, either through sedimentation or diagenetically.

STRATIGRAPHY AND PALAEOGEOGRAPHIC INTERPRETATION

The stratigraphy of the Dannemora syncline is divided into three depositional sequences of the 1st order (Plates 1 and 2). The depositional sequences 1 and 2 of the 1st order constitute the basal part of the lower formation. The depositional sequence 3 of the 1st order consists of the upper part of the lower formation, and the basal and upper unit of the upper formation (Plates 1 and 2).

The lower formation has mainly been investigated by sporadic drill-cores and therefore information about its original topographic relationships at different stages of the evolution is lacking. These relationships have, however, been satisfactorily reconstructed for the upper formation by access to a large number of underground galleries and drill-cores (the latter often in sections every 25 m). Faults are abundant in the area, causing a tectonic repetition of beds in some sections and cutting out of units in others. To what extent this has occurred in the lower formation has not been possible to determine.

The lower formation

The lower formation is solely composed of primary pyroclastic and redeposited pyroclastic rocks. A schematic subdivision of the lithostratigraphy of the lower formation and the basal parts of the upper formation (in section $y=2150$ m) has been constructed in Plate 2. Only three types of deposits have been discerned in the lower formation: pyroclastic flow, pyroclastic fall, and redeposited pyroclastic deposits. Within certain parts of the stratigraphy, these types alternate too intimately to be presented on Plates 1 and 2 in the current scale. In these cases, only the dominant unit has been displayed.

The depositional sequence 1 of the 1st order

The depositional sequence 1 begins with pyroclastic flow deposits (pumice flow deposits or ignimbrites), which are composed of 25 beds, 2–15 metres thick (unit A in Plate 2). The pyroclastic flow deposits contain abundant epidote-rich lithoclasts. They are overlain by around 100 beds, 0.5–3 metres thick, which appear to be composed of primary eruptive products (pyroclastic flow deposits)

or volcanoclastic, mass-flow deposits. Above these beds, several hundreds of 1 to 50 cm thick beds of redeposited pyroclastic units, volcanoclastic turbidites, and probably tempestites (unit B in Plate 2) occur. The sequence ends with a 100 m thick stratified unit of pyroclastic fall deposits (unit C in Plate 2).

The depositional sequence 1 is not complete as the bottom unit probably is lacking. Units A and B (Plate 2) are interpreted as subaqueous because the pyroclastic flow deposits are in some cases intercalated with volcanoclastic turbidites and also overlain by such deposits. No hummocky cross-stratification or oscillatory ripple marks have been observed, and hence the prevailing water depth has been impossible to determine. Such structures are, however, hard to discern in the thin drill-cores that were used for this study. Units A and B are assumed to be open marine deposits like parts of the upper unit of the upper formation (the upper part of depositional sequence 3). There, typical marine sediments are found, e.g. volcanoclastic tidal flat deposits with wavy, lenticular, and flaser bedding and bipolar cross-lamination. No carbonate deposits have been observed in units A and B, also pointing at deposition in an open marine environment, while carbonate deposits seem to be built up in more protected water bodies (Plate 5). The great number of epidote lithoclasts in the pyroclastic flow deposits implies that carbonate deposits exist further away, in the neighbourhood of the volcanic vent, fragmented by the eruptions and transported and altered to epidote by the flows. The unit C is interpreted as deposited in a subaerial environment as it is not interlayered by any volcanic turbidites.

The depositional sequence 2 of the 1st order

The depositional sequence 2 is initiated with volcanoclastic turbidites or tempestites (unit D in Plate 2), which are superposed by a pyroclastic flow deposit (pumice flow deposit or ignimbrite) composed of 6 beds, 7–15 metres thick (unit E in Plate 2). Also this deposit contains abundant lithic epidote-rich clasts. The sequence ends with a pyroclastic flow deposit (pumice flow deposit or ignimbrite) composed of 13 red beds, between 1.5 m and 14 m thick

(unit F in Plate 2), followed by 25 grey to greyish red, 1–9 m thick beds with dispersed black, cusped clasts (unit G in Plate 2). These latter beds have been interpreted as pyroclastic fall deposits but the lower part may be mingled with pyroclastic flow deposits originating from the earlier eruption.

The turbidites in the unit D, and locally the intercalated turbidites in unit E, indicate that these units were deposited in a subaqueous environment. They may be open marine deposits for the same reasons as stated for the units A and B. The great number of epidote lithoclasts in the pyroclastic flow deposits suggests also in this case that carbonate deposits exist further away in the neighbourhood of the volcanic vent. Unit F is thought to be terrestrial because the pyroclastic flow deposits are more reddish (more oxidized) than the open marine variety E and also more intensely flattened. They are not interlayered with volcanoclastic turbidites.

The depositional sequence 3 of the 1st order

The depositional sequence 3 starts with brown, volcanoclastic turbidites (unit H in Plate 2), followed by pyroclastic flow deposits (ash flow deposits), composed of 113 flow beds, 0.5–15 m thick (unit I in Plate 2). The flow deposits contain abundant lithic epidote-rich clasts.

The units H and I are interpreted as subaqueous and also open marine deposits for the same reasons as stated for the units D and E. The great number of epidote lithoclasts in the pyroclastic flow deposits once again indicates that carbonate deposits exist further away, in the neighbourhood of the volcanic vent. The sequence continues upwards with the upper formation (Plate 2).

The upper formation

The upper formation constitutes the uppermost part of the depositional sequence of the 1st order. It is divided into a basal unit and an upper unit (Plates 1c and 2) with respect to the occurrence of lithic clasts of magnetite and beds of iron ore and limestone. In the basal unit, lithic clasts of magnetite are common, but beds of iron ore and limestone are completely missing. On the other hand, beds of iron ore and limestone are common in the top unit.

The basal unit: The stratigraphy of the basal unit of the upper formation is presented in Plate 2. This part of the formation is composed of alternating pyroclastic flow deposits (ash flow deposits), pyroclastic fall deposits and volcanoclastic turbidites, which are not separated in Plate 2. The pyroclastic flow deposits contain a great number of epidote-rich lithic clasts and clasts of magnetite. Some beds of the pyroclastic fall deposits are characterized by

accretionary lapilli and some beds of the volcanoclastic turbidites by ripple marks.

The interbedding between the volcanoclastic turbidites and the pyroclastic rocks indicates that the depositional environment was subaqueous. The existence of accretionary lapilli and ripple marks suggests a deposition in shallow water. The basal unit is assumed to be an open marine deposit like parts of the upper unit of the upper formation. The common epidote-rich lithic clasts and clasts of iron ore in the ash flow deposits imply that carbonate rocks and iron ores occurred in the vicinity of the investigated area.

The upper unit: The lithostratigraphic section in the upper formation within the investigated parts of the WNW limb is presented schematically in Plate 1c. The basal unit is followed upwards by the upper unit, which is characterized by pyroclastic fall and redeposited pyroclastic deposits, carbonate rocks, and Mn-rich and Mn-poor iron ore. Other lithologies also occur, e.g. chlorite fels and skarn, but their limited thickness and lateral extent do not allow representation on the map.

The lateral variations in thickness of different layers of the upper unit of the upper formation (Plate 1c) are related to the varying extents of erosion and sedimentation in different parts of the depositional basin. The thickness variations of the layers reflect the approximate shape of sedimentary basins during different stages of the evolution. Through detailed studies of the stratigraphy it has been possible to subdivide the unit into 14 depositional sequences of the 2nd order by studying the erosional surfaces and correlation of their lateral changes (Plate 1b). Note that iron ore-bearing beds occur in 8 of the sequences, where they are found in the central portions of the upper parts. It seems very likely that the carbonate rocks and the majority of the pyroclastic fall deposits and redeposited pyroclastic rocks were deposited in subaqueous environments in depositional basins of different size.

Plate 1a attempts to illustrate the temporal variations of the lateral sizes of the basins. The basins are numbered from 1 to 14 in chronological order. Each basin represents a corresponding depositional sequence. Plate 1a illustrates that the basins increased and decreased in size through time and that they during some periods were divided into two separate basins. Repeated transgressions and regressions must thus have occurred. Basins 1 to 3 all had a large lateral extent and also extended into surrounding areas. A comparison with Plate 1b indicates, however, that all three are missing in the central parts. The following three basins (4–6) were each separated into two basins, divided by a geographical high. This can be explained by the existence of a (volcano-induced) dome, which slowly uplifted the area after the end of the 3rd depositional sequence. Along the

SSW side the uplift was accompanied by a growth fault. Sequences 1–3, as well as other parts of the lower portion of the upper unit of the upper formation, deposited on the emergent central high, were eroded away with time. Erosion also took place in adjacent basins, since these were gullies in the early stage of depositional sequence 4. At this time, erosion of sequences 2 and 3 continued. In basins 4 to 6 these gullies were filled in. The following basin, number 7, overflowed and deposited sediments over the entire region. After the completion of basin 7 the whole area was drained, subsidence followed due to compaction of earlier sub-basins, and new basins formed, especially in the SSW. The entire landscape suffered from intense erosion, especially the SSW sub-basin as it was transformed to a drainage pathway. It was eventually filled in during the formation of basin 8, and in basins 9 and 10 the whole landscape was blanketed with sediments. Continued compaction, especially in the right hand sub-basin (Plate 1) again created a basin, which was filled by sequence 11. The remaining basins (12–14) con

tinued to supply material to further blanket the landscape and fill depressions in the topography.

The lithostratigraphy in the top of the upper formation within the investigated parts of the WNW limb is summarised in Plate 3. The lithostratigraphy is presented by a number of logs labelled B–F and their positions are marked in Plate 1. The logs represent locations in the centre of the basins, and hence the stratigraphy of the peripheral parts is uncertain. The logs are divided into 14 depositional sequences of the 2nd order. The stratigraphy presented in Plate 3 is a composite of many sections from different levels within the mine. In total, 10 different rock types and 11 sedimentary structures have been identified (see Plate 3), which in different combinations compose all the different sedimentary facies. The erosional unconformities delimit the depositional sequences. Certain facies types are missing in some sequences whereas others are repeated. The logs (Plate 3) show that the depositional sequences started with transgressive and terminated with regressive sedimentation.

MODEL OF SUPRACRUSTAL EVOLUTION

The lower formation and the basal unit of the upper formation

The volcanic rocks in south central Sweden have essentially a rhyolitic composition. Allen et al. (1996) presented facies analyses of rhyolitic, pyroclastic rocks of the same age as the Dannemora rocks from a number of localities in central Sweden. Here, volcanism is thought to be linked to shallow marine to subaerial, rhyolitic pyroclastic caldera volcanoes. The depositional environments for the proximal and medial facies associations are interpreted as principally from shallow water to subaerial, and for the medial to distal ash–siltstone facies associations as primarily shallow to deep marine environments. Observed transgressions and regressions were interpreted as related to subsidence and uplift in connection with the regional magmatic extensional-compressional cycles or variations of the latter related to the evolution of individual volcanoes.

The volcanoclastic rocks in the lower formation and the basal unit of the upper formation in the Dannemora syncline alternate between pyroclastic flow, pyroclastic fall, and redeposited pyroclastic rocks in a similar fashion as in other regions in central Sweden. Also in the Dannemora area, the volcanism could have been tied to rhyolitic, pyroclastic caldera volcanoes. The depositional environment was medial and changed between shallow marine and subaerial. If the presented interpretation of the lower

formation is right then the investigated part of the lower formation has undergone three stages of regression and two stages of transgression, which have caused the 1st order depositional sequences 1–3 (Plate 2). If the general interpretations by Allen et al. (1996) are applied to the Dannemora area, the regressions could be the response to uplift and the transgression to subsidence, all tied to the volcanic activity. The regressions could of course also be related to basin infill by pyroclastic and redeposited pyroclastic material and sea-level changes. The transgressions could also have resulted from both burial compaction and sea-level changes.

The upper formation

The third depositional sequence of the 1st order continues upwards with the upper unit of the upper formation. Fourteen depositional sequences of the 2nd order have been discerned in that unit (Plates 1b and 3). Plate 3 illustrates that many of the sequences are initiated with redeposited pyroclastic units and terminated with iron ore or pyroclastic fall deposits (chlorite fels or skarn). This suggests that volcanic activity has had a major influence on water depth and depositional environment. Subsidence appears to have occurred after each pyroclastic eruption with influx of seawater in the depositional basin as a result. Before each eruption, it appears that doming raised the basins above sea level. Hence, a model for the develop-

ment of a depositional sequence of the 2nd order is proposed. According to that model the lithostratigraphy of a hypothetical depositional sequence of the 2nd order has been constructed (using the data in Plate 3) and compared against an assumed curve of volcano-induced subsidence and uplift (Plate 4). It should be noted that the observed transgressions may have, at least partially, been caused by sea-level changes and sediment compaction and proven regressions by sea-level changes and sediment progradation. Plate 4 also lists sedimentary environments, depositional sequences of the 3rd order, and other geological events. Plate 5 shows paleogeographic reconstructions for five main stages (stages 1–5) of the suggested depositional sequence.

Stage 1

Due to volcanic subsidence, the subsequent transgressions migrated in over the pyroclastic material and each depositional sequence started with erosion and deposition of volcanoclastic beach and shoreface deposits (facies P and M; Plate 4 and Table 3). Tidal flats developed and prograded, and transformed into volcanoclastic tidal flat deposits (facies O). Renewed subsidence occurred with accompanied deposition of transgressive, volcanoclastic beach, shoreface and tidal flat deposits. As progradation and transgressions occurred a number of times, new volcanoclastic depositional sequences of the 3rd order were formed. The volcanoclastic tidal flats were transversed by a number of tidal channels, in which volcanoclastic tidal channel sediments were deposited (facies N). When the transgression was faster than the progradation of tidal sediments, these were replaced by fining-upwards sequences of volcanoclastic beach and shoreface deposits, and turbidites or tempestites (facies M, P, and L). At the end of this stage of the evolution, an open lagoon was gradually created through the formation of a barrier of redepos-

ited pyroclastic materials. This barrier protected the basin brine against the equilibrating effects of the oceans to some extent. Silica and iron precipitated, which were later transformed to jaspilite or chert and siderite.

Stage 2

Algal mats, aragonite, and calcite formed in the tidal sediments surrounding the lagoon. Storm floods created storm layers of carbonates and also turbidites or tempestites of carbonates and volcanoclastic material, which were deposited in the deeper parts of the lagoon. The basin slowly transformed into a rapidly prograding sabkha. In the inter- and supratidal parts of the sabkha, gypsum precipitated diagenetically due to evaporation. Gypsum also precipitated as gypsum mush after evaporation from storm floods. New storm floods quickly eroded previous mush layers and instead deposited clastic gypsum layers. Also silica precipitated (facies J; Plate 4 and Table 3). Gypsum was altered to anhydrite, which formed nodules (facies K) or “chicken wire structures” (see Shinn 1983). Evaporation and diagenetic alterations resulted in fractures and “tepee structures” (see Burri et al. 1973, Warren & Kendall 1985). The supratidal parts of the sabkhas were exposed to extensive erosion through deflation. The deposition of eolian and locally volcanoclastic material may have occurred during this time. The erosional effect of the wind created uneven surfaces in the volcanoclastic eolian sediments. The carbonate and evaporite sediments in these parts were dolomitized according to the “sabkha model” for dolomitization (Kinsman 1964, Shinn & Loyd 1969, McKenzie et al. 1980, Shinn 1983, Warren 1989). The volcanoclastic sediments in the carbonates were simultaneously altered to the precursor of the chlorite fels (facies I).

Renewed transgression swept in over the sabkha, which then started to prograde. This was repeated, resulting in

Table 3. Different facies and sedimentary environments in Plate 4.

Facies	Sedimentary environment
A Pyroclastic fall deposit	Terrestrial
B Skarn altered, volcanoclastic eolian deposit	Terrestrial
C Dolomitic limestone with pseudomorphs after massive halite	Sublittoral
D Dolomitic limestone with pseudomorphs after bottom-growing gypsum	Sublittoral
E Dolomitic limestone with stromatolite-like structures	Sublittoral
F Spotted dolomitic limestone	Sublittoral
G Massive dolomitic limestone	Subtidal
H White- and grey-bedded dolomitic limestone	Subtidal
I Nodular dolomitic limestone	Sabkha
J Calcite limestone with pseudomorphs after algal mats and chert	Sabkha
Calcite limestone with pseudomorphs after gypsum mush	Sabkha
K Nodular calcite limestone	Sabkha
L Volcanoclastic turbidites or tempestites bedded with calcite limestone	Subtidal
M Transgressive, volcanoclastic beach and shoreface deposit	Beach, shoreface
N Volcanoclastic tidal channel deposit	Tidal channel
O Volcanoclastic tidal flat deposit	Tidal flat
P Regressive, volcanoclastic shoreface deposit	Shoreface

depositional sequences of the 3rd order, or "shallowing-upwards sequences", being deposited (see James 1984). Finally, the prograding sabkha could not keep up with the continued transgression and sedimentation was replaced by turbidites or tempestites of carbonate (facies H; Plate 4 and Table 3) and finally by massive carbonate deposited from suspension (facies G). Possibly, the water in the lagoon became stratified and a lower reducing layer formed, which was caused by a rich organic production. Organic material was preserved in the sediments due to the reducing environment and is present today as graphite, a product of later metamorphic alterations.

Stage 3

The dormant volcano resumed activity with doming or uplift as result. A regression began, which caused a gradual isolation of the lagoon and a closed salina evolved. Seawater recharge occurred through intra-sediment flow. Groundwater was also discharged into the basin. Due to hot climate, an intense evaporation of the basin water commenced. The lake diminished until only a central, shallow, saline lake with surrounding carbonate mud flats remained. In this lake, fine-grained carbonate turbidites were deposited, interlayered with algal mats. Displacive gypsum crystals gradually formed in the sediments (facies F; Plate 4 and Table 3).

During continued evaporation, bottom-nucleated gypsum began to grow on the lake bottom. The first crystals to form were large and partly fan-shaped with many dissolution surfaces, which gave rise to stromatolite-like structures (facies E; Plate 4 and Table 3). Algal mats may also have occurred between the gypsum crystals. When the salinity increased, more and more bottom-growing, vertically elongated gypsum crystals began to grow (facies D), mainly due to fewer dissolution surfaces. Finally, when evaporation reached its maximum, bottom-growing, massive, halite crystals were deposited (facies C). In connection with the transition to an increasingly pluvial climate, the lake area expanded and migrated over the mud flats with possible dissolution of the salt layers as a result. During alternating arid and pluvial conditions, repeated depositional sequences of evaporites formed. This type of event of the 3rd order may be called a "drying-upwards sequence". The gypsum is partially altered to nodules of

anhydrite, even in the salina environment.

The salina sediments were dolomitized diagenetically, which probably occurred in pulses in several ways. An initial dolomitization may have taken place according to the "brine reflux model" described by e.g. Warren (1989). A later and more complete dolomitization was probably caused by laterally flowing hydrothermal fluids in connection with the ore forming hydrothermal event.

Stage 4

During the final stage of the doming, the volcanic activity yielded plenty of metalliferous hydrothermal fluids. From the elevated, surrounding hinterlands, these fluids migrated laterally into the central parts of the salinas. The salt pan sediments functioned as a trap for the fluids, resulting in metal-precipitation and replacement. Initially, the fluids were mainly Fe- and Mn-bearing, which resulted in iron ores. Later, when the fluids were warmer and Zn-, Pb- and Cu-bearing, updoming was maximal. The rocks were then fractured and suitable for sulphide precipitation. The sulphur was introduced through bacterial sulphate reduction.

Supralittoral parts of the salina complex were exposed to considerable erosion through deflation. Deposition of eolian carbonate as well as volcanoclastic material could occur also on top of bottom-growing evaporites. In some places, the whole complex was covered with volcanoclastic eolian material, which was changed to chlorite fels during the dolomitization of the carbonate rocks. This material was later altered to skarn (facies B; Plate 4 and Table 3) by the same hydrothermal fluids that formed the ores and mineralizations.

Stage 5

At the end of the development of the depositional sequence of the 3rd order, the volcano erupted and pyroclastic material (facies A; Plate 4 and Table 3) was deposited. One or more layers of pyroclastic flow and/or fall material were deposited over parts or the entire salina complex. The pyroclastic material was either deposited in water or on land. This was controlled by the moment of the volcanic eruption related to the stage of development of the depositional sequence.

DISCUSSION

The proposed model for development of the depositional sequences of the 2nd order is not valid in all parts, for all sequences. There are deviations. The suggested first phase of the model with open marine environment is based upon the occurrence of tidal flat and tidal channel deposits in the depositional sequences 8 and 9 (Plate 3). These deposits have been interpreted as tidal with help of the occurrence of bipolar cross-bedding and wavy, lenticular and flaser bedding. Such structures have not been found in the other sequences, where there is abundant evidence for subaqueous deposition but no proof of marine. Nevertheless, stage 1 could have been open marine even during the deposition of these sequences, because the transgressions could have been too rapid for the development of prograding tidal flats with tidal channels.

Chert and siderite are commonly intercalated, especially with volcanoclastic turbidites at the basal parts of many sequences (Plate 3 and Fig. 21). Maybe it is easier to explain deposition of chert and siderite, during a transgressive phase, in a more protected waterbody, than in an open marine environment, e.g. in a closed salina. There, stratification of the water column could occur after dilution. Even if some of the sequences start with deposition in a closed salina, the essence of the proposed model should be true. Volcano-induced subsidence could have caused transgressions into the salina with help of seawater

recharge through the barrier. The carbonate sabkha deposits in Plate 4 are, in that case, carbonate mudflat deposits and the depositional sequences of the 4th order of primary stormbeds, chert, algal mats, and evaporites are sublittoral instead of supratidal (see Fig. 54 and "Evidence of primary organic life" above).

The proposed model is based on observed, repeated sequences of facies with interpreted sedimentary environments. The observed bipolar cross-bedding and wavy, lenticular and flaser bedding in the deposits interpreted to be tidal flats and channels can also be found in fluvial deposits, but more seldom. Irrespective of these deposits being fluvial instead of tidal, there is no evidence of superficial connection with the marine environment. The deposition could have taken place in an inland playa lake as well as in a closed salina. If deposition occurred in an inland playa lake, the transgressions and regressions were not volcano-induced but rather due to changes between pluvial and arid climate. The repeated dolomitization would be more difficult to explain if the depositional environment was an inland playa lake.

The proposed model for development of the depositional sequences of the 2nd order seems therefore most plausible. Some of the sequences begin with open marine deposits in the basal parts and others with closed salina deposits.

CONCLUSION

A performed basin analysis suggests that the stratigraphy of the Dannemora syncline consists of three transgressive-regressive depositional sequences of the 1st order (Plate 2). It seems plausible that each sequence consists of open marine deposits in the basal parts and terrestrial deposits in the upper parts. The depositional sequences 1 and 2 of the 1st order constitute the basal part of the lower formation. The depositional sequence 3 of the 1st order consists of the upper part of the lower formation, and the basal and upper unit of the upper formation (Plates 1 and 2). The lower formation is composed exclusively of volcanoclastic rocks. The basal unit of the upper formation also consists solely of volcanoclastic rocks, but the volcanic rocks contain lithic clasts of iron ore, which are lacking in the lower formation. Beds of iron ore and carbonate rocks are completely missing there. The upper unit of the upper formation on the other hand, is composed both of beds of volcanoclastic rocks and beds of iron ore and carbonate rocks. The upper unit of the upper formation is suggested to have been deposited in repeated open marine, open la-

goon, closed salina, and terrestrial environments (Plates 1 and 3). The carbonate rocks were deposited in the open lagoon and the closed salina environment. Some of them were primary evaporites. The iron ore was emplaced by hydrothermal fluids in the closed salina environment. If this is valid, the carbonate rocks and the iron ores formed just at the transition from open marine to terrestrial environment.

During the development of the depositional sequences 1 and 2, there were changes from open marine to terrestrial environments, but no carbonate rocks or iron ores have been found there within the investigated area. The lack of carbonate rocks may be caused by too voluminous deposition of pyroclastic deposits at the critical stage. The lack of iron ores may be explained by too long distance to the volcanic centre and the hydrothermal solutions. A great number of epidote lithoclasts in the pyroclastic flow deposits in these sequences implies that carbonate rocks existed further away. The carbonate rocks have been deposited in the neighbourhood of a volcanic vent and have

been fragmented by eruptions. Flows have transported the fragments and altered them to epidote. During the development of the basal unit of the upper formation there was no passage from open marine to terrestrial environment,

but common epidote-rich lithic clasts and clasts of iron ore in ash flow deposits suggest that carbonate rocks and iron ores occurred in the vicinity of the investigated area.

ACKNOWLEDGEMENTS

The author is most grateful to Christer Åkerman, Rodney Allen, Risto Kumpulainen, Ingmar Lundström, and Pär

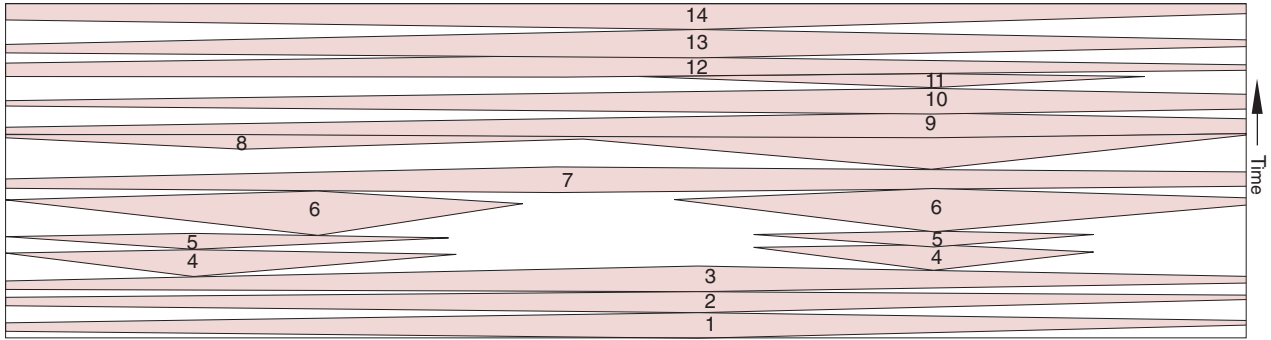
Weihed for substantial improvements of this manuscript. Patrik Witt-Nilsson translated the manuscript into English.

REFERENCES

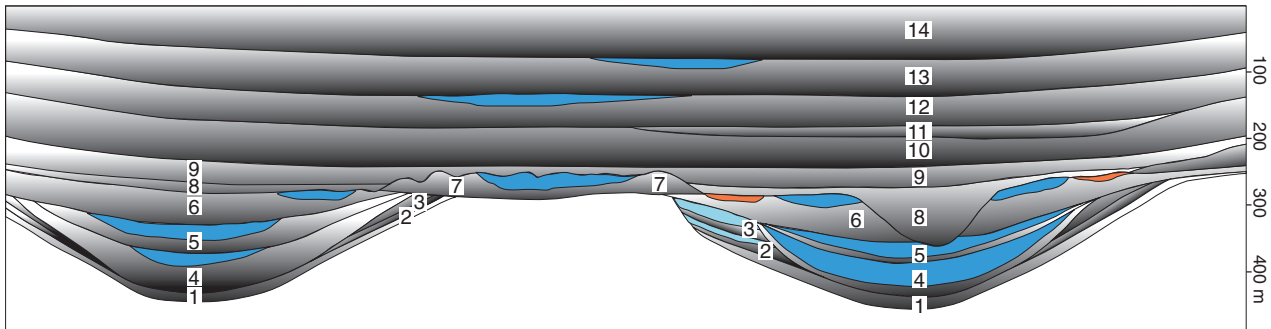
- Allen, R.L., Lundström, L., Ripa, M., Simeonov, A. & Christoferson, H., 1996: Facies Analysis of a 1.9 Ga, Continental Margin, Back-Arc, Felsic Caldera Province with Diverse Zn-Pb-Ag-(Cu-Au) Sulfide and Fe Oxide Deposits, Bergslagen Region, Sweden. *Economic Geology* 91, 979–1008.
- Baekström, O., 1923: Bidrag till kännedomen om sulfidmalmernas geologi inom Dannemorafältet. *Geologiska Föreningens i Stockholm Förhandlingar* 45, 286–294.
- Beales, F.W. & Hardy, J.L., 1980: Criteria for the recognition of diverse dolomite types with an emphasis on studies on host rocks for Mississippi Valley-type ore deposits. *Society of Economic Paleontologists and Mineralogists, Special Publication*, nr 32, 197–213.
- Björk, L., 1986: Beskrivning till berggrundskartan Filipstad NV. *Sveriges geologiska undersökning, Af 147*, 110 pp.
- Burri, P., du Dresnay, R. & Wagner, C.W., 1973: Tepee structures and associated diagenetic features in intertidal carbonate sands (Lower Jurassic, Morocco). *Sedimentary Geology* 9, 221–228.
- Bush, P.R., 1973: Some aspects of the genetic history of the sabkha in Abu Dhabi, Persian Gulf. In B.H. Purser (ed.): *The Persian Gulf. Springer-Verlag*. Berlin, 395–407.
- Butler, G.P., 1965: *Early diagenesis in the recent sediments of the Trucial coast of the Persian Gulf*. London University. Ph.D. Thesis. 251 pp.
- Butler, G.P., 1970: Holocene gypsum and anhydrite of Abu Dhabi Sabkha, Trucial Coast: an alternative explanation of origin. In J.L. Rau, & L.F. Dellwig (eds.): *Third Symposium on Salt, Northern Ohio Geological Society*, 120–152.
- Cas, R.A.F. & Wright, J.V., 1987: *Volcanic successions: Modern and ancient. A geological approach to processes, products and successions*. Allen and Unwin, London. 518 pp.
- Cas, R.A.F. & Wright, J.V., 1991: Subaqueous pyroclastic flows and ignimbrites: An assessment. *Bulletin of Volcanology* 51, 357–380.
- Clifton, H.E., 1982: Estuarine Deposits. In P.A. Scholle & D. Spearing (eds.): *Sandstone Depositional Environments. The American Association of Petroleum Geologists*. Tulsa, Oklahoma. 179–189.
- Dronkert, H., 1977: A preliminary note on a recent sabkha deposit in S. Spain. *Publicaciones del Instituto de Investigaciones Geológicas de la Diputación de Barcelona* 32, 153–166.
- Erdmann, A., 1851: *Dannemora jernmalmsfält i Upsala län*. Avtryck ur Kungliga Vetenskapsakademiens Handlingar för år 1850. Norstedt & Söner, Stockholm. 138 pp.
- Eriksson, K.A., Truswell, J.F. & Button, A., 1976: Paleoenvironmental and geochemical models from an early Proterozoic carbonate succession in South Africa. In M.R. Walter (eds): *Stromatolites*. Elsevier Scientific Publishing Company. Amsterdam. 635–643.
- Geijer, P. & Magnusson, N.H., 1944: De mellansvenska järnmalmernas geologi. *Sveriges Geologiska Undersökning Ca 35*, 527–538.
- Hoffman, P., 1976: Stromatolite morphologies in Shark Bay, Western Australia. In M.R. Walter (ed.): *Stromatolites*. Elsevier. Amsterdam. 261–272.
- Howells, M.F., Reedman, A.J. & Campbell, S.D.G., 1991: *Ordovician (Caradoc) marginal basin volcanism in Snowdonia (north-west Wales)*. British Geological Survey, London. 191 pp.
- James, N.P., 1984: Shallowing upward sequences in carbonates. In R.G. Walker (ed.): *Facies models. Geological Association of Canada. Toronto. Geoscience Canada Reprint Series 1*, 213–228.
- Kendall, A.C., 1984: Evaporites. In R.G. Walker (ed.): *Facies models. Geological Association of Canada. Toronto. Geoscience Canada Reprint Series 1*, 259–296.
- Kendall, C.G.S.C. & D.E. Skipwith, S.P.A., 1969: Holocene shallow-water carbonate and evaporite sediments of Khor al Bazam, Abu Dhabi, Southwest Persian Gulf. *American Association of Petroleum Geologists Bulletin* 53, 841–869.
- Kinsman, D.J.J., 1964: The recent carbonate sediments near Halat el Bahrani, Trucial Coast, Persian Gulf. In *Deltaic and shallow marine deposits-developments in sedimentology*. Elsevier Sci. Pub. Amsterdam. 185–192.
- Kinsman, D.J.J., 1969: Modes of formation, sedimentary associations and diagnostic features of shallow-water and supratidal evaporites. *American Association of Petroleum Geologists Bulletin* 53, 830–840.
- Lager, I., 1986: The Dannemora iron ore deposit. In I. Lundström & H. Papunen (eds): *Mineral deposits of south-western Finland and Bergslagen province, Sweden. Sveriges*

- geologiska undersökning Ca 61*, 26–30.
- Lundqvist, 1979: The Precambrian of Sweden. *Sveriges geologiska undersökning C 768*, 87 pp.
- Lundström, I., 1995: Beskrivning till berggrundskartorna Filipstad SO och NO. *Sveriges geologiska undersökning Af 177*, 185, 218 pp.
- Lundström, I., Allen, R.L., Persson, P.-O. & Ripa, M., 1998: Stratigraphies and depositional ages of Svecofennian, Palaeoproterozoic metavolcanic rocks in E. Svealand and Bergslagen, south central Sweden. *Geologiska Föreningens i Stockholm Förhandlingar 120*, 315–320.
- Magnusson, N. H., 1925: Persbergs malmtrakt och berggrunden i de centrala delarna av Filipstads bergslag. *Beskrivningar av mineralfyndigheter, n:r 2. Kungl. Kommerskollegium*, 475 pp.
- McClay, K.R. & Carlile, D.G., 1978: Mid-Proterozoic sulfate evaporites at Mt. Isa mine, Queensland, Australia. *Nature 274*, 240–241.
- McCubbin, D.G., 1982: Barrier-Island and Strand-Plain Facies. In P.A. Scholle & D. Spearing (eds): *Sandstone Depositional Environments. The American Association of Petroleum Geologists*. Tulsa, Oklahoma. 247–279.
- McKenzie, J.A., Hsü, K.J. & Schneider, J.F., 1980: Movement of subsurface waters under the sabkha, Abu Dhabi, UAE, and its relation to evaporite dolomite genesis. In D.H. Zenger, J.B. Dunham & R.L. Ethington (eds): *Concepts and models of dolomitization. Society of Economic Paleontologists and Mineralogists, Special Publication nr 28*, 11–30.
- McPhie, J., Doyle, M. & Allen, R., 1993: *Volcanic Textures. A guide to the interpretation of textures in volcanic rocks*. University of Tasmania, Hobart. 196 pp.
- Nyström, E., 1922: Petrographical and chemical observations on the hälleflintas of the Dannemora mining field. *Geologiska Föreningens i Stockholm Förhandlingar 44*, 761–772.
- Oen, I. S., 1987: Rift-related Igneous Activity and Metallogenesis in SW Bergslagen, Sweden. *Precambrian Research 35*, 367–382.
- Persson, L. & Persson, P.-O., 1999: U-Pb zircon age of the Vätö granite, south central Sweden. In S. Bergman (ed.): *Radiometric dating results 4. Sveriges geologiska undersökning C 831*, 91–99.
- Reading, H.G., 1986: *Sedimentary Environments and Facies*. Second, Blackwell Scientific Publications, Oxford. 615 pp.
- Richter-Bernburg, G., 1973: Facies and paleogeography of the Messinian evaporites in Sicily. In C.W. Drooger, (ed.): *Messinian Events in the Mediterranean*. North Holland Publishing Co. Amsterdam. 124–141.
- Schreiber, B.C., 1978: Environments of subaqueous gypsum deposition. In *Marine evaporites: SEPM Short Course Notes 4*. Oklahoma City. 43–73.
- Schreiber, B.C. & Hsü, K.J., 1980: Evaporites. In G.D. Hobson (ed.): *Developments in Petroleum Geology*. Applied Science Publishers LTD. London. 87–138.
- Schreiber, B.C. & Kinsman, J.J., 1975: New observations on the Pleistocene evaporites of Montallegro, Sicily and a modern analog. *Journal of Sedimentary Petrology 45*, 469–479.
- Shearman, D.J., 1966: Origin of marine evaporites by diagenesis. *Institution of Mining & Metallurgy, Section B 75*, 208–215.
- Shinn, E.A., 1968: Practical significance of birdseye structures in carbonate rocks. *Journal of Sedimentary Petrology 38*, 215–223.
- Shinn, E.A., 1983: Tidal flat environment. In P.A. Scholle, D.G. Bebout & C.H. Moore (eds): *Carbonate depositional environments. The American Association of Petroleum Geologists memoir nr 33*. Tulsa, Oklahoma. 172–210.
- Shinn, E.A. & Loyd, R.M., 1969: Anatomy of modern carbonate tidal-flat, Andros Island, Bahamas. *Journal of Sedimentary Petrology 39*, 1202–1228.
- Stephens, M. B., Ahl, M., Bergman, T., Lundström, I., Persson, L., Ripa, M. & Wahlgren, C.-H., 2000: Syntes av berggrundsgeologisk och geofysisk information, Bergslagen och omgivande områden. In H. Delin (ed.): *Regional berggrundsgeologisk undersökning – sammanfattning av pågående undersökningar 1999. Sveriges geologiska undersökning Rapporten och meddelanden 102*, 78–97.
- Stålhös, G., 1991: Beskrivning till berggrundskartorna Östhammar NV, NO, SV, SO. *Sveriges geologiska undersökning Af 161, 166, 169, 172*, 249 pp.
- Sundius, N., 1923: Grythyttfältets geologi. *Sveriges geologiska undersökning C 312*. 354 pp.
- Tegengren, F., 1924: Sveriges ädlare malmer och bergverk. *Sveriges geologiska undersökning Ca 17*, 299–302.
- Törnebohm, A., 1878: *Beskrivning till geologisk atlas över Dannemora gruvor*. Beckman, Stockholm. 85 pp.
- Vai, G.B. & Ricci-Lucchi, F., 1977: Algal crusts autochthonous and clastic gypsum in a cannibalistic evaporite basin: a case history from the Messinian of the Northern Apennines. *Sedimentology 24*, 211–244.
- Walter, M.R., 1976: *Stromatolites*. Elsevier Scientific Publishing Company, New York. 790 pp.
- Warren, J.K., 1982: The hydrological setting, occurrence and significance of gypsum in late Quaternary salt lakes in south Australia. *Sedimentology 29*, 609–638.
- Warren, J.K., 1989: *Evaporite sedimentology*. Prentice Hall, Inc., London. 285 pp.
- Warren, J.K. & Kendall, C.G.S.C., 1985: Comparison of sequences formed in marine sabkha (subaerial) and salina (subaqueous) settings-modern and ancient. *American Association of Petroleum Geologists Bulletin 69*, 1013–1023.
- Weimer, R.J., Howard, J.D. & Lindsay, D.R., 1982: Tidal Flats and Associated Tidal Channels. In P.A. Scholle & D. Spearing (eds): *Sandstone Depositional Environments. The American Association of Petroleum Geologists memoir nr 33*. Tulsa, Oklahoma. 191–245.

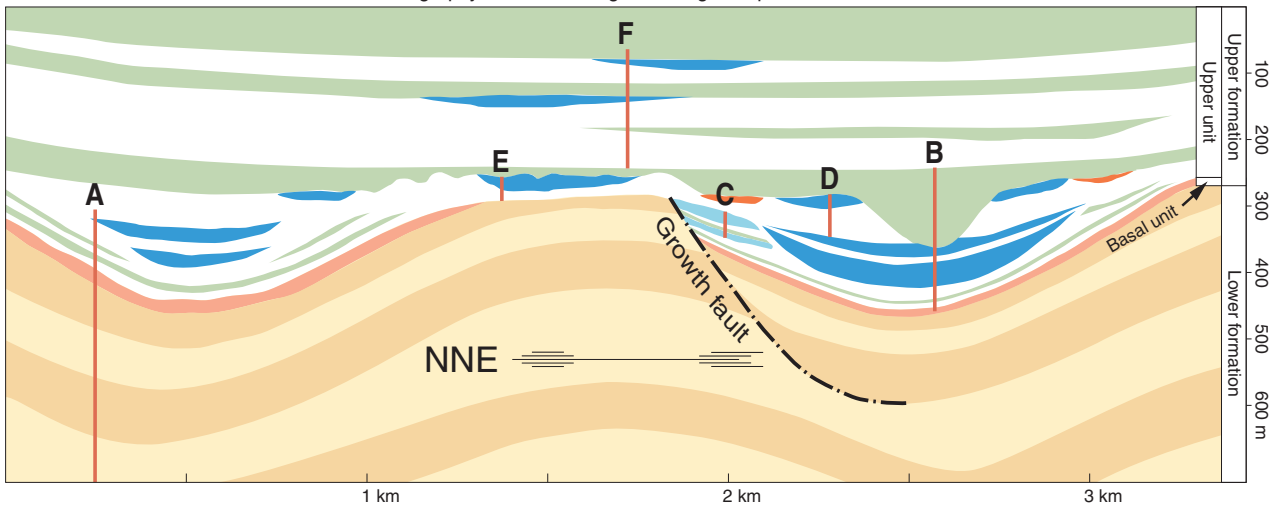
a. Basin extensions with time in the upper unit of the upper formation.



b. Depositional sequences (14) of the 2nd order in the upper unit of the upper formation.



c. A schematic reconstruction of the lithostratigraphy after stretching out along fault planes.



**a. Upper formation
Upper unit**

- Depositional basins
- Erosion or no deposition

A Locations of the Section A (Plate 2) and the geologic logs B-F (Plate 3)

**b. Upper formation
Upper unit**

- Depositional sequences
- Mn-poor iron ore
- Mn-rich iron ore
- Sulfide ore (in b. & c.)

**c. Upper formation
Upper unit**

- (Open marine, open lagoon, closed salina and terrestrial deposits)
- Pyroclastic fall and redeposited pyroclastic deposit
 - Limestone
 - Mn-poor iron ore
 - Mn-rich iron ore

Upper formation – Basal unit

(Open marine deposits)

- Pyroclastic flow, fall and redeposited pyroclastic deposit

Lower formation

(Open marine and terrestrial deposits)

- Pyroclastic flow deposit
- Pyroclastic fall and redeposited pyroclastic deposit

Plate 1. a) Basin extensions and b) depositional sequences of the 2nd order in the upper unit of the upper formation, and c) reconstructed lithostratigraphy in the main part of the north-western limb of the Dannemora syncline. Some of the beds have been emphasized to be visible, other, thin beds are discarded.

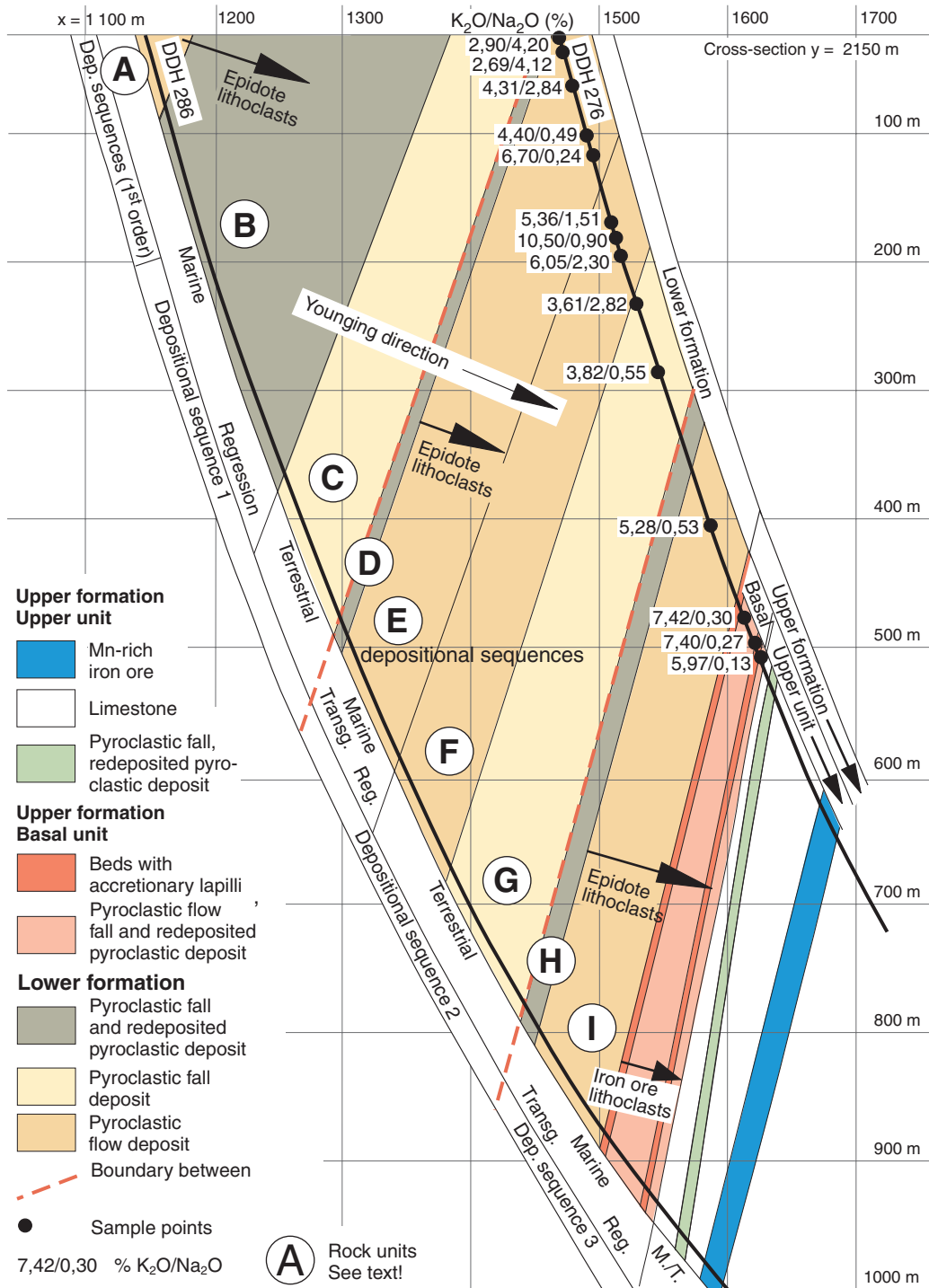


Plate 2. A reconstruction of the lithostratigraphy in part of the upper unit of the upper formation (open marine, open lagoon, closed salina, and terrestrial deposits), the basal unit of the upper formation (open marine deposits), and the lower formation (open marine and terrestrial deposits) with help of the cores from the diamond drill-holes 276 and 286 in the cross-section $y = 2150$ m. The location of the section is indicated as Section A in Figure 3 and Plate 1. A–I correspond to different rock units described in the text.

Lithologies

- Pyroclastic fall deposit
- Redeposited pyroclastic deposit
- Calcite limestone
- Dolomitic limestone
- Iron ore
- Chlorite fels
- Skarn (Ca-, Mg-, Fe- and Mn-silicates)
- Chert

Structures

- Massive
- Pebbles
- Accretionary lapilli
- Planar bedding
- Ripples
- Cross-bedding
- Nodules (P.a. gypsum mush)
- Pseudomorphs after bottom-growing gypsum
- Pseudomorphs after displacive gypsum
- Stromatolite-like structures
- Pseudomorphs after massive halite
- Spotty
- Bipolar cross-bedding

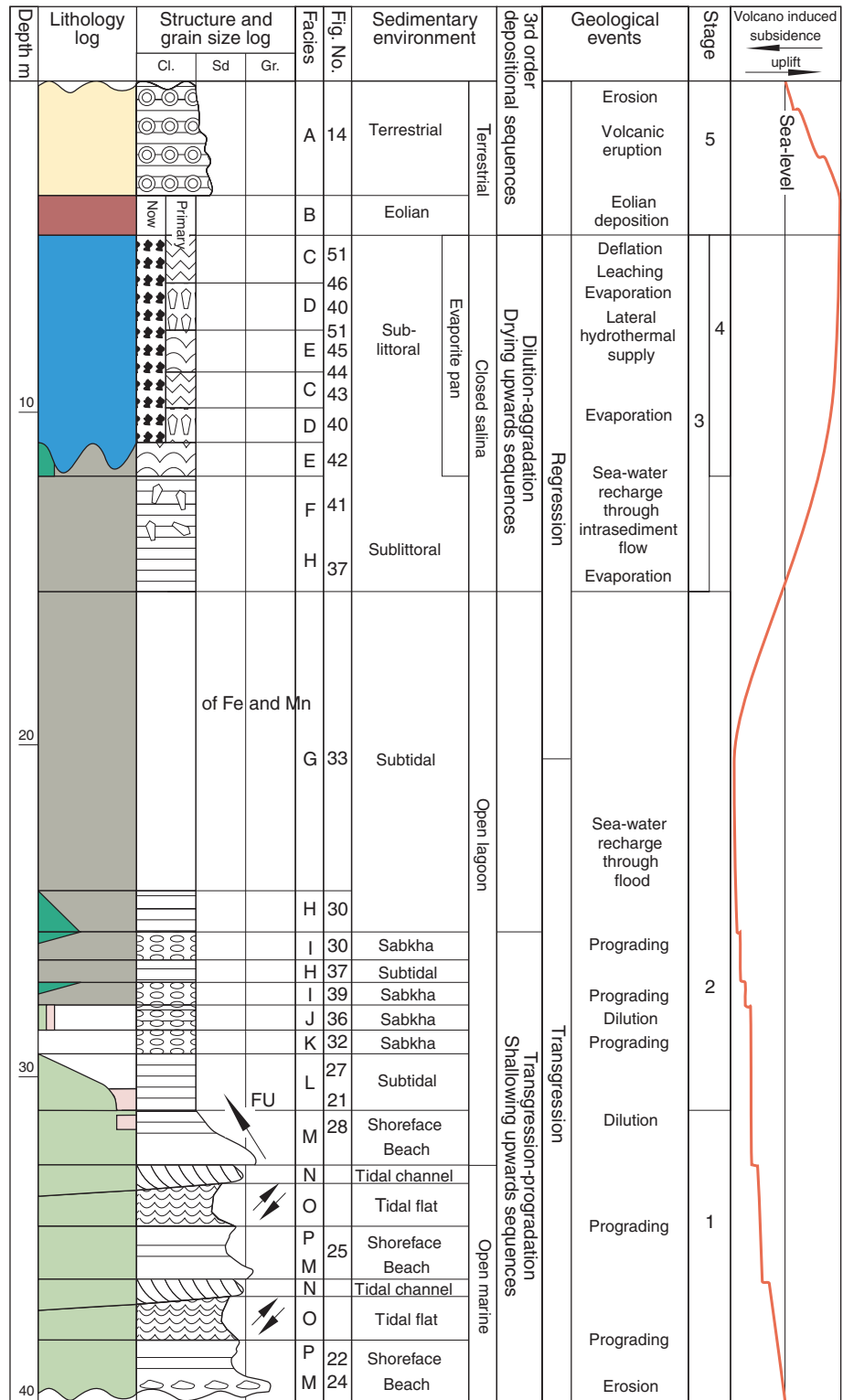


Plate 4. The lithostratigraphy in a hypothetical depositional sequence of the 2nd order deposited open marine, in an open lagoon, in a closed salina, and terrestrially, related to volcano-induced subsidence and uplift. Cl=clay, Sd=sand, Gr=granules.

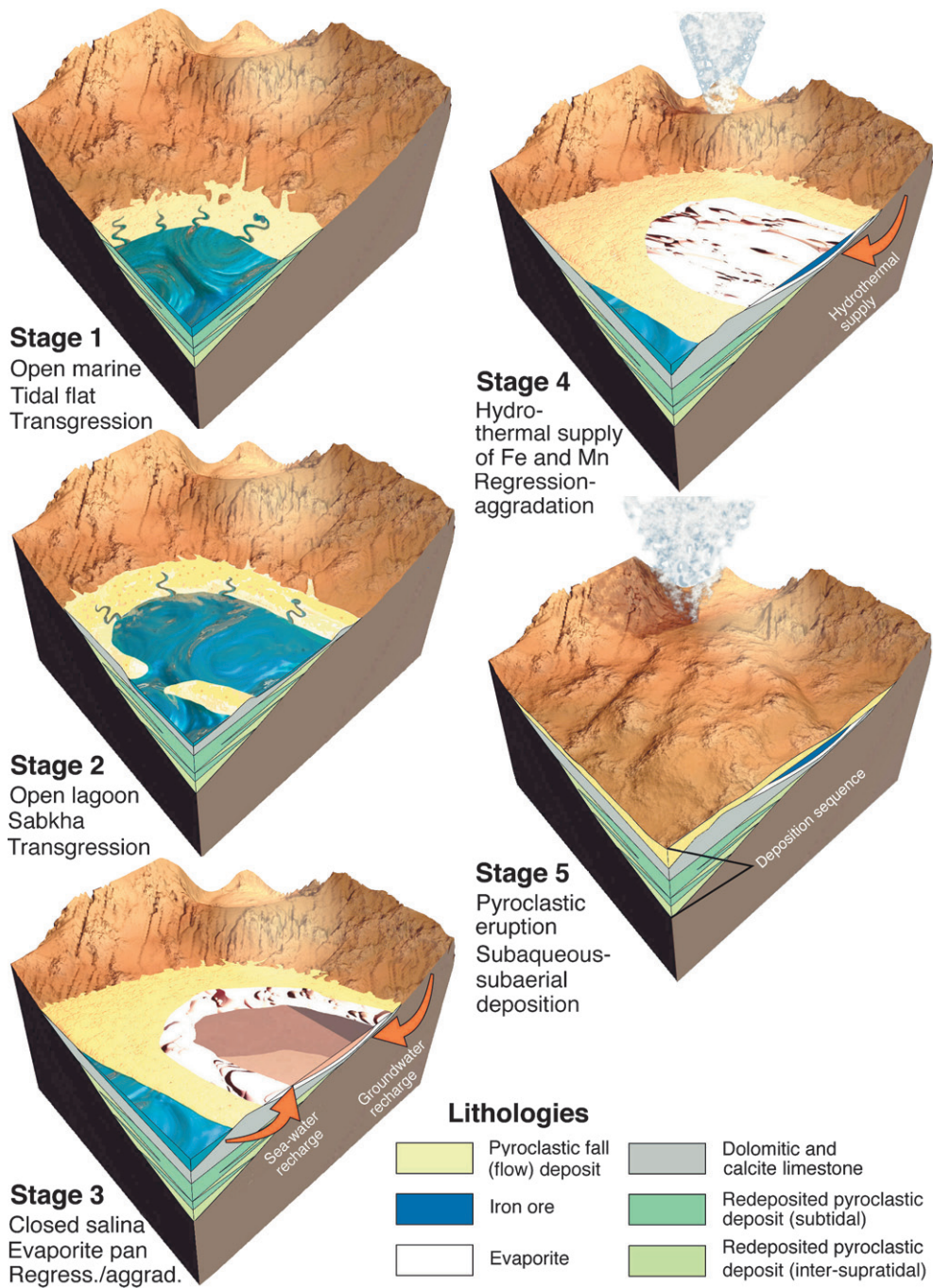


Plate 5. Landscape models of different stages in the hypothetical depositional sequence in Plate 4.



Geological Survey of Sweden
Box 670
SE-751 28 Uppsala
Phone: +46 18 17 90 00
Fax: +46 18 17 92 10
www.sgu.se

Uppsala 2001
ISSN 0349-2176
ISBN 91-7158-666-0
Print: Elanders Tofters AB